1 Appendix

1.1Materials and Methods

1.1.1 Solution Preparations

1.1.1.1 Sodium Chloride Solution

A 0.15 M sodium chloride solution (#96) was quantitatively prepared with 0.0438 g sodium chloride (#25) and water (#02). This stored at 5 degrees Celsius.

1.1.1.2 Sodium Hydroxide Solution

A 0.1 M sodium hydroxide solution (#97) was quantitatively prepared with 0.1967 g sodium hydroxide (#26) and water (#02). This stored at 5 degrees Celsius.

1.1.1.3 Hydrochloric Acid Solution

Solutions of 0.1 M and 0.01 M concentrations (#89) were quantitatively prepared from 2 M stock solution of hydrochloric acid (#13) and water (#02). This stored at 5 degrees Celsius.

1.1.2 Sample Preparation for UV-Vis. Transmission Spectroscopy

1.1.2.1 Blood

Blood (#16) was diluted in a 1:500 ratio by volume in PBS (#95), however the blood concentration was increased to a 1:250 ratio in PBS for higher haemoglobin absorbance. PBS was used as a baseline.

1.1.3 Sample Preparation for UV-Vis.-NIR Reflectance Spectroscopy

1.1.3.1 Calibration Validation for Disclaimer

The three tests below were carried out in numerical order to investigate effect of calibration settings on instrument calibration. Steps 2 and 3 were replicated. Mean, median and variances calculated using Microsoft Office 365 Excel® software.

1. Analysis with InGaAs detector installed
    a. With previous calibration settings as per previous user

b. Perform instrument alignment

c. Run sample in InGaAs method

2. Analysis with 2D detector installed

    a. Calibrate instrument

    b. Install InGaAs detector

    c. Run sample in InGaAs method

3. Analysis with InGaAs installed from test 2

    a. Calibrate instrument

    b. Run sample in InGaAs method

1.1.3.2 Biliverdin

Biliverdin (concentration in blood, #56) was diluted in a 1:2000 ratio by volume in PBS (#95). Baseline solution used was a drop each of sodium hydroxide (0.1 M, #97) hydrochloric acid (0.1M #89) and PBS solutions.

1.1.3.3 Bilirubin

Reference solution prepared for bilirubin at the concentration in blood (#35) was 4 drops of PBS (#95) solution, 5 drops of hydrochloric acid solution (#89) and 5 drops of sodium hydroxide solution (#97). This was mixed, and 1 drop used as the baseline.

1.1.4 Cryogenic Analysis

1.1.4.1 Dimethyl Sulfoxide (deuterated)

Started temperature control on run 4. At run 22 the temperature was set to 298 K and heating setting was changed to High. At run 64 the temperature was set to 298 K and heating setting was changed to High.

For the duplicate, at run 19 the temperature was set to 298 K and heating setting was changed to High. At run 65 the temperature was set to 298 K and heating setting was changed to High.

1.1.4.2 Human Haemoglobin in DMSO-d_6

At run 28, thermocouple reading was 75 K. At run 32 the temperature was set to 275 K and heating setting was changed to Medium. At run 36 the temperature was set to 298 K and heating setting was changed to High. The heater was set to Off at run 48 and the cryostat underwent second cooling with liquid nitrogen. At run 63 the temperature setting was set to 298 K and the heating setting was changed to Medium. At run 99, the heating setting was changed to High.

1.1.4.3 Biliverdin in DMSO-d_6

For the 0.25 mg/μL at run 12, thermocouple reading was 77 K and the heating setting was changed to High. At run 34 the temperature reading was 79 K and heating setting was changed to High.

For the 0.4 mg/μL at run 60, thermocouple reading was 78 K and the heating setting was changed to High.

1.1.5 Nuclear Magnetic Resonance (NMR) to Investigate Purity of Biliverdin and Bilirubin

Approximately 10 mg of sample was weighed using an analytical balance and transferred into an NMR tube. This was diluted to 2/3 the volume of the NMR tube with DMSO-d_6 (approximately 600 μL) and mixed until homogenous for analysis. Spectral data was saved as pdf files.

1.2Results

1.2.1 Additional UV-Vis.-NIR Results

1.2.1.1 Perkin Elmer Lambda 950 UV-Vis.-NIR Spectrophotometer

1.2.1.1.1 Validation Disclaimer for Calibration

Step 2 Output:

Connected to Lambda 950, serial number 950L1302081
Firmware version: 1.61.00 Lambda 900
Synchronizing instrument time and date with PC...
Instrument time and date successfully set
Ready...

Calibrating slits, this will take a few minutes, please wait...
Slit calibration successful
Slit calibration saved
Date: 2017/01/17 10:58:57
Calibration: pass
Gain 29
Energy 0.617E
Steps 605

Calibrating UV/Vis wavelength, this will take a few minutes, please wait...
UV/Vis wavelength calibration successful
UV/Vis wavelength calibration saved
Date: 2017/01/17 11:00:14
Factor: 0.00995877
Offset: -233
D2-Peak 656.1 Pass 1: pass(Peak:648.70nm,Energy:0.593E,Slit:1.00nm,Gain:61)
D2-Peak 656.1 Pass 2: pass(Peak:648.63nm,Energy:0.617E,Slit:0.10nm,Gain:93)
Peak 0.0 Pass 1: pass(Peak:-0.07nm,Energy:0.427E,Slit:1.00nm,Gain:26)
Peak 0.0 Pass 2: pass(Peak:0.04nm,Energy:0.540E,Slit:0.10nm,Gain:42)

Calibrating NIR wavelength, this will take a few minutes, please wait...
NIR wavelength calibration successful
NIR wavelength calibration saved
Date: 2017/01/17 11:03:36
Factor: 0.03982416
Offset: 20
D2-Peak 1312.2 Pass 1: pass(Peak:1312.20nm,Energy:0.524E,Slit:4.00nm,Gain:45)
D2-Peak 1312.2 Pass 2: pass(Peak:1312.28nm,Energy:0.683E,Slit:0.40nm,Gain:68)
Peak 0.0 Pass 1: pass(Peak:0.08nm,Energy:0.503E,Slit:4.00nm,Gain:60)
Peak 0.0 Pass 2: pass(Peak:-0.00nm,Energy:0.659E,Slit:0.40nm,Gain:88)

Calibrating 0% T, please wait...
0% T calibration successful
0% T calibration saved
Date: 2017/01/17 11:06:46
0T sample 1922,1924,1929,1938,1959,1997
0T reference 1921,1924,1928,1938,1957,1995

Restoring instrument settings, please wait...
Calibration complete
Ready...

Step 2 Duplicate Output:

Connected to Lambda 950, serial number 950L1302081

Firmware version: 1.61.00 Lambda 900
Synchronizing instrument time and date with PC...
Instrument time and date successfully set
Ready...

Calibrating slits, this will take a few minutes, please wait...
Slit calibration successful
Slit calibration saved
Date: 2017/01/17 12:20:11
Calibration: pass
Gain 44
Energy 0.543E
Steps 349

Checking Zero Peak, this will take a few minutes, please wait...
Peak 0.0 Pass 1: pass(Peak:-0.02nm,Energy:0.579E,Slit:0.10nm,Gain:30)

Checking UV/Vis D2 Peak, this will take a few minutes, please wait... (1)
D2-Peak 656.1 Pass 1: pass(Peak:656.07nm,Energy:0.141E,Slit:0.08nm,Gain:239)

Calibrating UV/Vis wavelength, this will take a few minutes, please wait...
UV/Vis wavelength calibration successful
UV/Vis wavelength calibration saved
Date: 2017/01/17 12:27:08
Factor: 0.00995931
Offset: -239
Old Peak One: -0.02
New Peak One: 0.00
Old Peak Two: 656.07
New Peak Two: 656.10

Checking Zero Peak, this will take a few minutes, please wait...
Peak 0.0 Pass 1: pass(Peak:-0.01nm,Energy:0.555E,Slit:0.10nm,Gain:30)

Checking NIR D2 Peak, this will take a few minutes, please wait... (1)
D2-Peak 1312.2 Pass 1: pass(Peak:1312.47nm,Energy:0.206E,Slit:0.40nm,Gain:90)

Calibrating NIR wavelength, this will take a few minutes, please wait...
NIR wavelength calibration successful
NIR wavelength calibration saved
Date: 2017/01/17 12:30:26
Factor: 0.03981651
Offset: 20
Old Peak One: -0.01
New Peak One: 0.00
Old Peak Two: 1312.47
New Peak Two: 1312.20

Calibrating 0% T, please wait...
0% T calibration successful
0% T calibration saved
Date: 2017/01/17 12:30:28
0T sample 1918,1920,1925,1935,1954,1994
0T reference 1918,1920,1925,1935,1954,1992

Restoring instrument settings, please wait...
Calibration complete
Ready...

Step 3 Output:

Connected to Lambda 950, serial number 950L1302081
Firmware version: 1.61.00 Lambda 900
Synchronizing instrument time and date with PC...
Instrument time and date successfully set
Ready...

Calibrating slits, this will take a few minutes, please wait...
Slit calibration successful
Slit calibration saved
Date: 2017/01/17 11:56:30
Calibration: pass
Gain 44
Energy 0.560E
Steps 601

Checking Zero Peak, this will take a few minutes, please wait...
Peak 0.0 Pass 1: pass(Peak:-0.05nm,Energy:0.655E,Slit:0.10nm,Gain:30)

Checking UV/Vis D2 Peak, this will take a few minutes, please wait... (1)
D2-Peak 656.1 Pass 1: pass(Peak:656.03nm,Energy:0.147E,Slit:0.08nm,Gain:224)

Calibrating UV/Vis wavelength, this will take a few minutes, please wait...
UV/Vis wavelength calibration successful
UV/Vis wavelength calibration saved
Date: 2017/01/17 12:02:56
Factor: 0.00995911
Offset: -237
Old Peak One: -0.05
New Peak One: 0.00
Old Peak Two: 656.03
New Peak Two: 656.10

Checking Zero Peak, this will take a few minutes, please wait...
Peak 0.0 Pass 1: pass(Peak:-0.02nm,Energy:0.618E,Slit:0.10nm,Gain:30)

Checking NIR D2 Peak, this will take a few minutes, please wait... (1)
D2-Peak 1312.2 Pass 1: pass(Peak:1312.16nm,Energy:0.236E,Slit:0.40nm,Gain:90)

Calibrating NIR wavelength, this will take a few minutes, please wait...
NIR wavelength calibration successful
NIR wavelength calibration saved
Date: 2017/01/17 12:06:19
Factor: 0.03982485
Offset: 20
Old Peak One: -0.02
New Peak One: 0.00
Old Peak Two: 1312.16
New Peak Two: 1312.20

Calibrating 0% T, please wait...
0% T calibration successful
0% T calibration saved
Date: 2017/01/17 12:06:20
0T sample 1918,1920,1925,1935,1955,1995
0T reference 1918,1920,1925,1935,1954,1993

Restoring instrument settings, please wait...
Calibration complete
Ready...

Step 3 Duplicate Output:

Connected to Lambda 950, serial number 950L1302081
Firmware version: 1.61.00 Lambda 900
Synchronizing instrument time and date with PC...
Instrument time and date successfully set
Ready...

Calibrating slits, this will take a few minutes, please wait...
Slit calibration successful
Slit calibration saved
Date: 2017/01/17 13:48:15
Calibration: pass
Gain 44
Energy 0.549E
Steps 597

Checking Zero Peak, this will take a few minutes, please wait...
Peak 0.0 Pass 1: pass(Peak:-0.04nm,Energy:0.630E,Slit:0.10nm,Gain:30)

Checking UV/Vis D2 Peak, this will take a few minutes, please wait... (1)

Checking UV/Vis D2 Peak, this will take a few minutes, please wait... (2)
Checking UV/Vis D2 Peak, this will take a few minutes, please wait... (3)
* Error in calibration - UV/Vis D2-peak check failed
Old settings retained.

Checking Zero Peak, this will take a few minutes, please wait...
Peak 0.0 Pass 1: pass(Peak:-0.05nm,Energy:0.599E,Slit:0.10nm,Gain:30)

Checking NIR D2 Peak, this will take a few minutes, please wait... (1)
D2-Peak 1312.2 Pass 1: pass(Peak:1312.03nm,Energy:0.228E,Slit:0.40nm,Gain:90)

Calibrating NIR wavelength, this will take a few minutes, please wait...
NIR wavelength calibration successful
NIR wavelength calibration saved
Date: 2017/01/17 14:06:54
Factor: 0.03982850
Offset: 23
Old Peak One: -0.05
New Peak One: 0.00
Old Peak Two: 1312.03
New Peak Two: 1312.20

Calibrating 0% T, please wait...
0% T calibration successful
0% T calibration saved
Date: 2017/01/17 14:06:55
0T sample 1917,1919,1924,1932,1951,1987
0T reference 1917,1919,1923,1932,1949,1985

Restoring instrument settings, please wait...
Calibration complete
Ready...

Checking Zero Peak, this will take a few minutes, please wait...
Peak 0.0 Pass 1: pass(Peak:-0.02nm,Energy:0.580E,Slit:0.10nm,Gain:30)

Checking UV/Vis D2 Peak, this will take a few minutes, please wait... (1)
Checking UV/Vis D2 Peak, this will take a few minutes, please wait... (2)
D2-Peak 656.1 Pass 1: pass(Peak:656.05nm,Energy:0.392E,Slit:0.12nm,Gain:239)

Calibrating UV/Vis wavelength, this will take a few minutes, please wait...
UV/Vis wavelength calibration successful
UV/Vis wavelength calibration saved
Date: 2017/01/17 14:13:12
Factor: 0.00995931
Offset: -241
Old Peak One: -0.02
New Peak One: 0.00

Old Peak Two: 656.05

New Peak Two: 656.10

Restoring instrument settings, please wait...

Calibration complete

Ready...

Method selection between 'InGaAs' and '2D detector' has no effect on calibration.

There is statistical variance in two main characteristic peaks analysed (oxyhaemoglobin) of 0.01-0.03 nm whether calibrated on 2D Detector or InGaAs instrument, as shown in the below Table. The soret peak demonstrates the most variance of approximately 45 nm.

Calibration Settings of Perkin Elmer Lamda 950	***OxyHb Spectra Peak Maxima (nm)***		
Previous User Calibration Settings	432.41	540.35	578.50
Calibrated on 2D Detector	423.50	540.97	576.07
Calibrated twice on 2D Detector	427.38	540.79	575.93
Calibrated on 2D Detector Replicate 1	430.28	540.69	575.78
Calibrated on 2D Detector Replicate 2	435.16	540.73	575.85
Calibrated on InGaAs Detector (Integrating Sphere)	429.40	540.68	575.85
Calibrated twice on InGaAs Detector (Integrating Sphere)	431.94	540.76	575.98
Calibrated on InGaAs Detector (Integrating Sphere) Replicate 1	419.21	541.02	576.06
Total Variance *Variance is calculated with respect to the statistical mean*	**26.83**	**0.04**	**0.84**
Total Mean	428.66	540.75	576.25
Total Median	429.84	540.75	575.96
Calibration on InGaAs Detector (Integrating Sphere) Variance	**45.39**	**0.03**	**0.01**
Mean	426.85	540.82	575.96
Median	429.40	540.76	575.98
Calibration on 2D Detector Variance	**24.14**	**0.02**	**0.02**
Mean	429.08	540.80	575.91
Median	428.83	540.76	575.89

Table 4-1: Summary of calculations for wavelength variance depending on calibration settings for Perkin Elmer Lambda 950 UV-Vis.-NIR Spectrophotometer.

1.2.1.1.2 Solvents

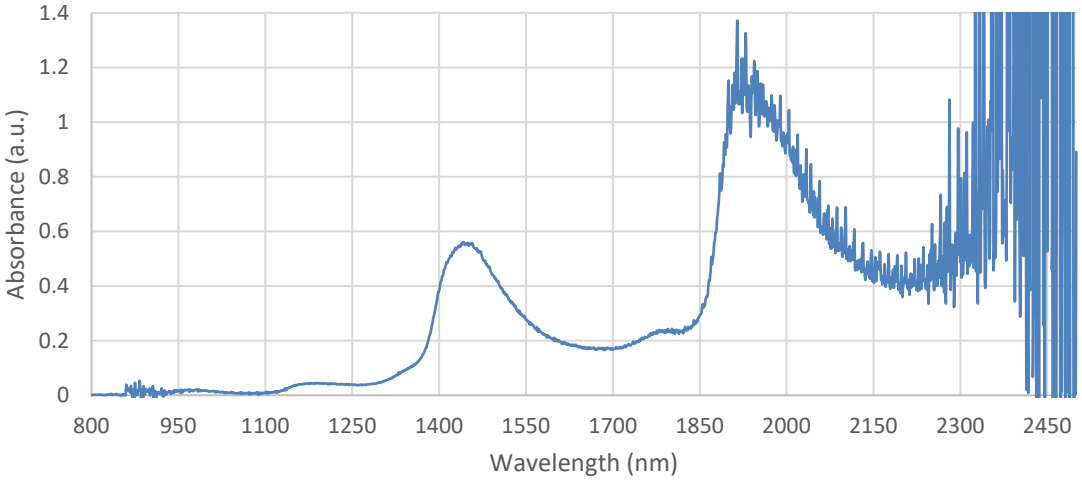

Figure 1-1: NIR reflectance spectrum of water (reference: filter paper), analysed using the UV-Vis.-NIR Lambda 950 Spectrophotometer at Flinders University.

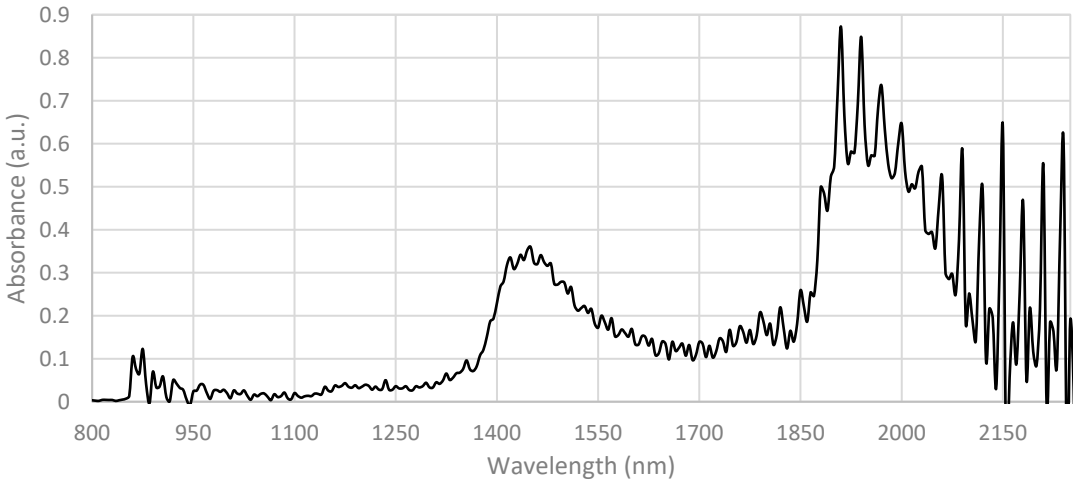

Figure 4-2: NIR reflectance spectrum of PBS solution (reference: filter paper), analysed using the UV-Vis.-NIR Lambda 950 Spectrophotometer at Flinders University.

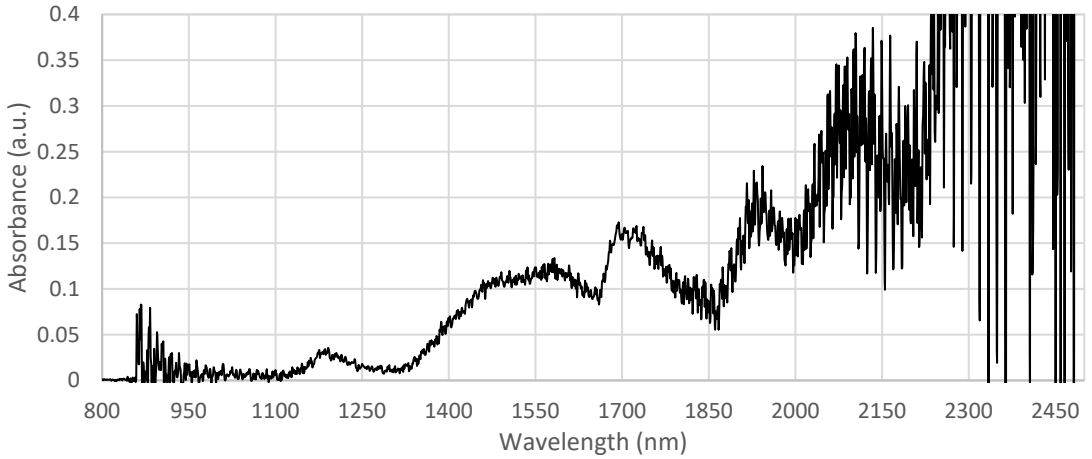

Figure 1-3: NIR reflectance spectrum of 100% ethanol (reference: filter paper), analysed using the UV-Vis.-NIR Lambda 950 Spectrophotometer at Flinders University.

Ethanol provides a NIR spectrum alike that recorded in literature [1]. Spectral information above 1850 nm possesses noise, which has been dramatically reduced by smoothing to assist in visual comparison. The baseline is sloping, more so than that of water. Ethanol dried quickly in comparison to water (filter paper was still moist post analysis).

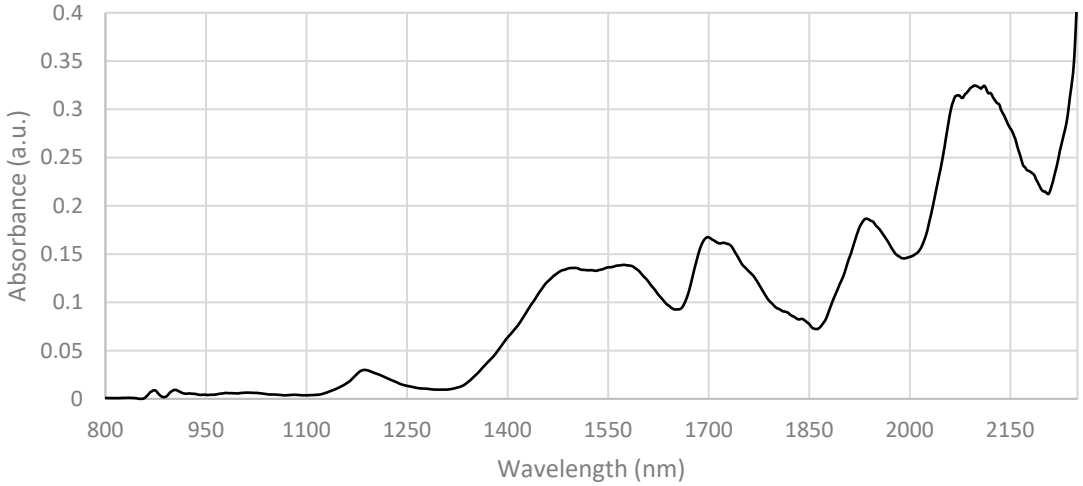

Figure 4-4: Smoothed (width 49) NIR reflectance spectrum of 100% ethanol (reference: filter paper), generated using the UV-Vis.-NIR Lambda 950 Spectrophotometer software at Flinders University. Please refer to the Appendix (Additional FIR Results) for a non-smoothed version.

1.2.1.1.3 Blood

The spectrum of stored neat Sheep's blood diluted in PBS that has been refrigerated contains oxyhaemoglobin (410, 539 & 576 nm) and methaemoglobin (502 & 630

nm) peaks.

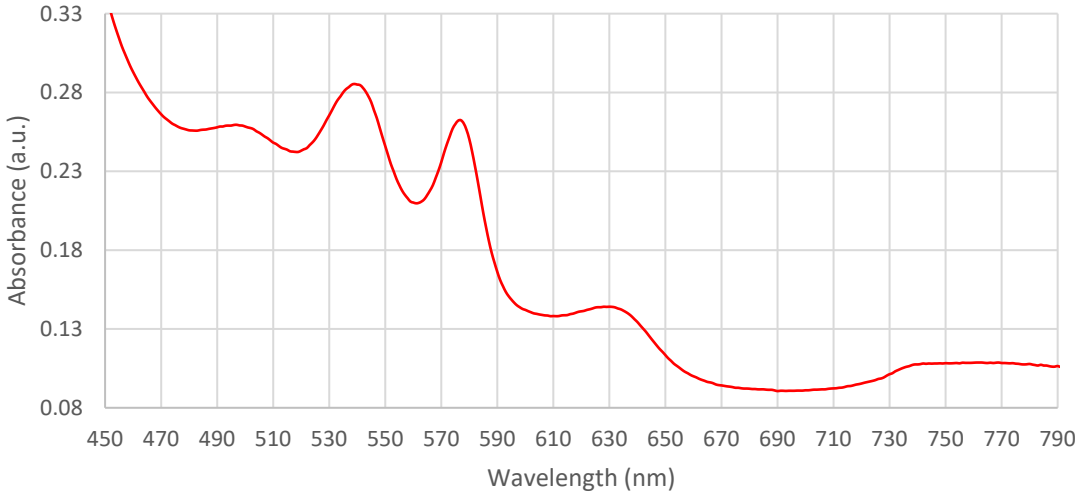

Figure 1-5: UV-Vis. spectrum of stored neat blood diluted in PBS (20 uL blood in 10 mL PBS) analysed at Flinders University with PBS as a baseline in a quartz cuvette.

Neat blood as it dries presents the below spectra overlay. At time zero, peaks are observed at 429, 500, 538, 576 and 627. Over time, there is an overall decrease in peak absorption, and increase in the ridge between the 538 and 576 nm peaks. Spectra in-between times 36 mins and 200 mins are similar to these.

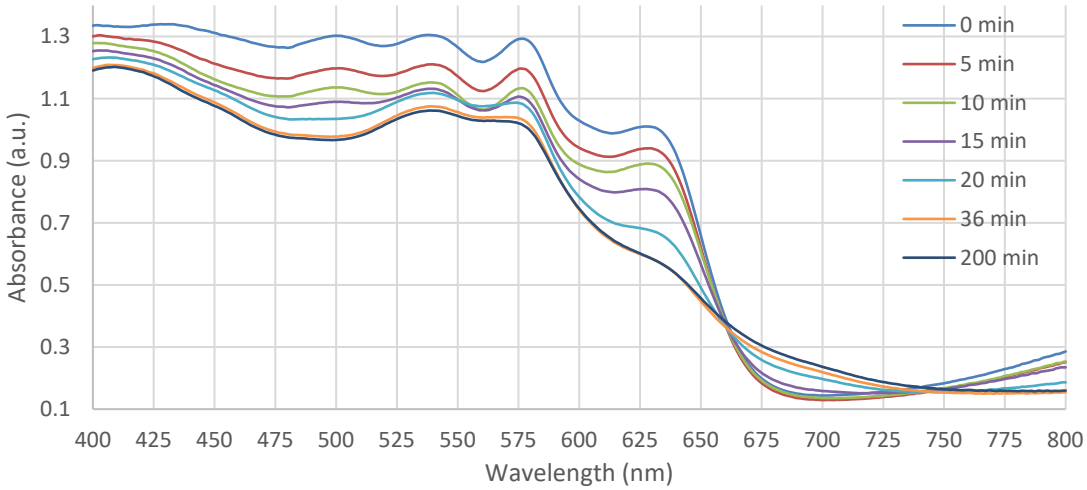

Figure 1-6: UV-Vis. (Flinders) spectra overlay of neat blood as it dries.

Humidity data:

18 dec 2014 – 9am 13%, 3pm 7%

19 dec 2014 – 9am 32%, 3pm 8%

20 dec 2014 – 9am 18%, 3pm 34%

18 Feb 2015 – 3pm 52%

Duplicate of previously refrigerated neat blood as it dries, but with smaller time intervals:

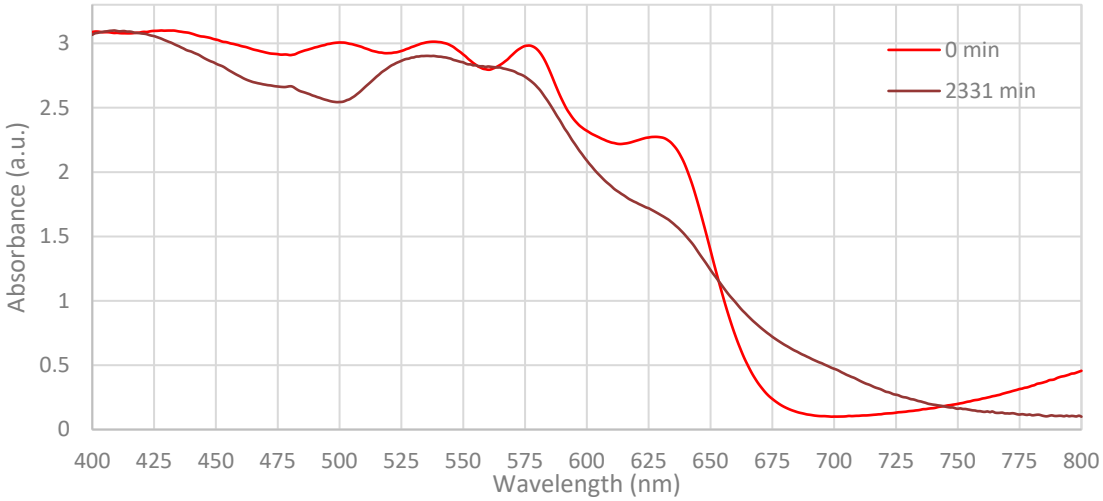

Figure 1-7: normalised UV-Vis. (Flinders) spectra overlay of neat blood as it dries.

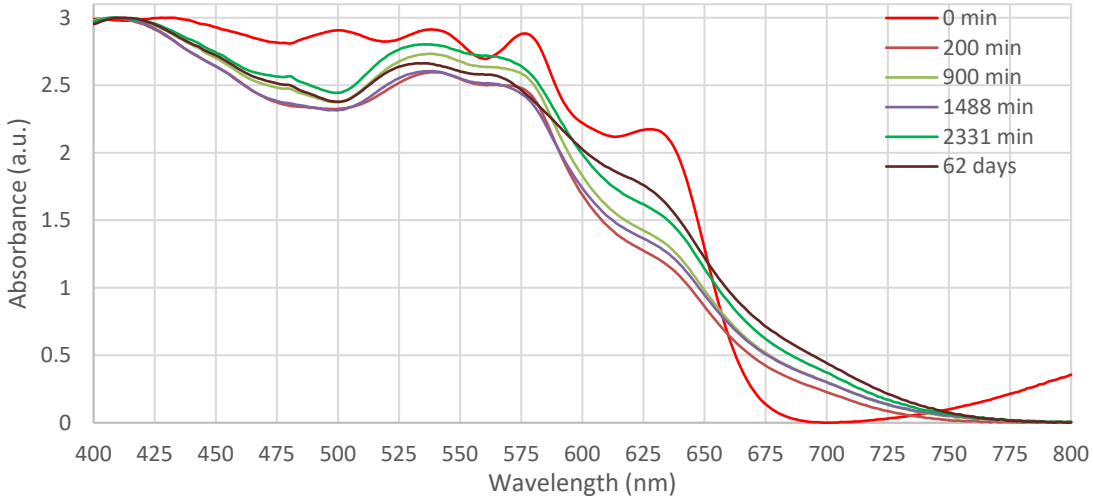

Figure 1-8: normalised UV-Vis. (Flinders) spectra overlay of neat blood as it dries.

1.2.1.1.4 Methaemoglobin

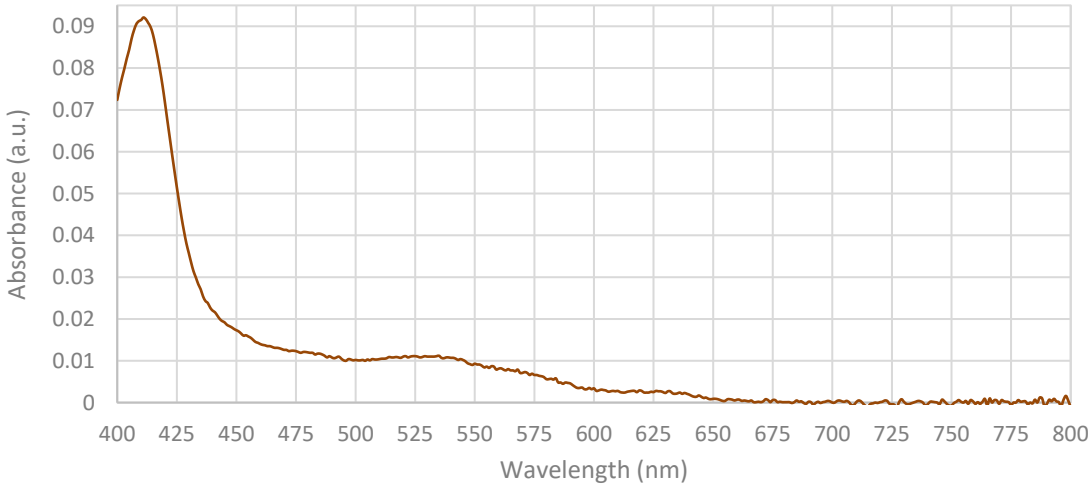

Figure 1-9: UV-Vis. reflectance spectrum of methaemoglobin preparation from neat sheep's blood (15 µL blood, 5 mL PBS & 24.3 mg sodium nitrite), analysed using a UV-Vis.-NIR Lambda 950 Spectrophotometer at Flinders University.

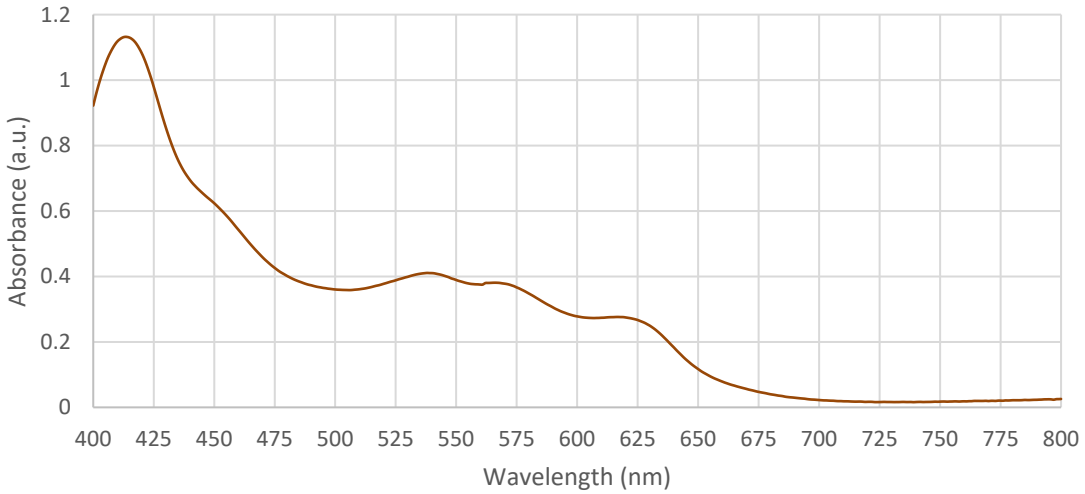

Figure 1-10: UV-Vis. reflectance spectrum of methaemoglobin preparation from neat sheep's blood (300 µL blood, 900 µL filtered plasma & 489.8 mg sodium nitrite), analysed after 2 days using a UV-Vis.-NIR Lambda 950 Spectrophotometer at Flinders University.

When leaving the methaemoglobin preparation for 12 days, it had a green discolouration and pH was tested as 6-7.

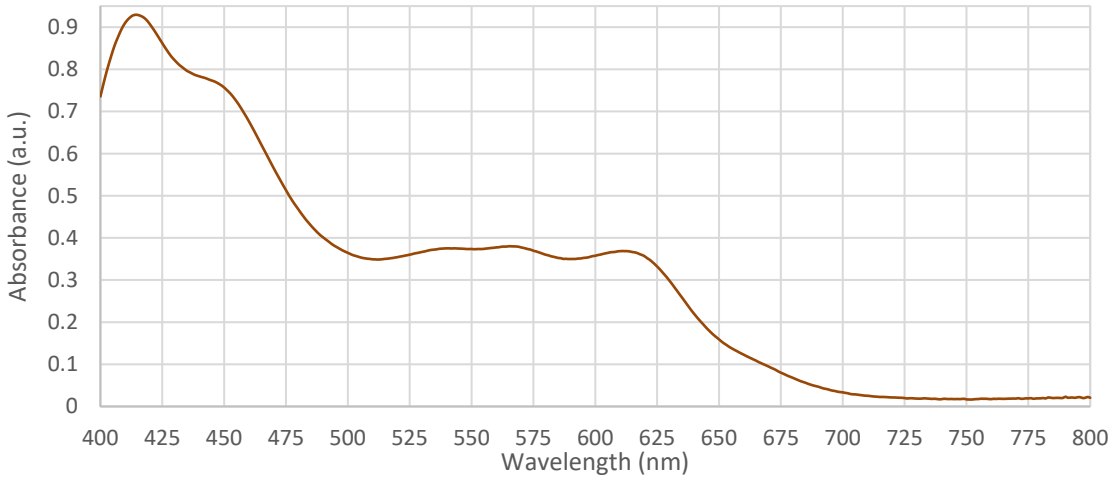

Figure 1-11: UV-Vis. reflectance spectrum of methaemoglobin preparation from neat sheep's blood (300 µL blood, 900 µL filtered plasma & 489.8 mg sodium nitrite), analysed after 12 days using a UV-Vis.-NIR Lambda 950 Spectrophotometer at Flinders University.

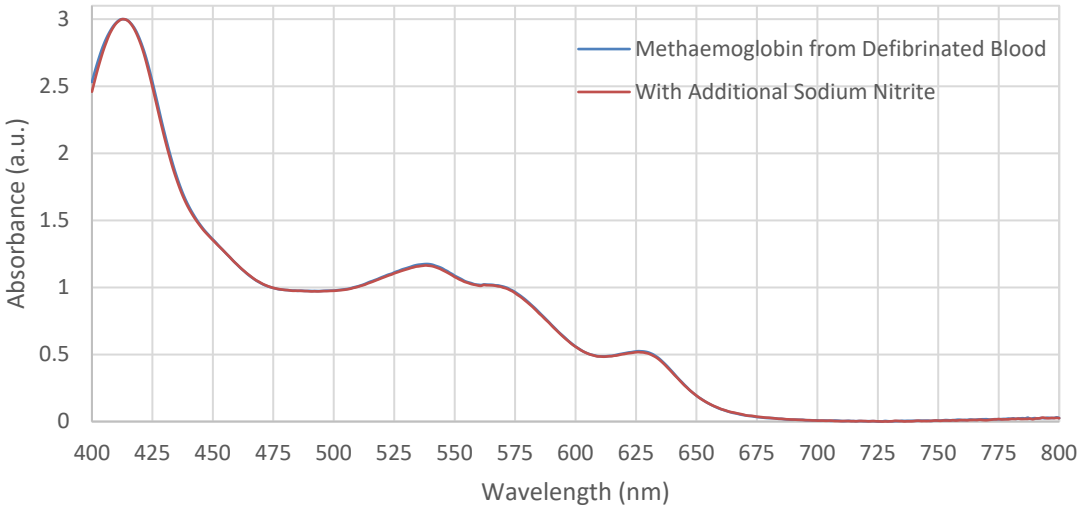

Figure 1-12: UV-Vis. reflectance spectrum of methaemoglobin preparation from defibrinated sheep's blood (300 µL blood, 1 mL filtered sheep blood plasma & 586.4 mg sodium nitrite), then with excess sodium nitrite, analysed using a UV-Vis.-NIR Lambda 950 Spectrophotometer at Flinders University.

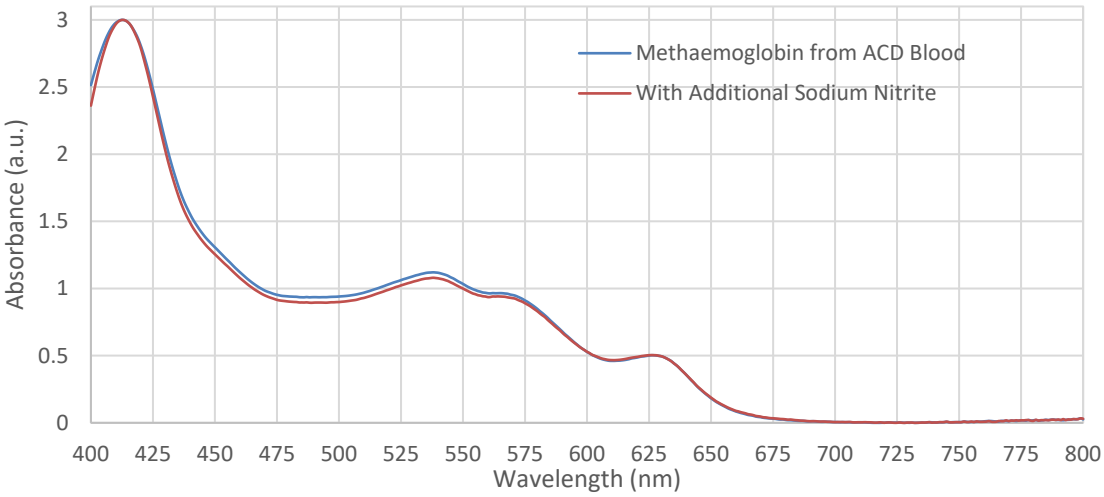

Figure 1-13: UV-Vis. reflectance spectrum of methaemoglobin preparation from sheep's blood containing ACD (100 µL blood, 1 mL PBS & 209.9 mg sodium nitrite), then with excess sodium nitrite (316.6 mg), analysed using a UV-Vis.-NIR Lambda 950 Spectrophotometer at Flinders University.

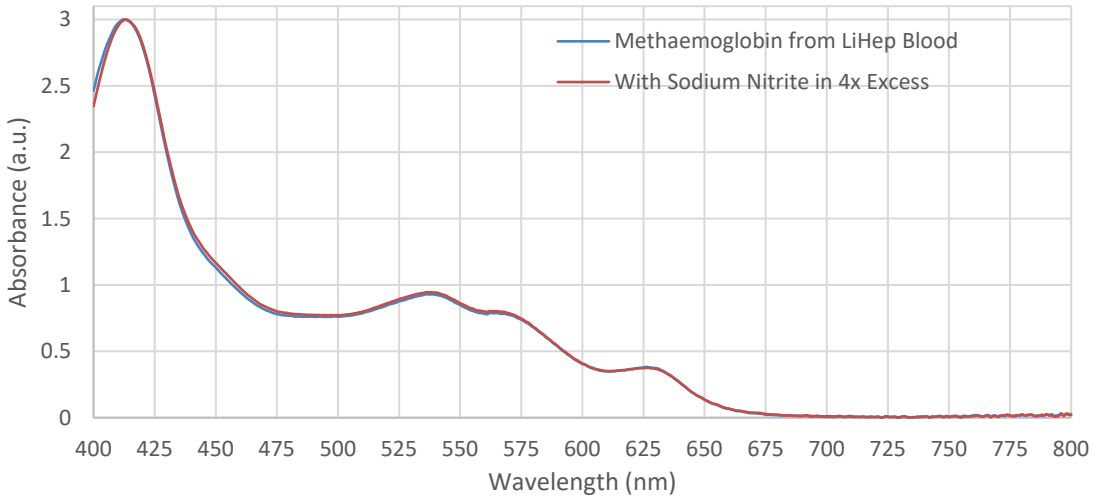

Figure 1-14: UV-Vis. reflectance spectrum of methaemoglobin preparation from sheep's blood containing LiHep (100 µL blood, 1 mL PBS & 211.4 mg sodium nitrite), then with excess sodium nitrite (205.3 mg), analysed using a UV-Vis.-NIR Lambda 950 Spectrophotometer at Flinders University.

1.2.1.1.5 Biliverdin

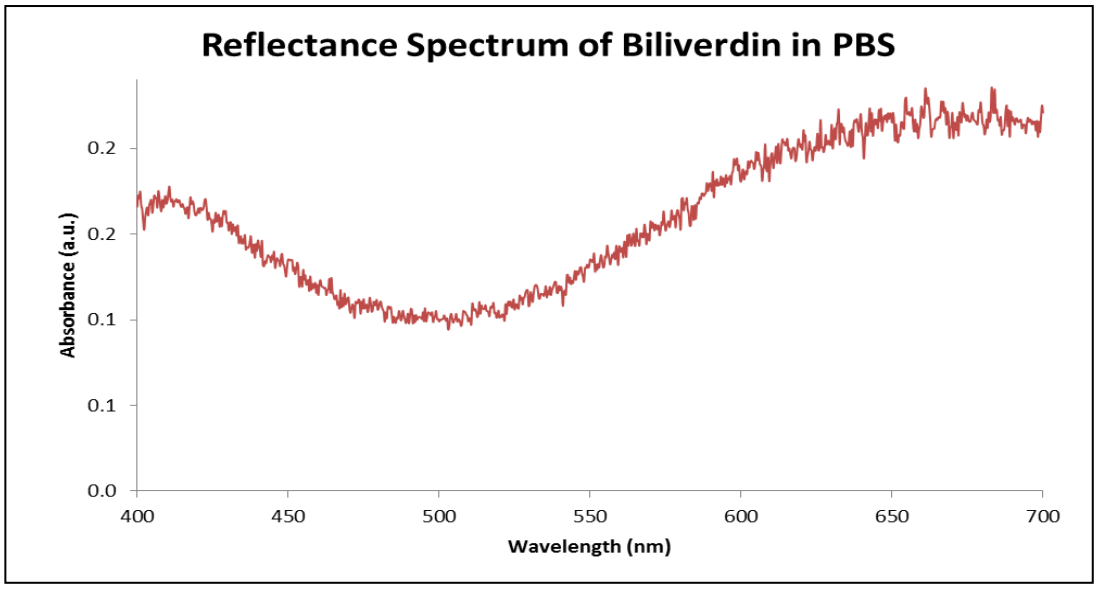

Figure 1-15: UV-Vis. spectrum of a biliverdin in PBS preparation (2.28 mg/mL), analysed using a Varian Cary 5G UV-Vis.-NIR Spectrometer with DRA-CA-50M Diffuse Reflectance Accessory at Flinders University.

1.2.1.1.6 Bilirubin

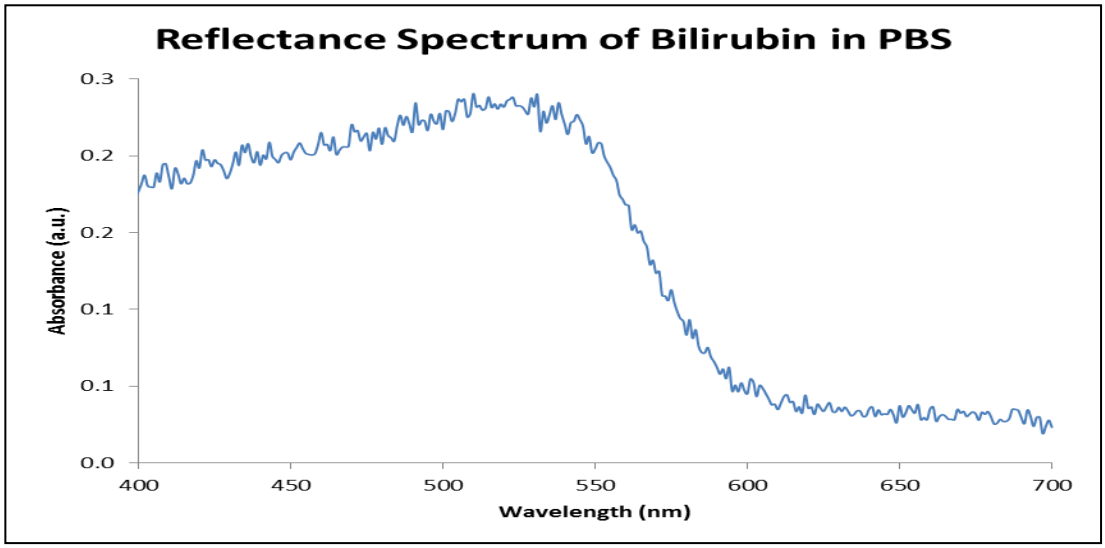

Figure 1-16: UV-Vis. spectrum of a bilirubin in pH shifted aqueous preparation (0.012 mol/L), analysed using a Varian Cary 5G UV-Vis.-NIR Spectrometer with DRA-CA-50M Diffuse Reflectance Accessory at Flinders University.

The below spectra of bilirubin from stored solution exhibit an additional peak. This solution was stored past recommended storage time.

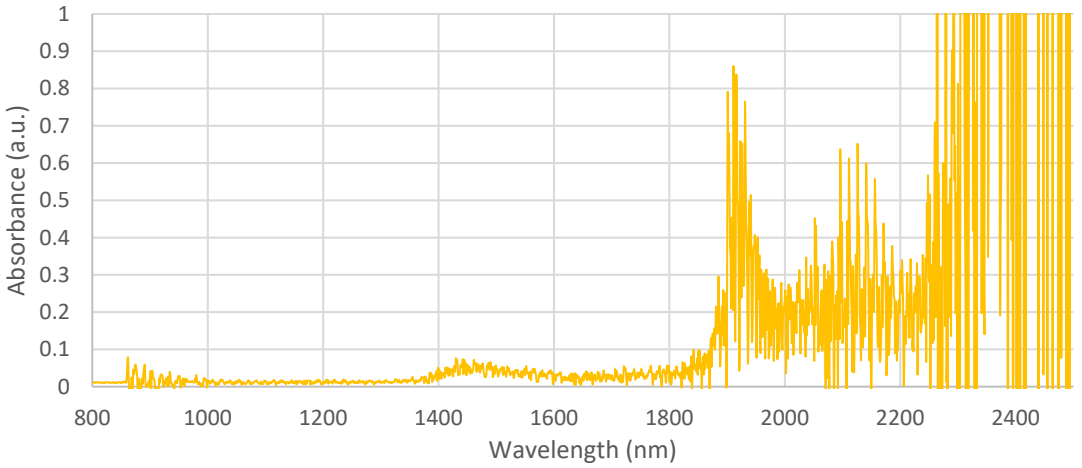

Figure 1-17: NIR reflectance spectrum of bilirubin in pH shifted preparation in sheep's blood (1.9×10^{-2} M), analysed using a UV-Vis.-NIR Lambda 950 Spectrophotometer at Flinders University.

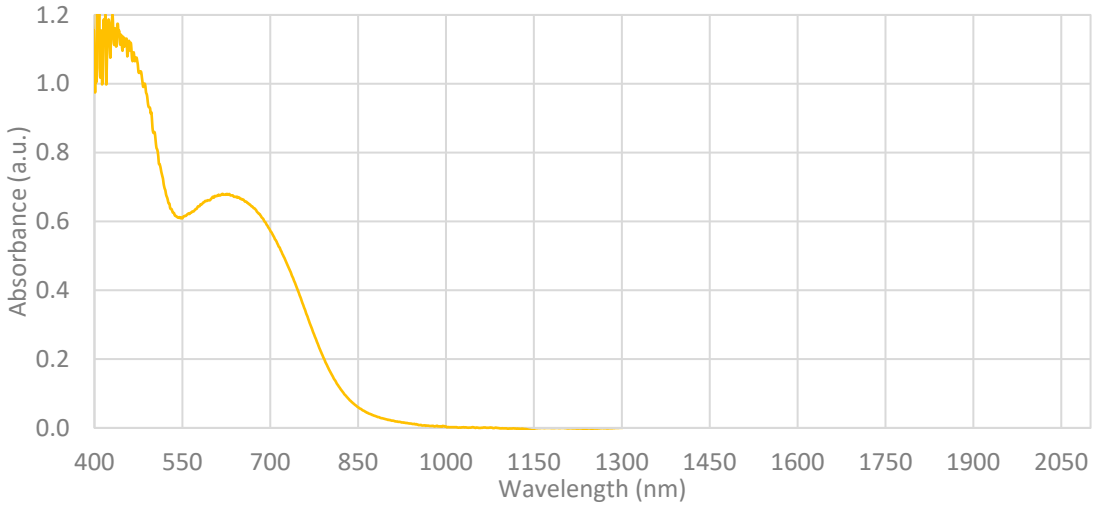

Figure 1-18: dried 0.012 M bilirubin stored in fridge. Drop each of PBS and NaOH as white ref. 641 nm peak

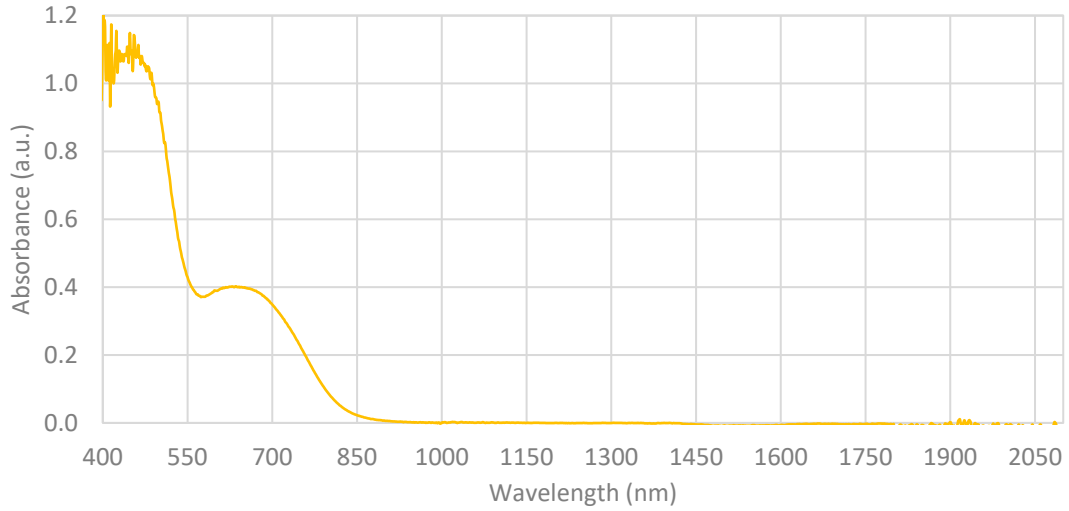

Figure 1-19: dried 0.012 M bilirubin stored in fridge. Drop each of PBS and NaOH as white ref. 670 nm peak

1.2.2 Additional MIR Results

1.2.2.1 FTIR Microscope with ATR Accessory to analyse dried Ferritins and Blood

1.2.2.1.1 Blood

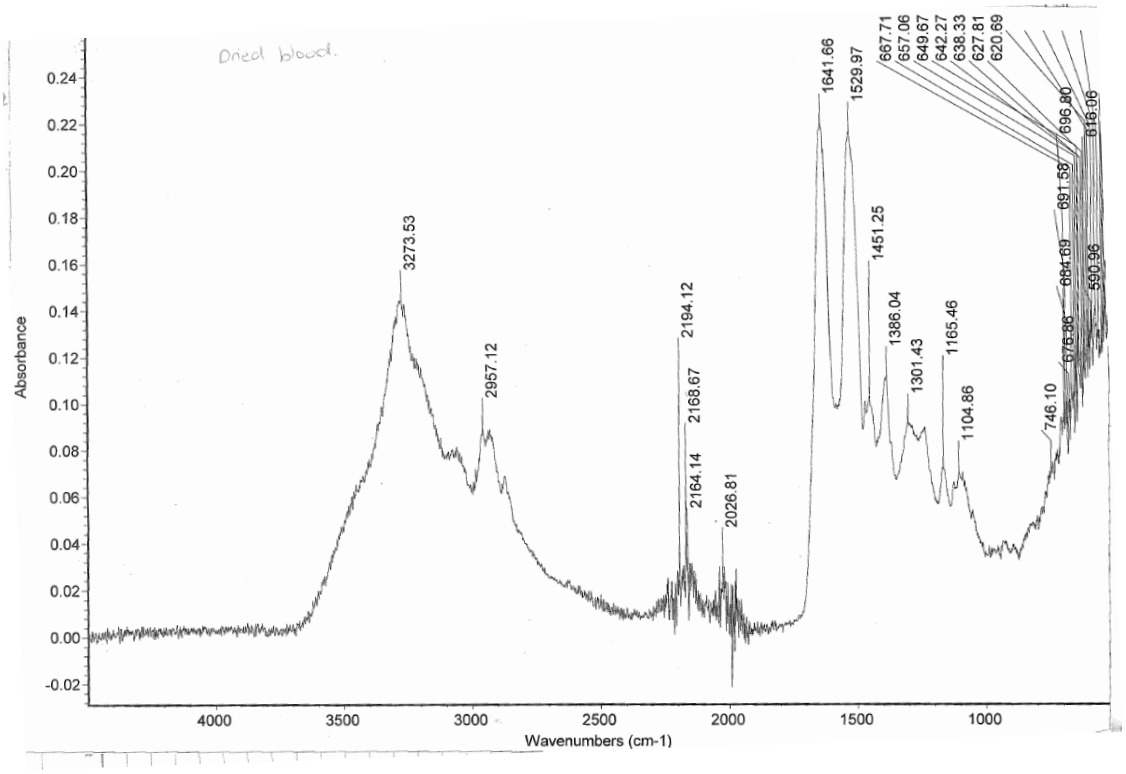

Figure 1-20: FTIR ATR of vacuum dried defibrinated blood.

1.2.2.1.2 Biliverdin

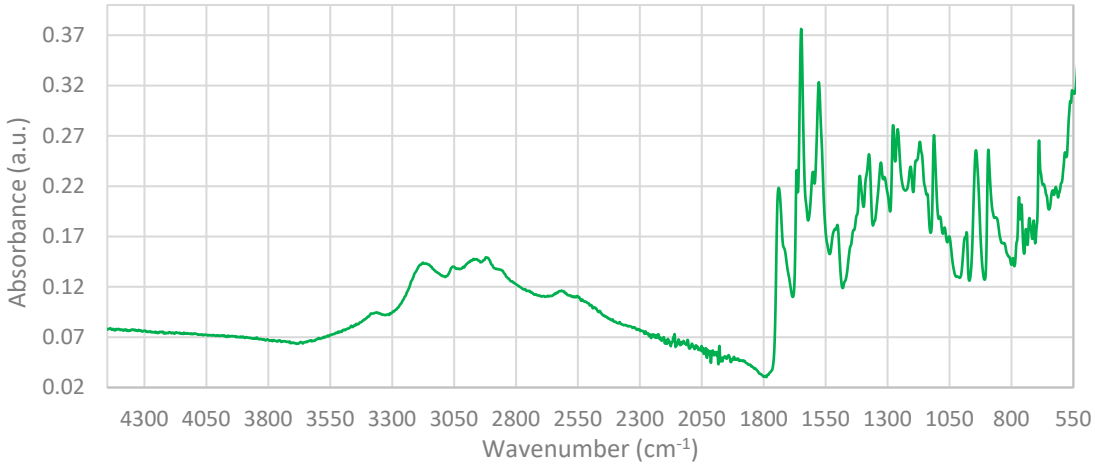

Figure 1-21: ATR-FTIR spectrum of biliverdin hydrochloride powder, analysed using an FT-IR Microscope with ATR accessory at Flinders University.

1.2.2.1.3 Bilirubin

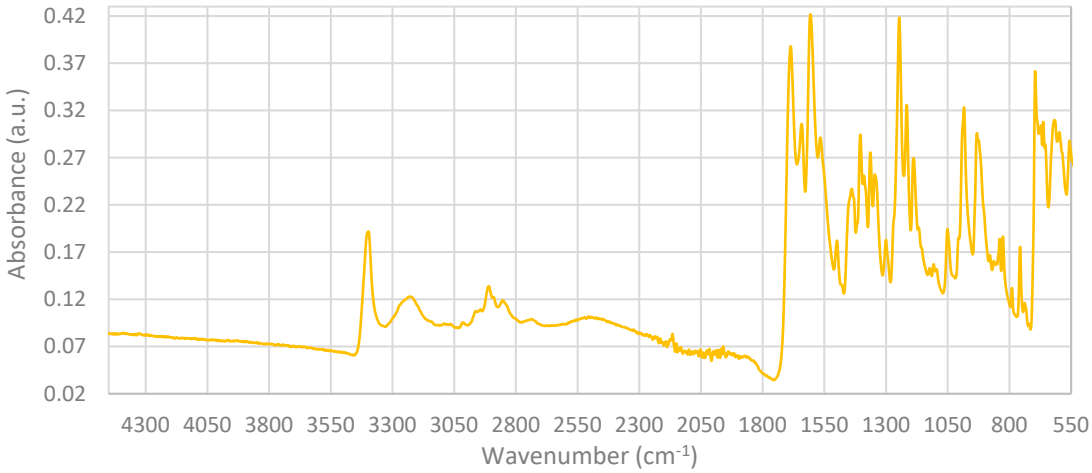

Figure 1-22: ATR-FTIR spectrum of bilirubin powder, analysed using an FT-IR Microscope with ATR accessory at Flinders University.

1.2.2.1.4 Biliverdin and Bilirubin Mixtures

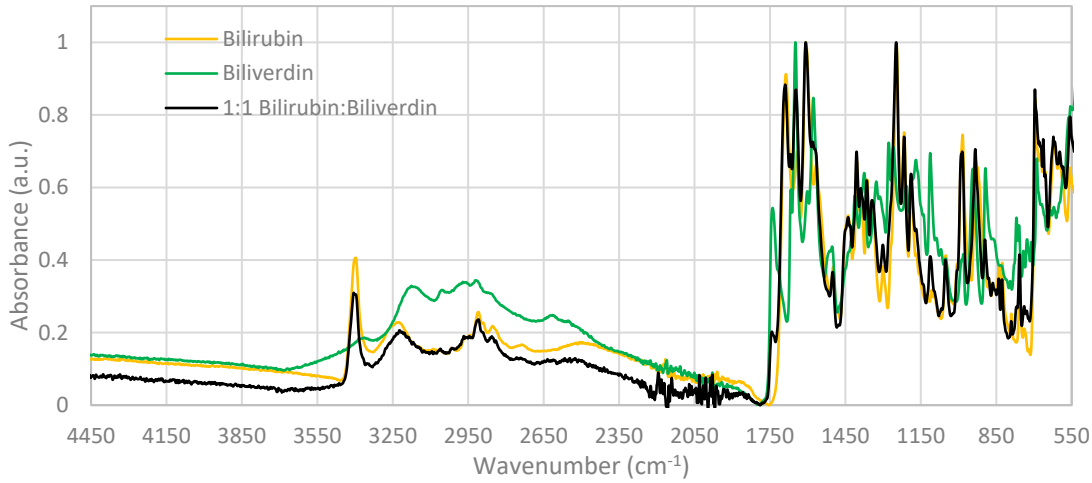

Figure 1-23: ATR-FTIR spectrum of biliverdin & bilirubin (1:1 mixture), normalised between 1750-550 cm^{-1} and 2350-4400 cm^{-1}, analysed using an FT-IR Microscope with ATR accessory at Flinders University.

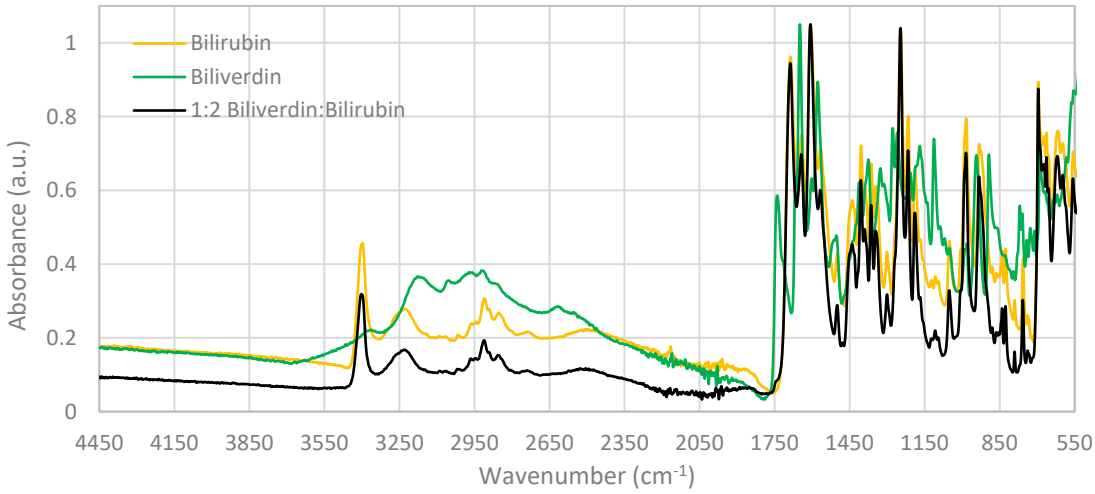

Figure 1-24: ATR-FTIR spectrum of bilirubin & biliverdin (1:2 mixture; 1.5 mg bilirubin & 0.6 mg biliverdin), normalised between 1750-550 cm^{-1} and 2350-4400 cm^{-1}, analysed using an FT-IR Microscope with ATR accessory at Flinders University.

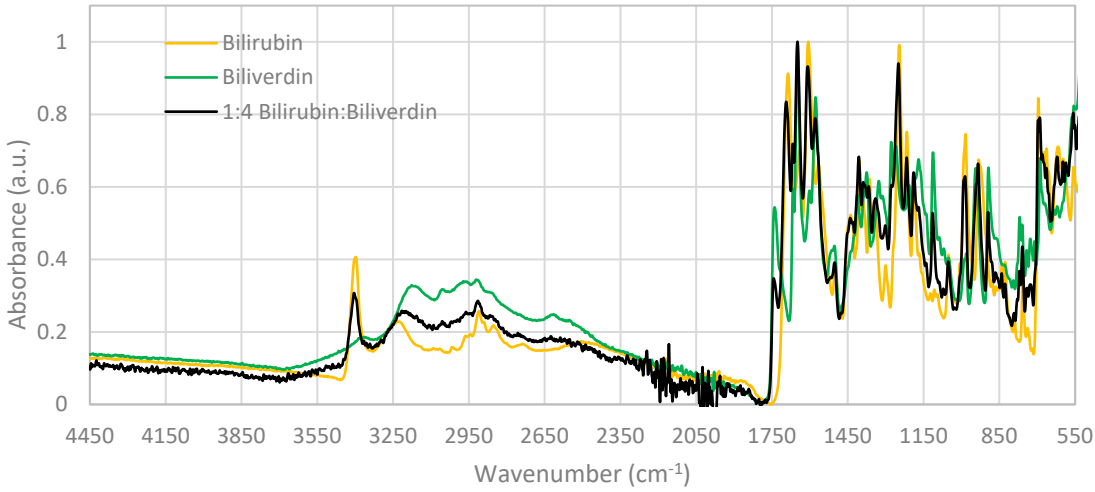

Figure 1-25: ATR-FTIR spectrum of bilirubin & biliverdin (1:4 mixture; 0.6 mg bilirubin & 2.6 mg biliverdin), normalised between 1750-550 cm^{-1} and 2350-4400 cm^{-1}, analysed using an FT-IR Microscope with ATR accessory at Flinders University.

1.2.2.1.5 Ferritin

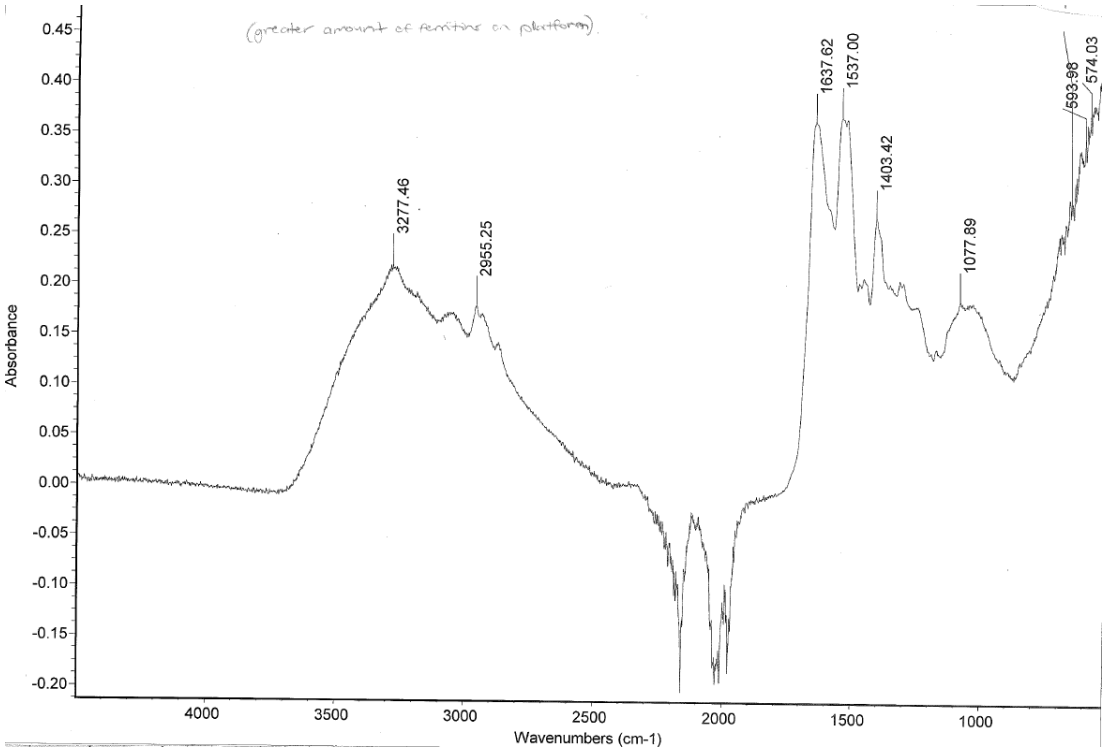

Figure 1-26: FTIR ATR of vacuum dried ferritins in NaCl.

1.2.3 Additional Far Infrared (FIR) Results

1.2.3.1 Blood

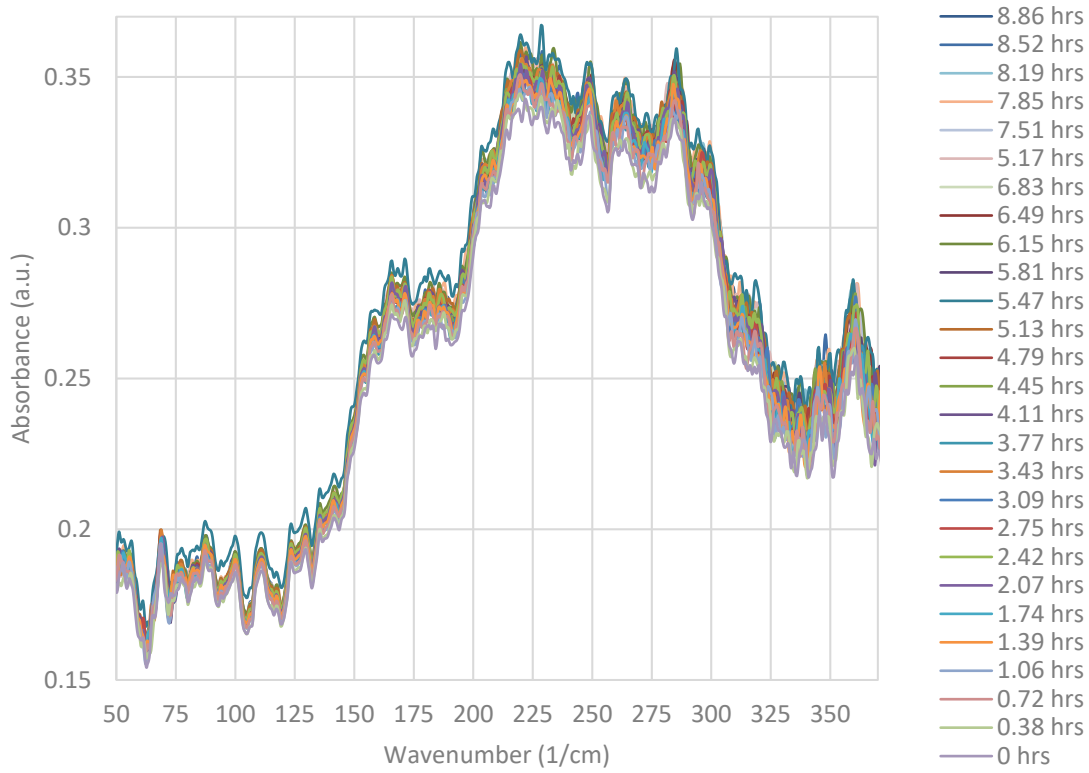

Figure 1-27: FIR overlayed spectra of overnight (8.86 hours) pressed airdried defibrinated blood in PE pellet (20 µL in 30 mg PE), analysed at the Australian Synchrotron (FIR Beamline) with SiBolo detector. Pellet weight was approximately 1 mg. Amplitude approximately 2800. Delay between Measurements (runs) parameter in acquisition was set to 1200 secs and Repeat the Measurement (runs) set to 100.

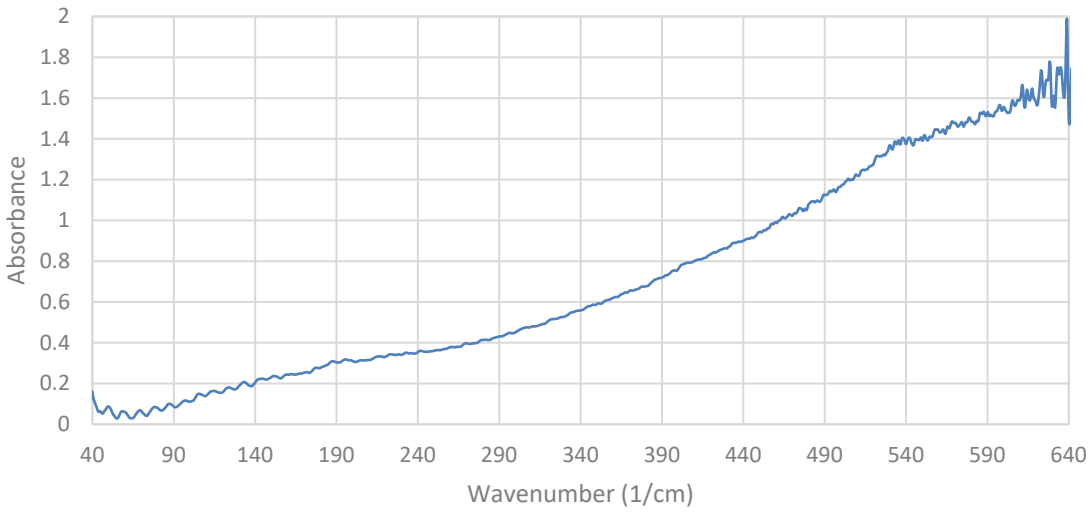

Figure 1-28: Thin layer of vacuum dried neat sheep heart blood previously pipetted on to pressed 7 mm PE pellet, analysed at the Australian Synchrotron (FIR Beamline) with SiBolo detector. Pellet weight was approximately 2 mg.

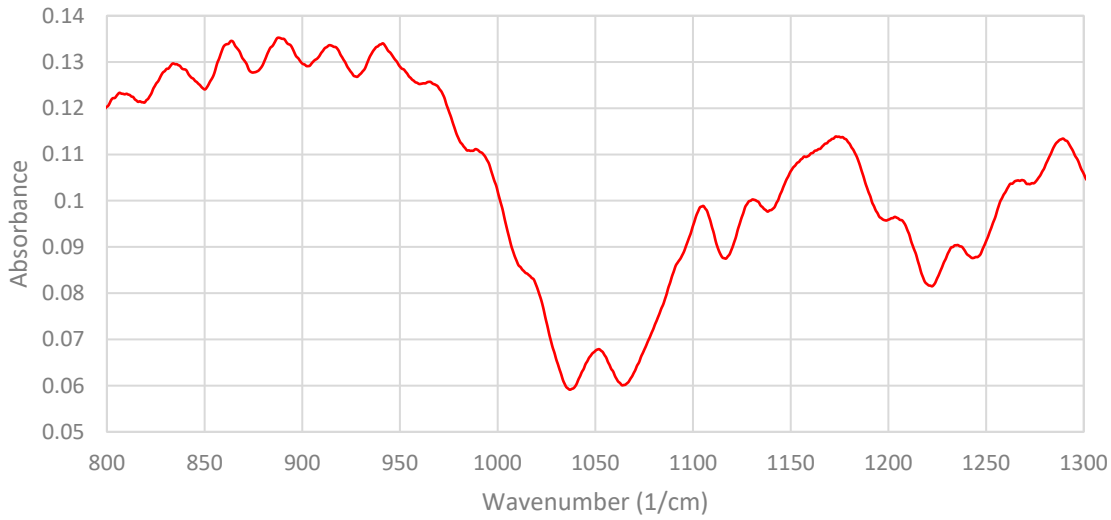

Figure 1-29: FIR spectrum of pressed 5% vacuum-dried defibrinated blood in KBr pellet (weight approx. 1 mg) analysed on the THz/FIR beamline at the Australian Synchrotron using an MCT_N detector with amplitude of 23800. This spectrum is not averaged hence presents noise.

In the below figure, weak peaks are observed using the Si:B detector at 405, 434, 460, 490, 520, 544, 576, 604, 629, 657, 687 and 719 wavenumbers. Fringing and oscillation corroborate effects due to protein structure as discussed for ferritin. Extensive fringing is a direct result from beamline issues unable to be troubleshooted by the Beamline Scientist during that beamtime.

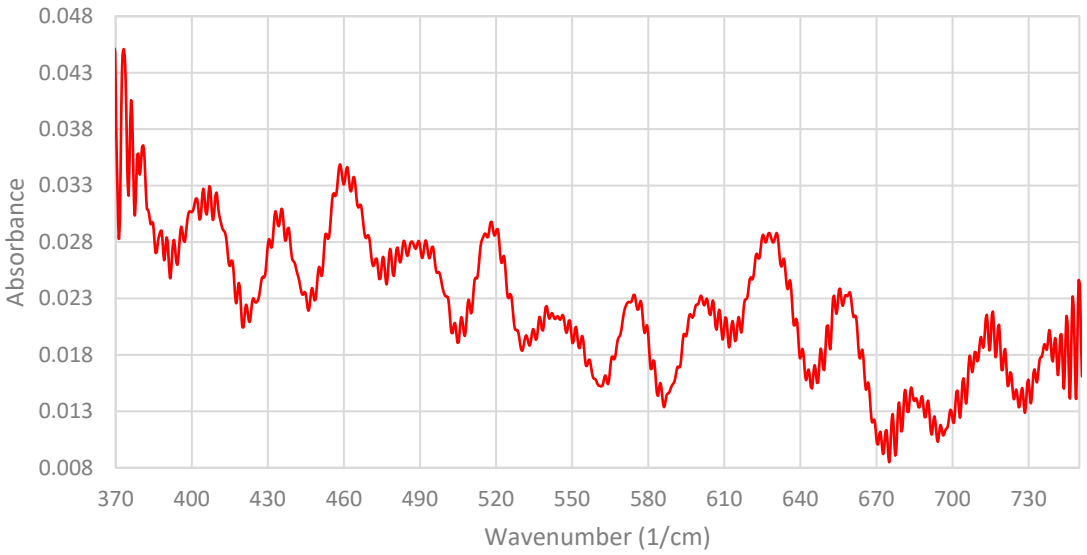

Figure 4-30: FIR spectrum of pressed 5% vacuum-dried defibrinated blood in KBr pellet (weight approx. 1 mg) analysed on the THz/FIR beamline at the Australian Synchrotron using a Si:B detector with amplitude of 12000.

Below is a 3D Plot and Waterfall Plot to help illustrate the changes of airdried defibrinated blood over time.

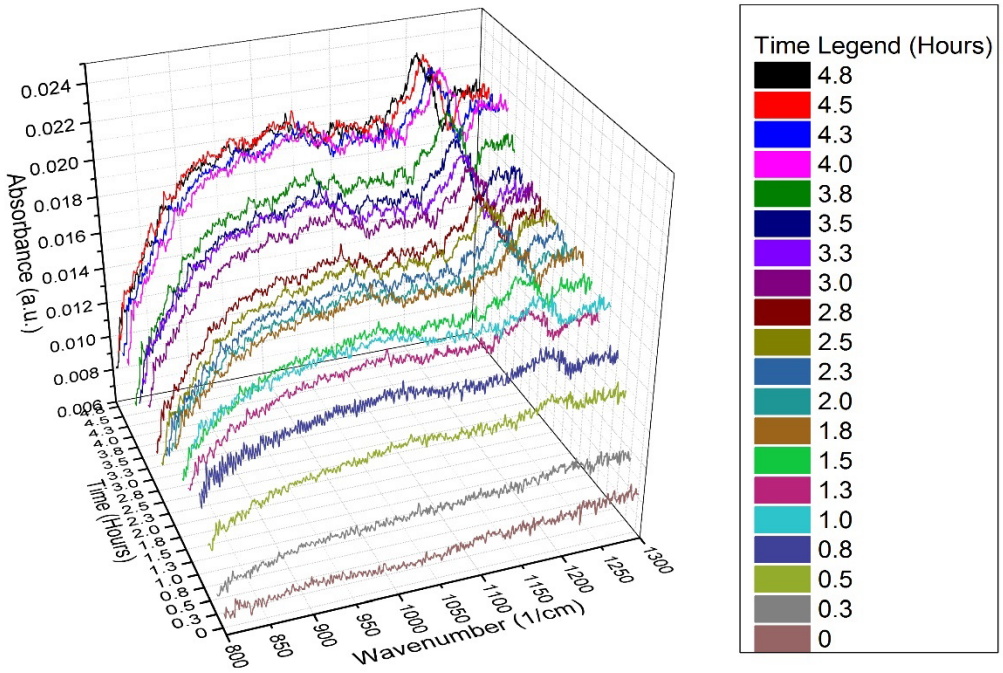

Figure 4-31: 3D ribbon plot of overlayed MIR spectra of overnight (4.79 hours) pressed 5% airdried defibrinated blood in KBr pellet (weight approx. 1 mg), analysed at the Australian Synchrotron (THz/FIR Beamline) using MCT$_N$ detector with amplitude of approx 20289. Delay between Measurements parameter in acquisition was set to 900 secs and Repeat the Measurement was set to 100.

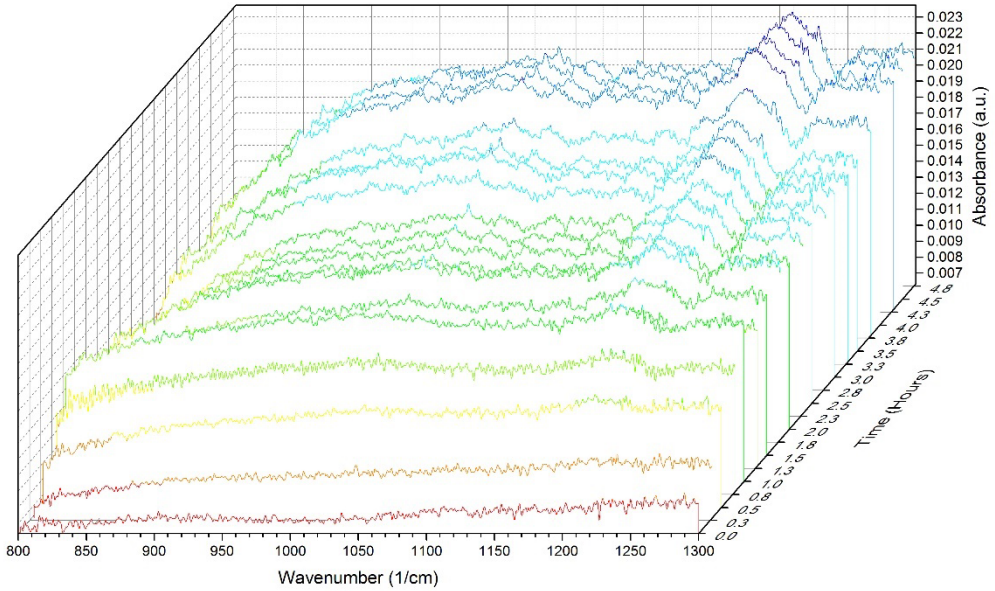

Figure 4-32: Waterfall plot of overlayed spectra of overnight (4.79 hours) pressed 5% airdried defibrinated blood in KBr pellet (weight approx. 1 mg), analysed at the Australian Synchrotron (THz/FIR Beamline) using MCT$_N$ detector with amplitude of approx 20289. Delay between Measurements parameter in acquisition was set to 900 secs and Repeat the Measurement was set to 100.

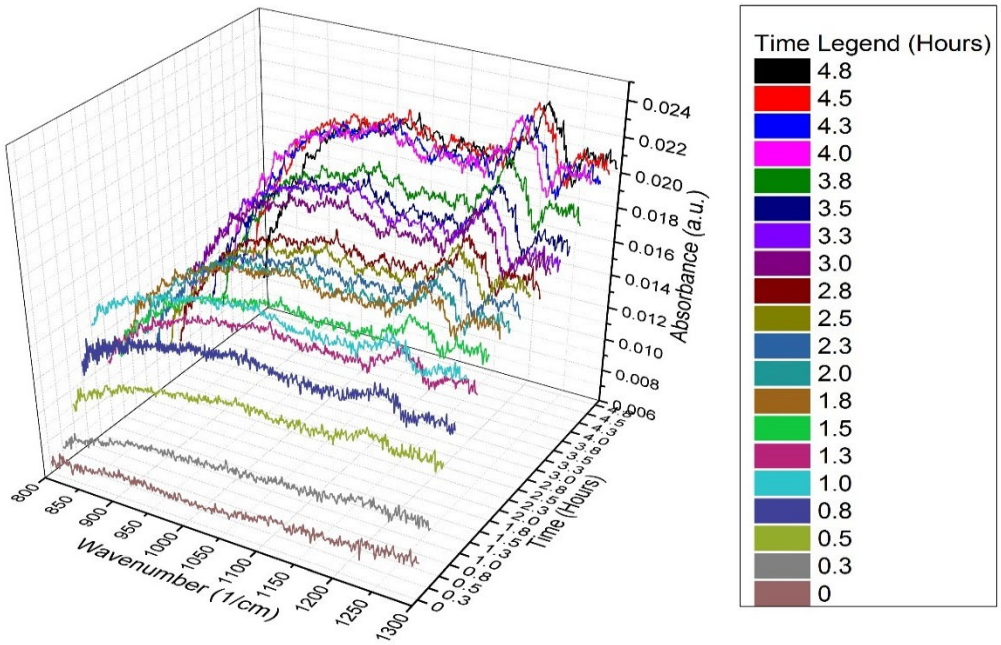

Figure 1-33: 3D ribbon plot of overlayed spectra of overnight (4.79 hours) pressed 5% airdried defibrinated blood in KBr pellet, analysed at the Australian Synchrotron (FIR Beamline) with MCT$_N$ detector. Pellet weight was approximately 1 mg. Amplitude approximately 20289. Delay between Measurements (runs) parameter in acquisition was set to 900 secs and Repeat the Measurement (runs) set to 100.

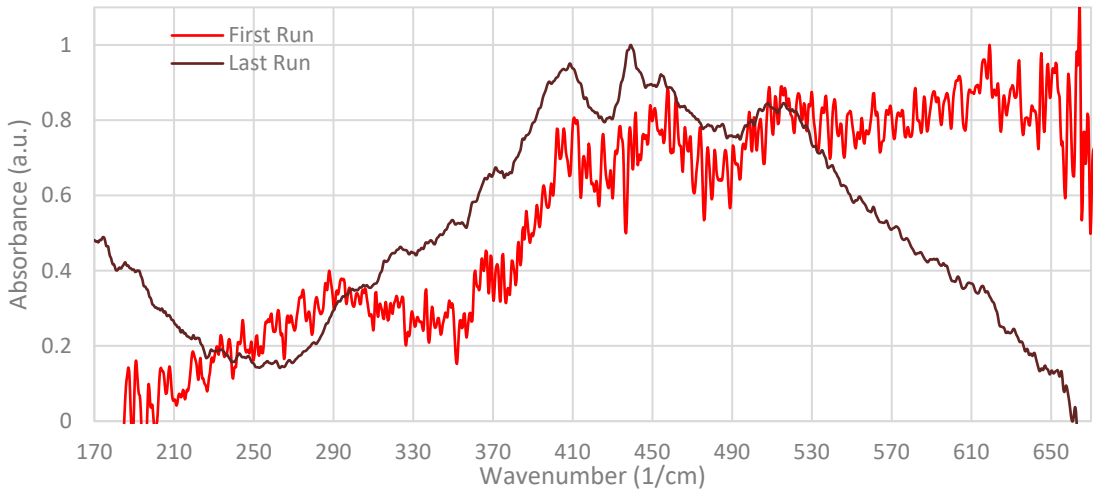

Figure 4-34: FIR-ATR overlayed spectra of defibrinated sheep's blood as it dries, analysed at the Australian Synchrotron (THz/FIR beamline) with SiBolo detector and starting amplitude of 5100.

1.2.3.2 Human Haemoglobin

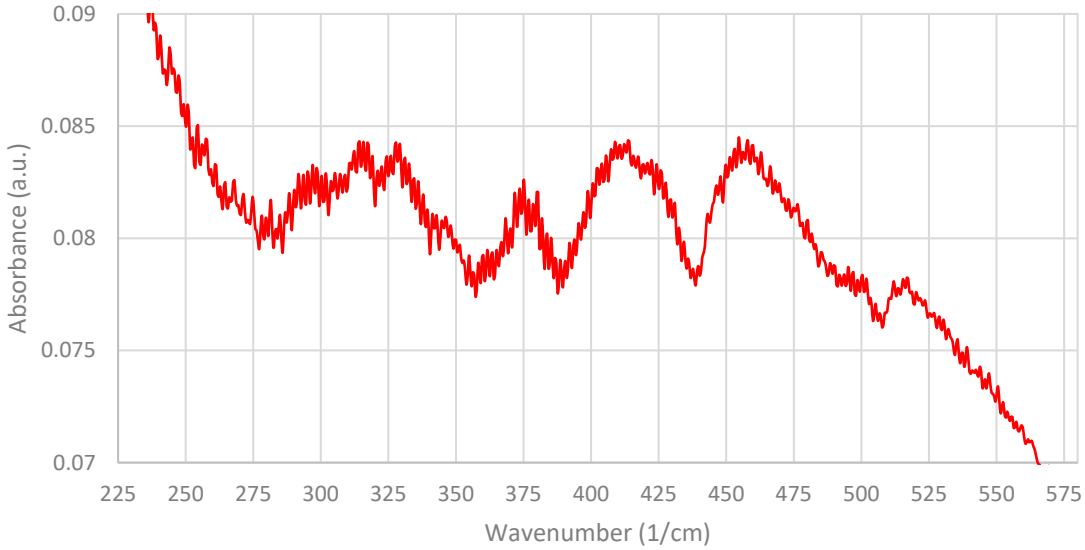

Figure 1-35: FIR-ATR spectrum of human haemoglobin (ground) analysed at the Australian Synchrotron (THz/FIR beamline) with SiBolo detector.

1.2.3.3 Solvents

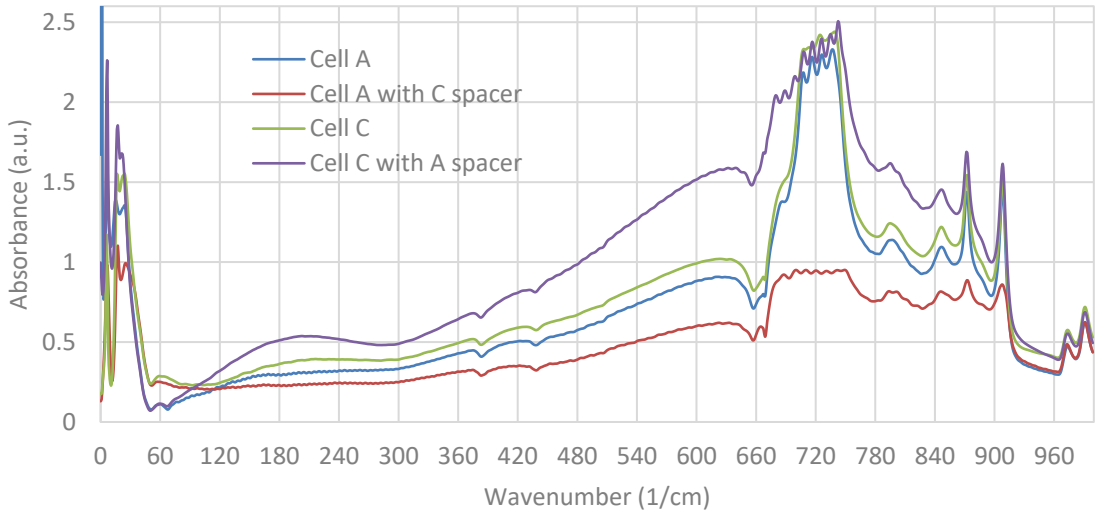

Figure 1-36: Absorbance overlayed spectra of water in DWLC's A and C with swapped 5 µm spacer, analysed at the Australian Synchrotron (FIR Beamline) with SiBolo detector. Amplitude 23300 for Cell A, 20300 for Cell C, 23500 for Cell A with C's spacer and 1600 for Cell C with Cell A's spacer.

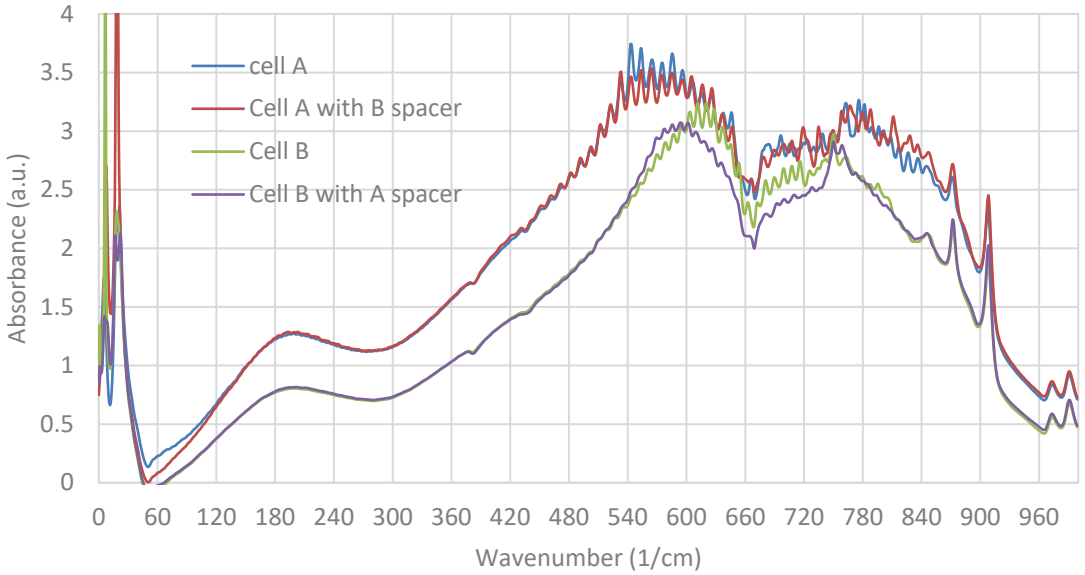

Figure 4-37: FIR overlayed spectra of water in DWLC's A and B with swapped 20 µm spacer, analysed at the Australian Synchrotron (THz/FIR Beamline) using a SiBolo detector with amplitudes of 3200 (Cell A), 7100 (Cell B), 3700 (Cell A with B's spacer) & 7100 (Cell B with Cell A's spacer).

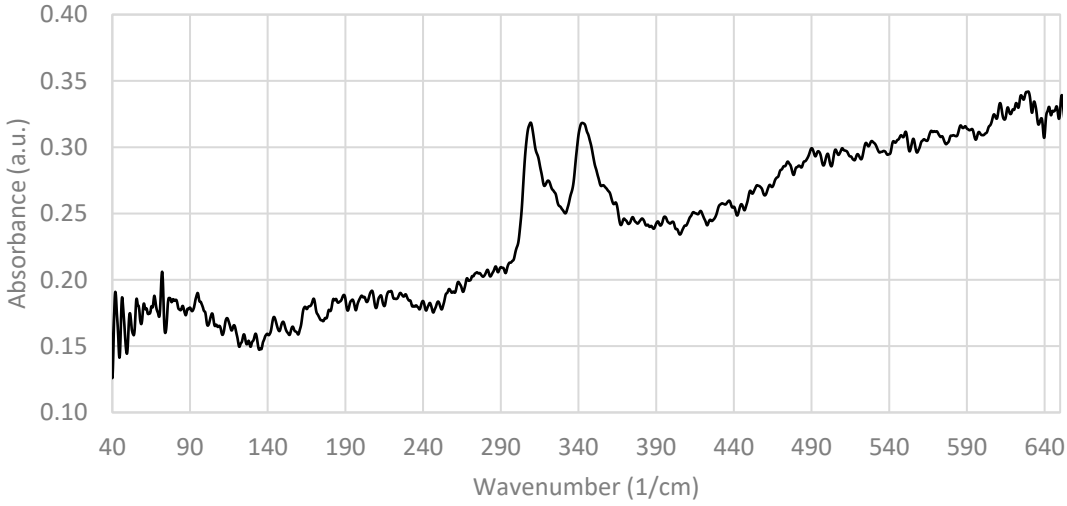

Figure 1-38: FIR spectrum of DMSO-d6 in DWLC A with a 10 µm spacer, analysed at the Australian Synchrotron (FIR Beamline) with SiBolo detector. Amplitude 6090.

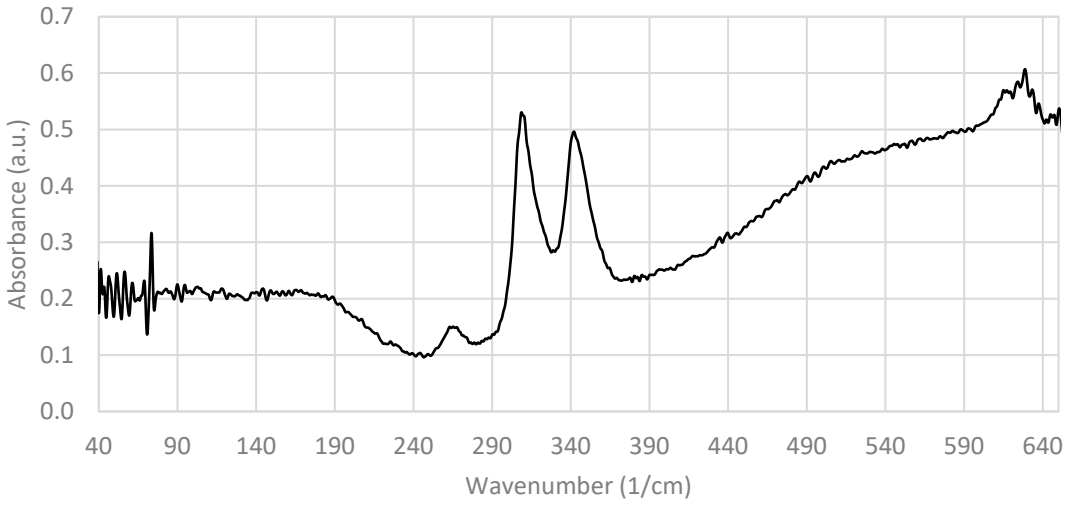

Figure 1-39: FIR spectrum of DMSO-d6 in DWLC C with a 10 µm spacer, analysed at the Australian Synchrotron (FIR Beamline) with SiBolo detector. Amplitude 5670.

DWLC A compared to C above: Cell C gives greater resolved and quality spectrum with less noise. This was duplicated to give the same results.

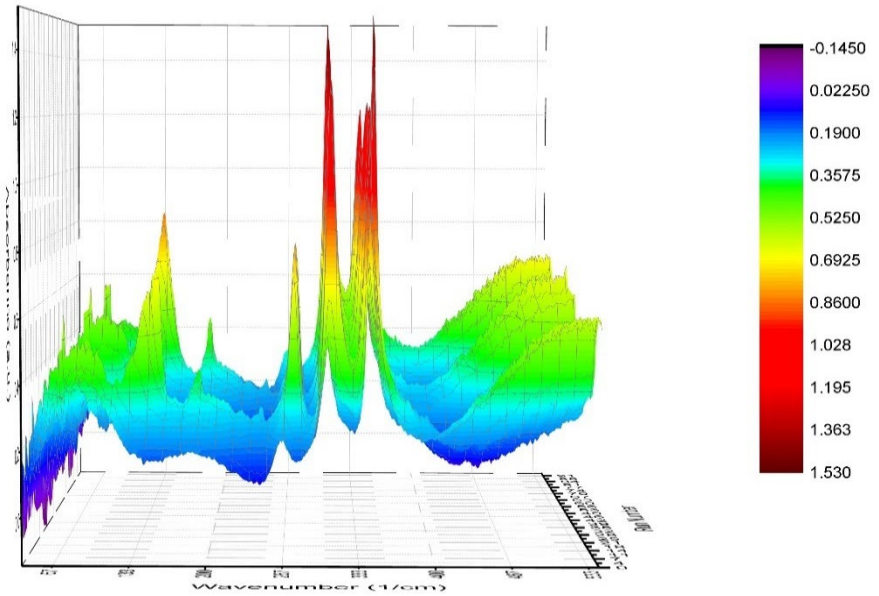

Figure 1-40: 3D Colourmap Surface Contour plot of FIR absorbance spectra for DMSO-d_6 in DWLC C using 20 µm spacer, when cooled (78 K) and heated (298 K) twice, analysed at the Australian Synchrotron (FIR Beamline) with SiBolo detector.

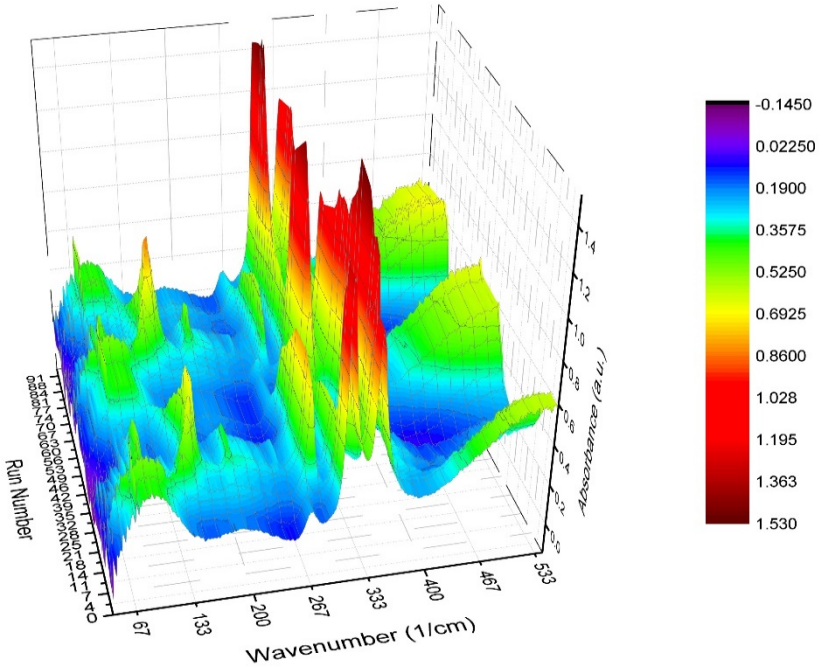

Figure 1-41: 3D Colourmap Surface Contour plot of FIR absorbance spectra for DMSO-d_6 in DWLC C using 20 µm spacer, when cooled (78 K) and heated (298 K) twice, analysed at the Australian Synchrotron (FIR Beamline) with SiBolo detector.

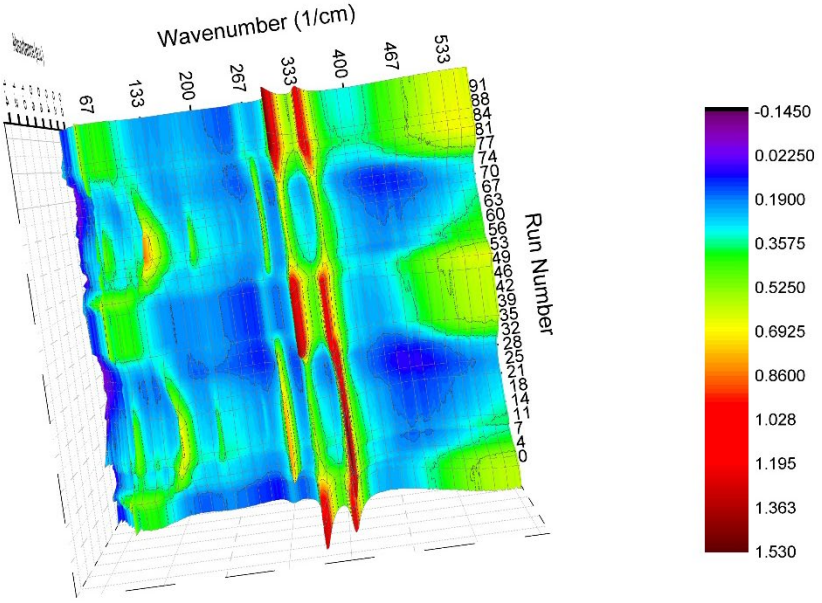

Figure 1-42: 3D Colourmap Surface Contour plot of FIR absorbance spectra for DMSO-d_6 in DWLC C using 20 µm spacer, when cooled (78 K) and heated (298 K) twice, analysed at the Australian Synchrotron (FIR Beamline) with SiBolo detector.

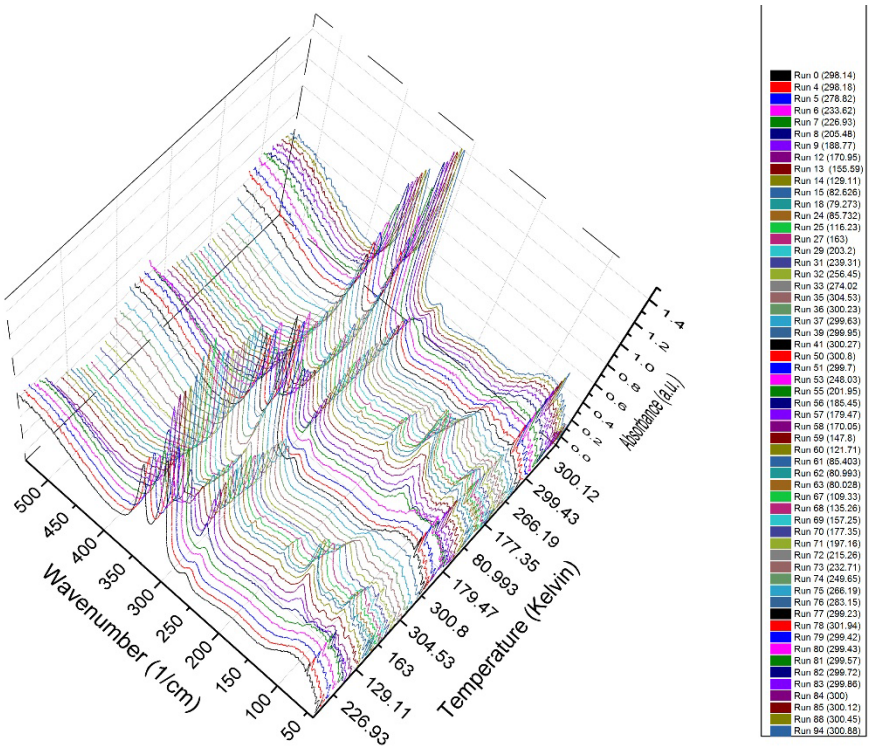

Figure 1-43: 3D Ribbon Plot of FIR absorbance spectra for DMSO-d_6 in DWLC C using 20 µm spacer, when cooled (78 K) and heated (298 K) twice, analysed at the Australian Synchrotron (FIR Beamline) with SiBolo detector.

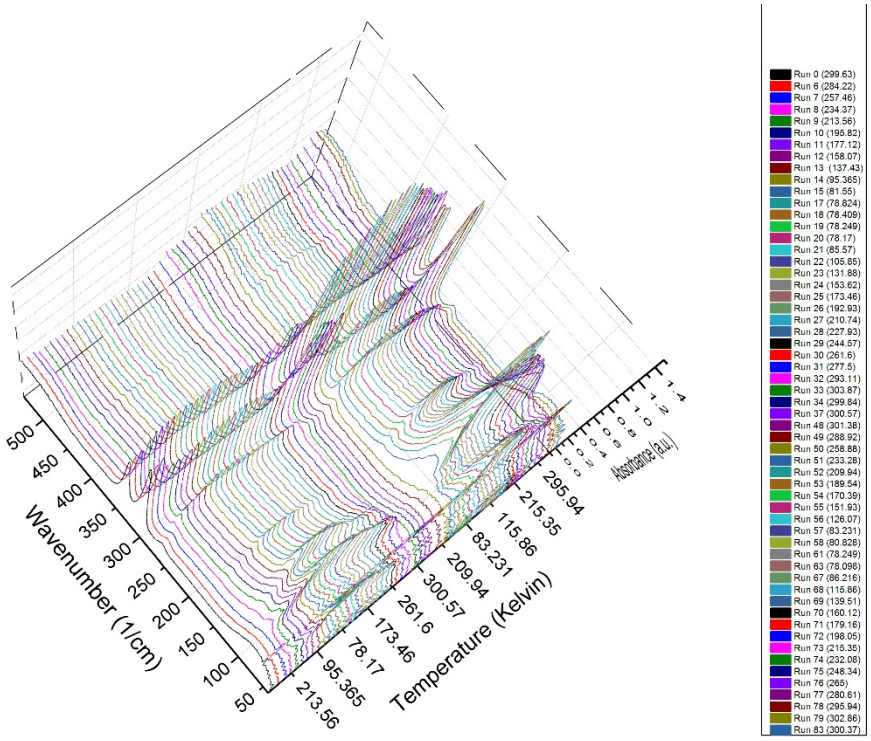

Figure 1-44: 3D Ribbon Plot of FIR absorbance spectra for duplicate DMSO-d_6 in DWLC C using 20 µm spacer, when cooled (78 K) and heated (298 K) twice, analysed at the Australian Synchrotron (FIR Beamline) with SiBolo detector.

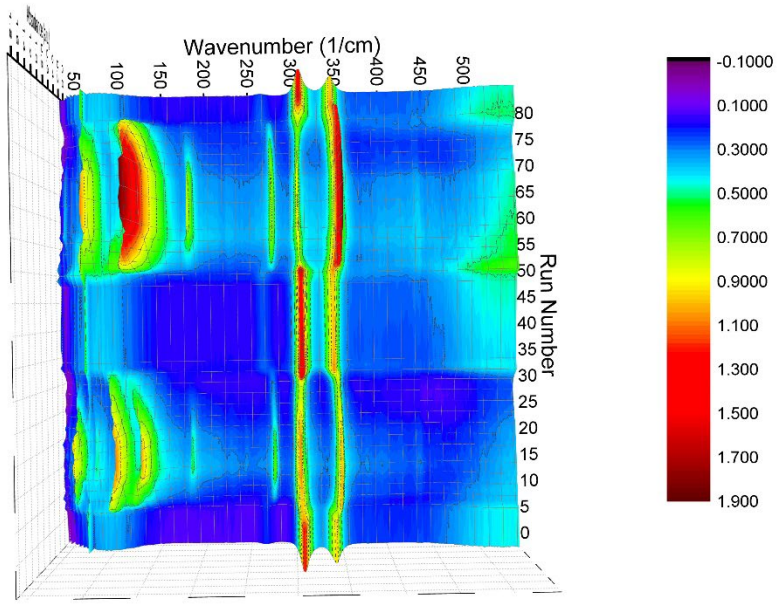

Figure 1-45: 3D Colourmap Surface Contour plot of FIR absorbance spectra for duplicate DMSO-d_6 in DWLC C using 20 µm spacer, when cooled (78 K) and heated (298 K) twice, analysed at the Australian Synchrotron (FIR Beamline) with SiBolo detector.

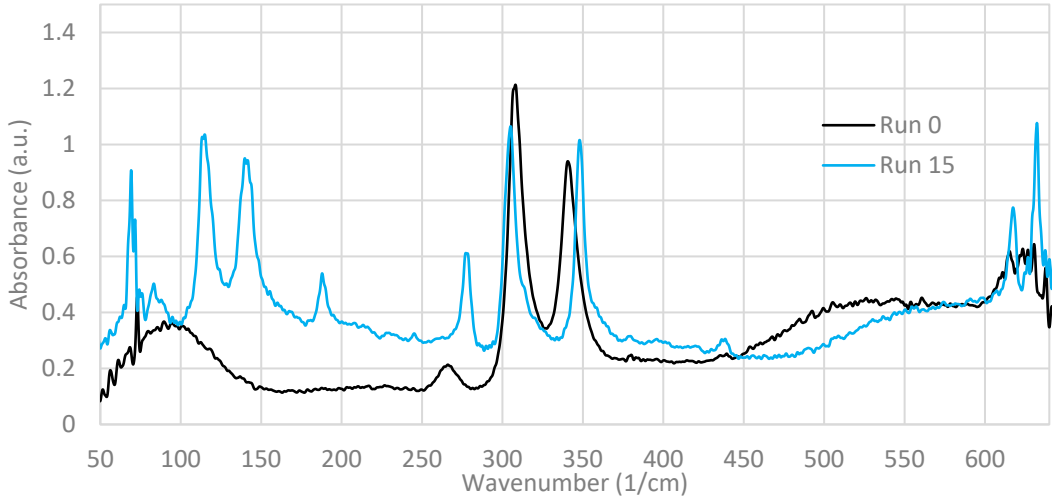

Figure 1-46: Overlayed FIR spectra of duplicate DMSO-d_6 in DWLC C with a 20 µm spacer when cooled (to 78 K) for the first time, analysed at the Australian Synchrotron (FIR Beamline) with SiBolo detector. Starting amplitude 5500.

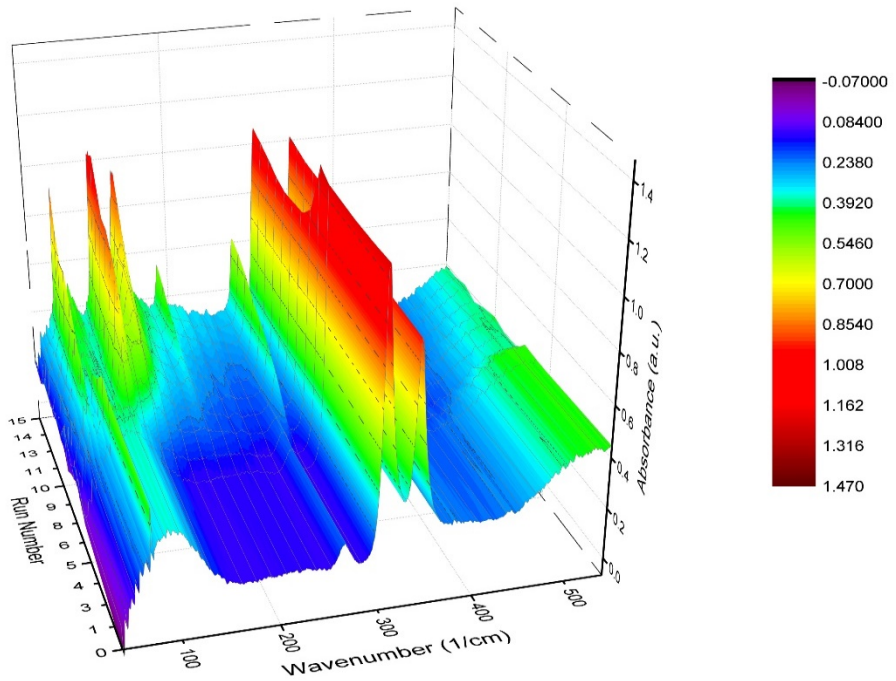

Figure 1-47: 3D Colourmap Surface Contour plot of FIR absorbance spectra for duplicate DMSO-d_6 in DWLC C using 20 µm spacer, when cooled (to 78 K) for the first time, analysed at the Australian Synchrotron (FIR Beamline) with SiBolo detector.

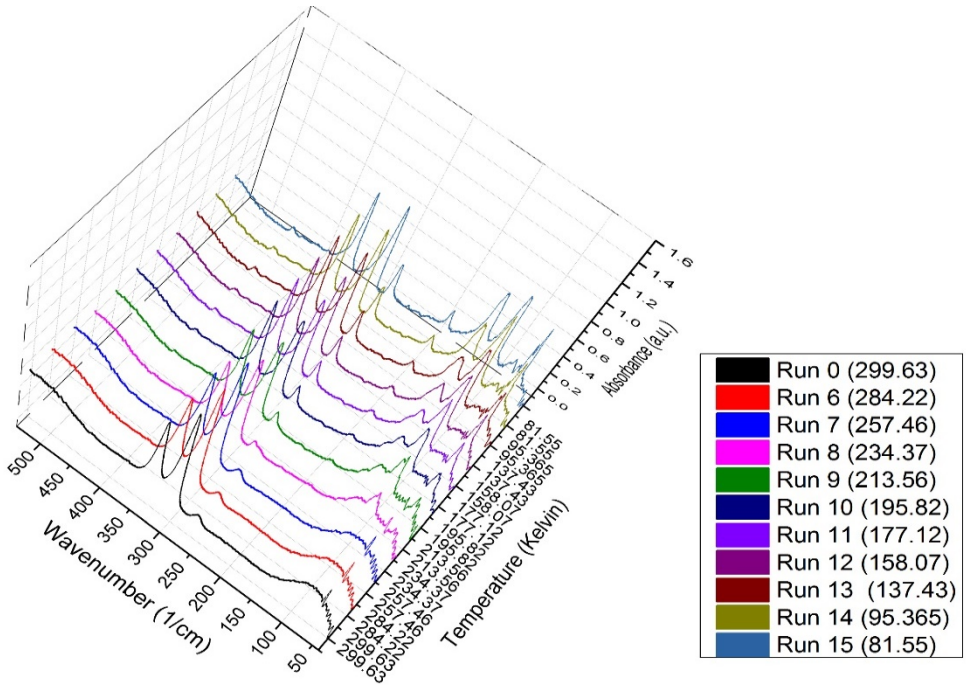

Figure 1-48: 3D Ribbon plot of FIR absorbance spectra for duplicate DMSO-d_6 in DWLC C using 20 µm spacer, when cooled (to 78 K) for the first time, analysed at the Australian Synchrotron (FIR Beamline) with SiBolo detector.

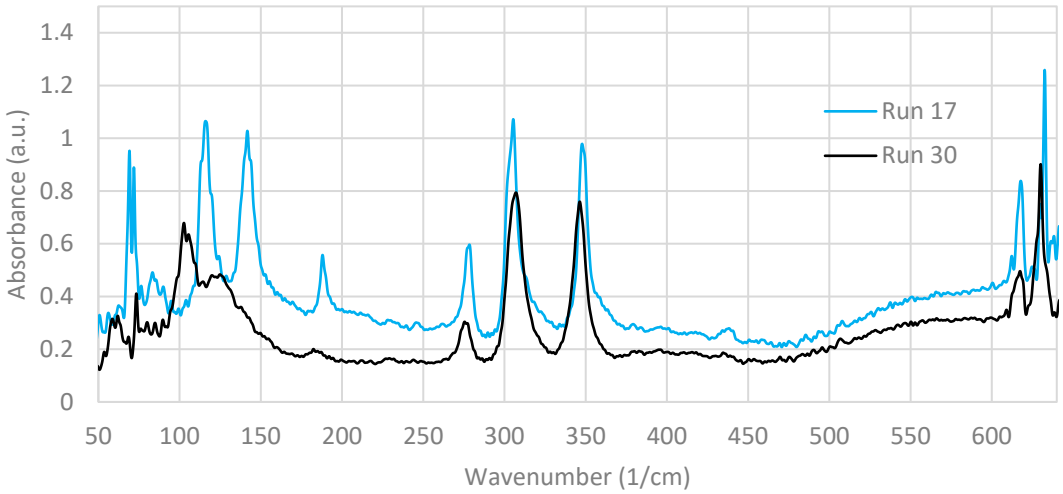

Figure 1-49: Overlayed FIR spectra of duplicate DMSO-d6 in DWLC C with a 20 µm spacer when heated (to 298 K) for the first time, analysed at the Australian Synchrotron (FIR Beamline) with SiBolo detector.

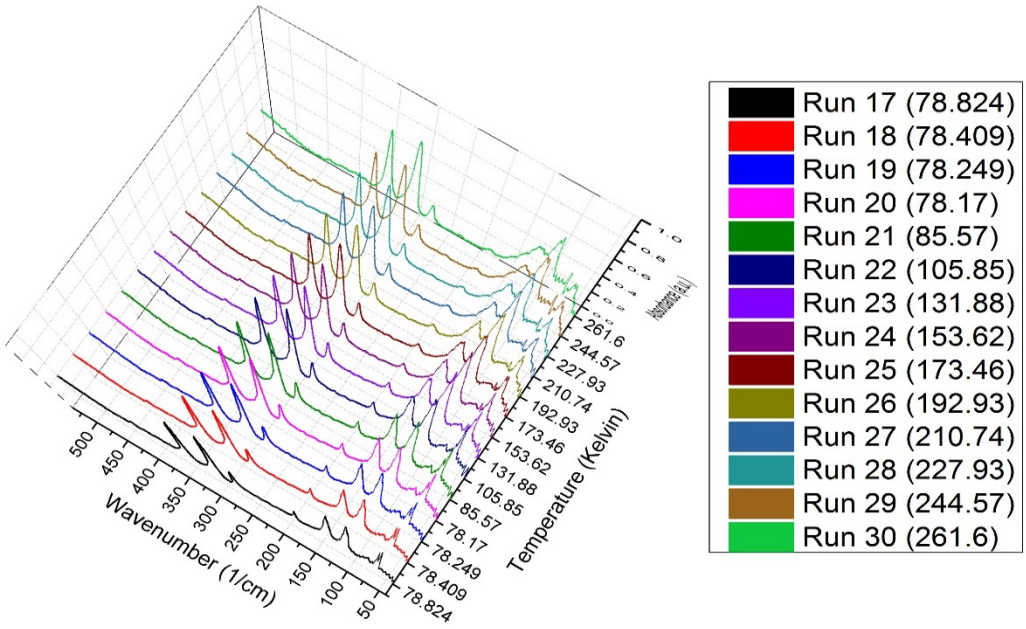

Figure 1-50: 3D Ribbon plot of FIR absorbance spectra for duplicate DMSO-d_6 in DWLC C using 20 µm spacer, when heated (to 298 K) for the first time, analysed at the Australian Synchrotron (FIR Beamline) with SiBolo detector.

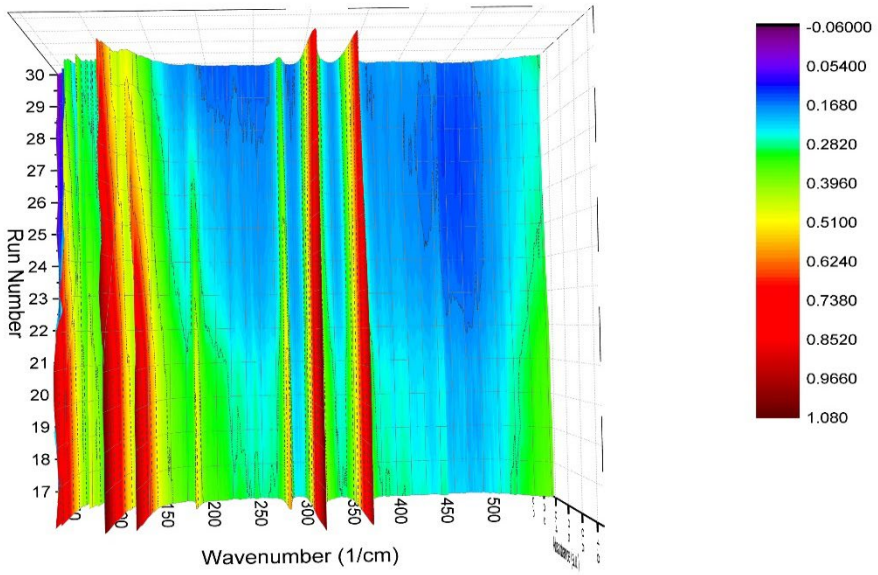

Figure 1-51: 3D Colourmap Surface Contour plot of FIR absorbance spectra for duplicate DMSO-d6 in DWLC C using 20 µm spacer, when cooled (to 78 K) for the second time, analysed at the Australian Synchrotron (FIR Beamline) with SiBolo detector.

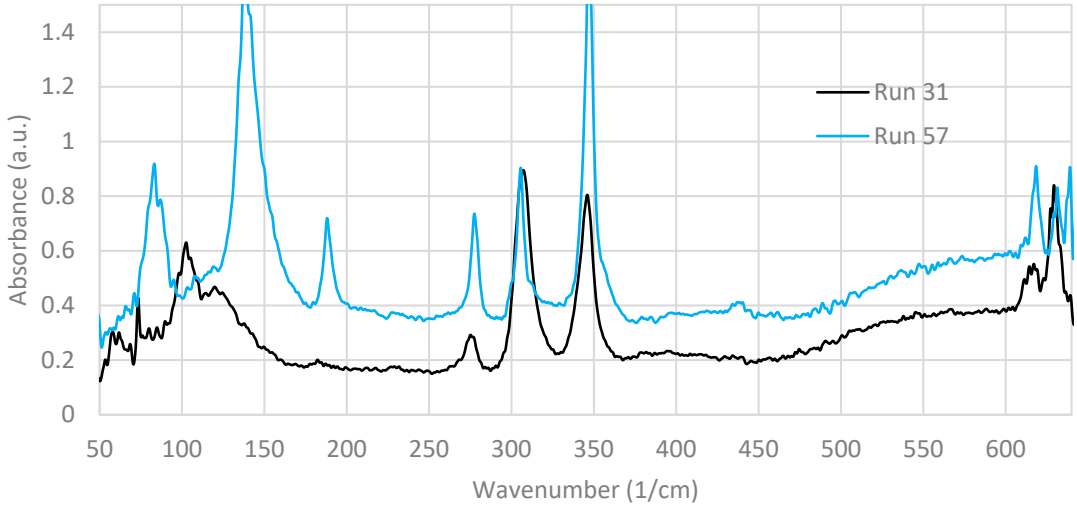

Figure 1-52: Overlayed FIR spectra of duplicate DMSO-d6 in DWLC C with a 20 µm spacer when cooled (to 78 K) for the second time, analysed at the Australian Synchrotron (FIR Beamline) with SiBolo detector.

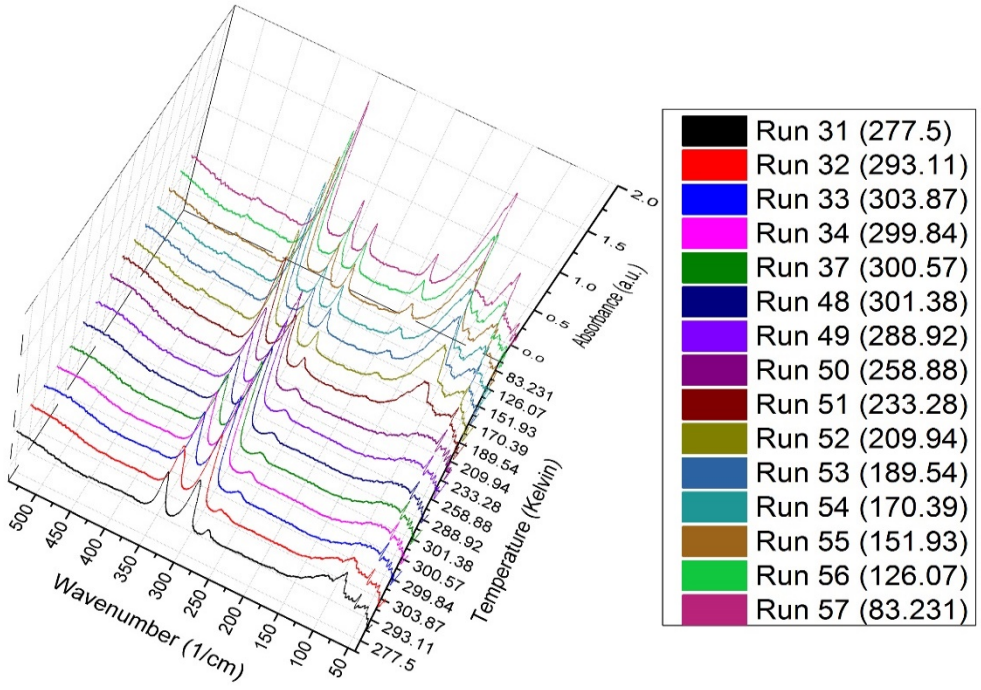

Figure 1-53: 3D Ribbon plot of FIR absorbance spectra for duplicate DMSO-d_6 in DWLC C using 20 µm spacer, when cooled (to 78 K) for the second time, analysed at the Australian Synchrotron (FIR Beamline) with SiBolo detector.

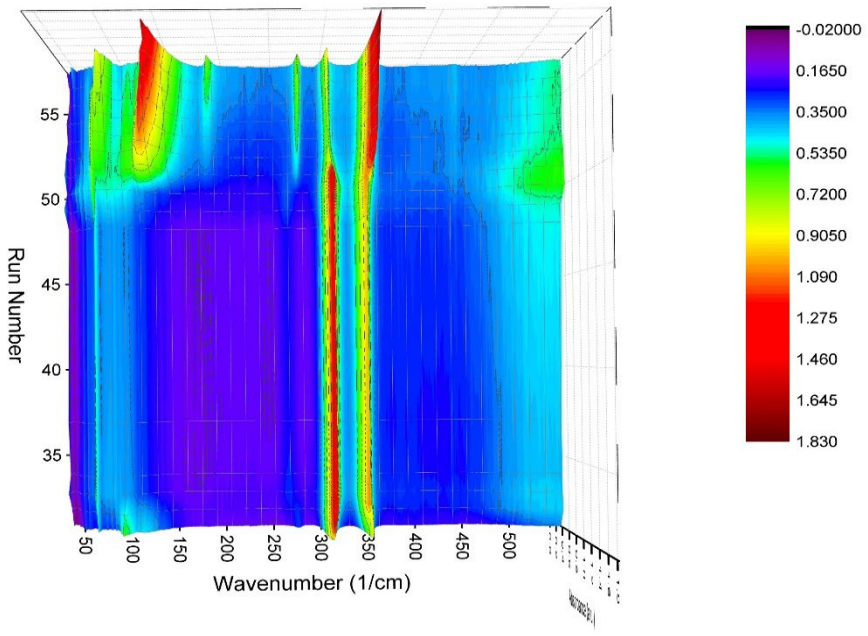

Figure 1-54: 3D Colourmap Surface Contour plot of FIR absorbance spectra for duplicate DMSO-d6 in DWLC C using 20 µm spacer, when cooled (to 78 K) for the second time, analysed at the Australian Synchrotron (FIR Beamline) with SiBolo detector.

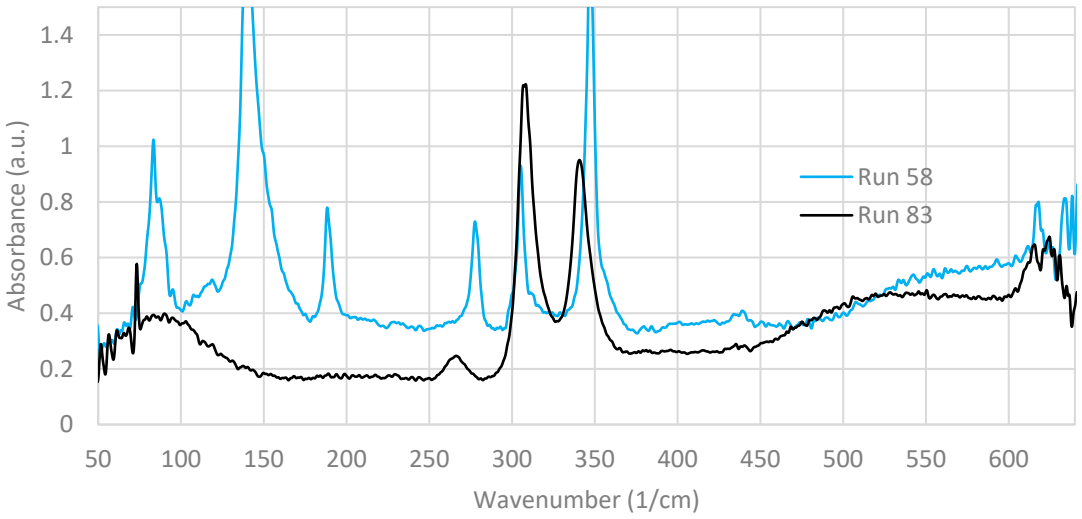

Figure 1-55: Overlayed FIR spectra of duplicate DMSO-d6 in DWLC C with a 20 µm spacer when heated (to 298 K) for the second time, analysed at the Australian Synchrotron (FIR Beamline) with SiBolo detector.

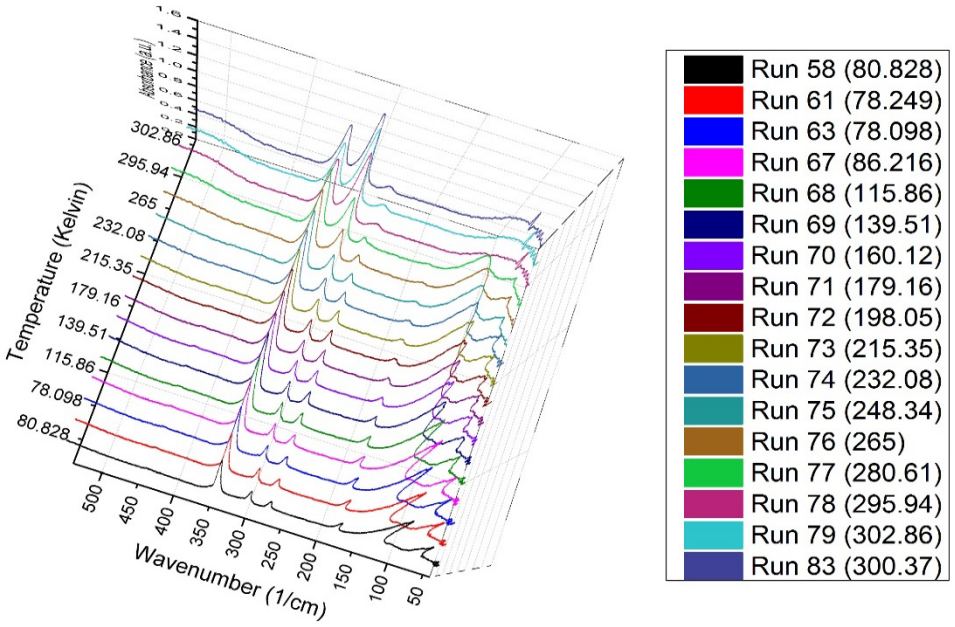

Figure 1-56: 3D Ribbon plot of FIR absorbance spectra for duplicate DMSO-d6 in DWLC C using 20 µm spacer, when heated (to 298 K) for the second time, analysed at the Australian Synchrotron (FIR Beamline) with SiBolo detector.

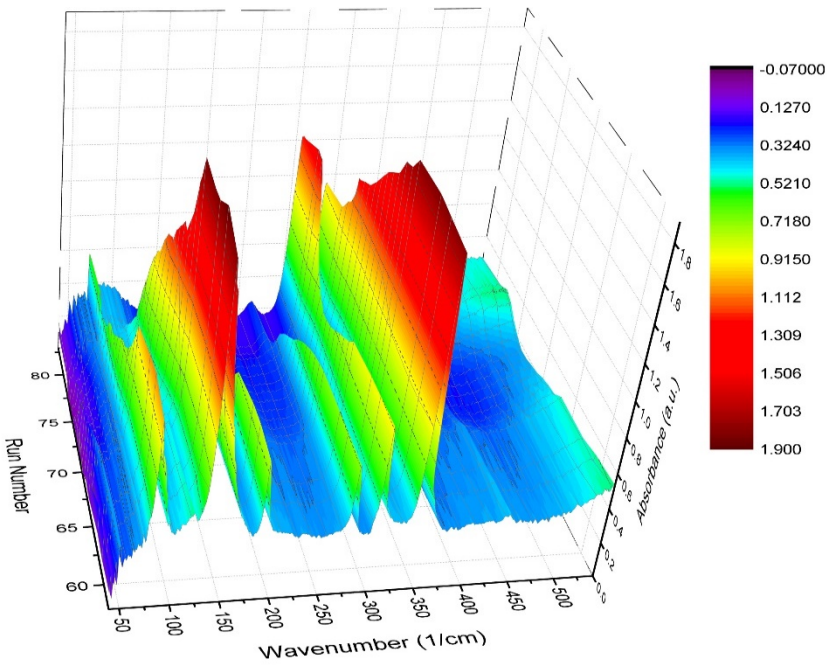

Figure 1-57: 3D Colourmap Surface Contour plot of FIR absorbance spectra for duplicate DMSO-d6 in DWLC C using 20 µm spacer, when heated (to 298 K) for the second time, analysed at the Australian Synchrotron (FIR Beamline) with SiBolo detector.

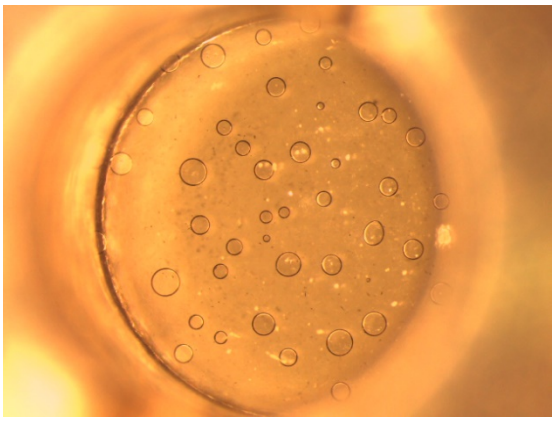

Figure 1-58: Image of duplicate assembled DWLC C using 20 µm spacer containing DMSO-d_6, after cryogenic analysis (two cooling cycles).

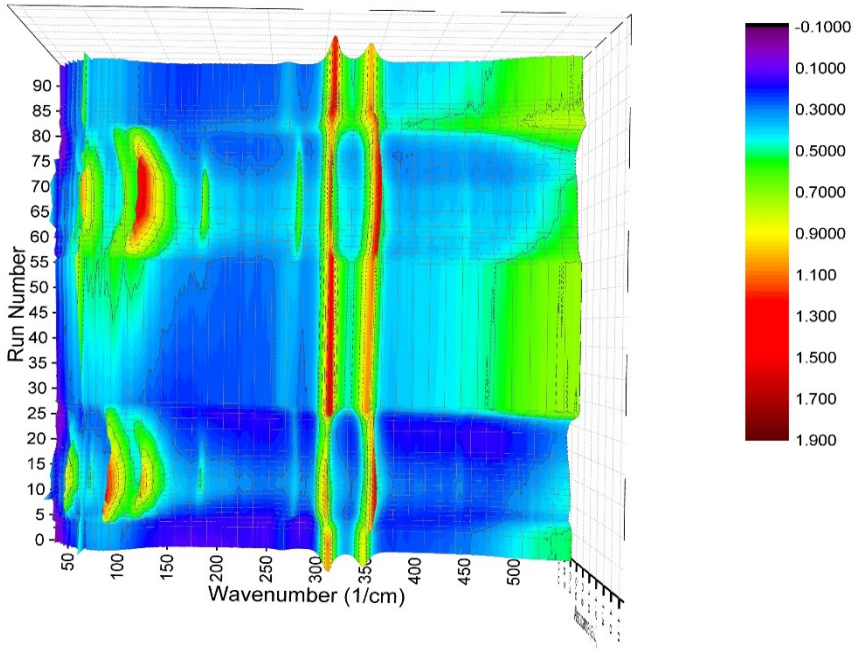

Figure 1-59: 3D Colourmap Surface Contour plot of FIR absorbance spectra for triplicate DMSO-d6 in DWLC C using 20 µm spacer, when cooled (78 K) and heated (298 K) twice, analysed at the Australian Synchrotron (FIR Beamline) with SiBolo detector.

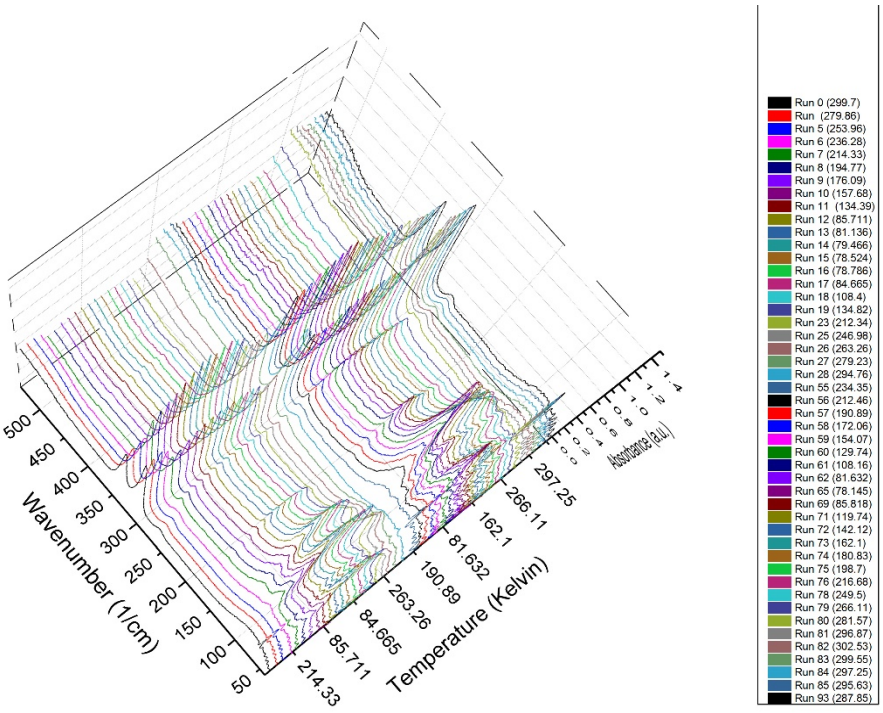

Figure 1-60: 3D Ribbon Plot of FIR absorbance spectra for triplicate DMSO-d6 in DWLC C using 20 µm spacer, when cooled (78 K) and heated (298 K) twice, analysed at the Australian Synchrotron (FIR Beamline) with SiBolo detector.

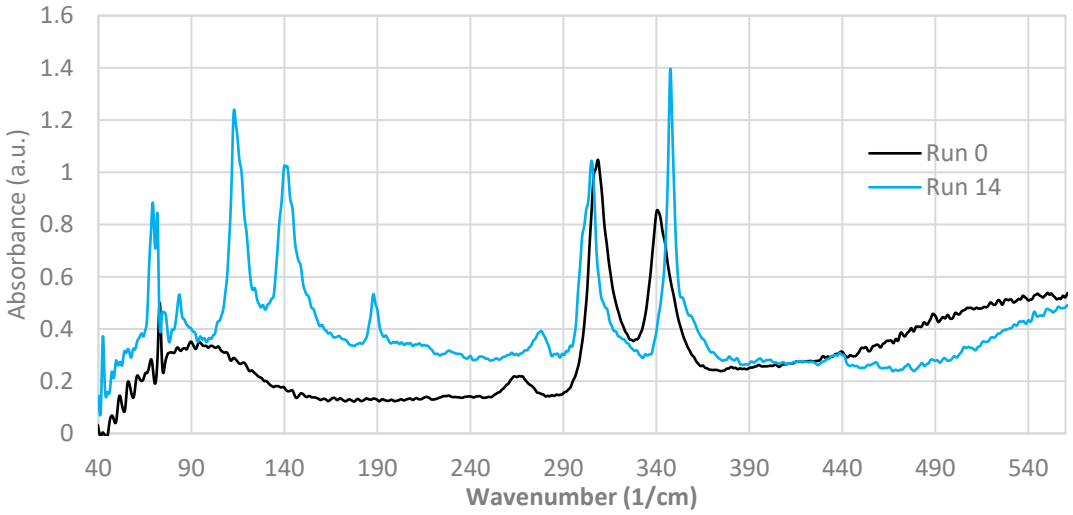

Figure 1-61: Overlayed FIR spectra of triplicate DMSO-d6 in DWLC C with a 20 µm spacer when cooled (to 78 K) for the first time, analysed at the Australian Synchrotron (FIR Beamline) with SiBolo detector. Starting amplitude 5400.

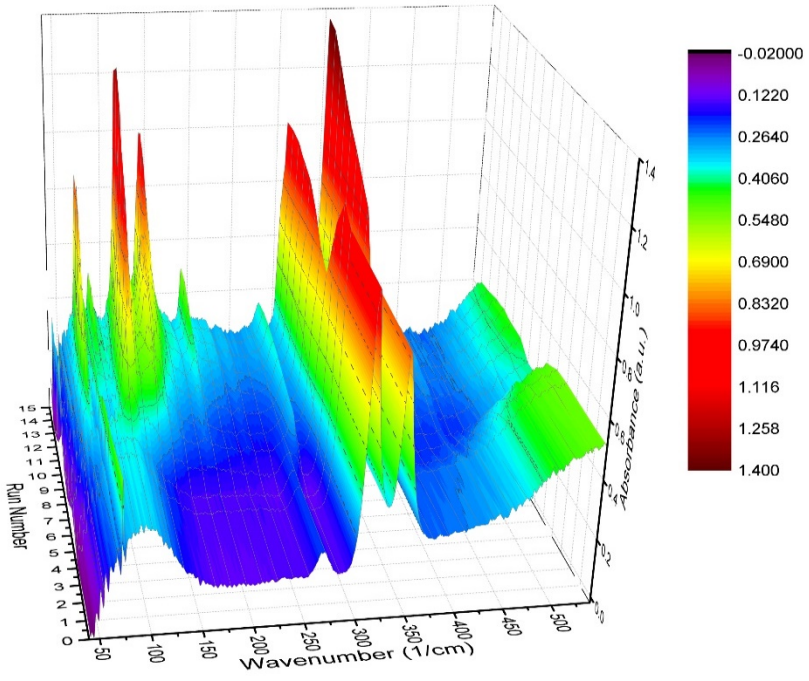

Figure 1-62: 3D Colourmap Surface Contour plot of FIR absorbance spectra for triplicate DMSO-d6 in DWLC C using 20 µm spacer, when cooled (to 78 K) for the first time, analysed at the Australian Synchrotron (FIR Beamline) with SiBolo detector.

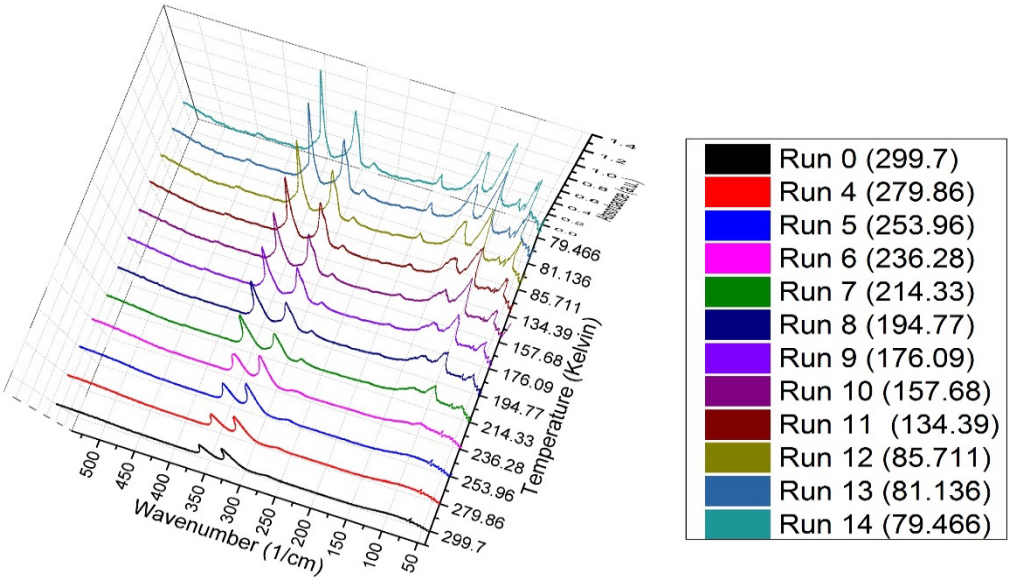

Figure 1-63: 3D Ribbon plot of FIR absorbance spectra for triplicate DMSO-d6 in DWLC C using 20 µm spacer, when cooled (to 788 K) for the first time, analysed at the Australian Synchrotron (FIR Beamline) with SiBolo detector.

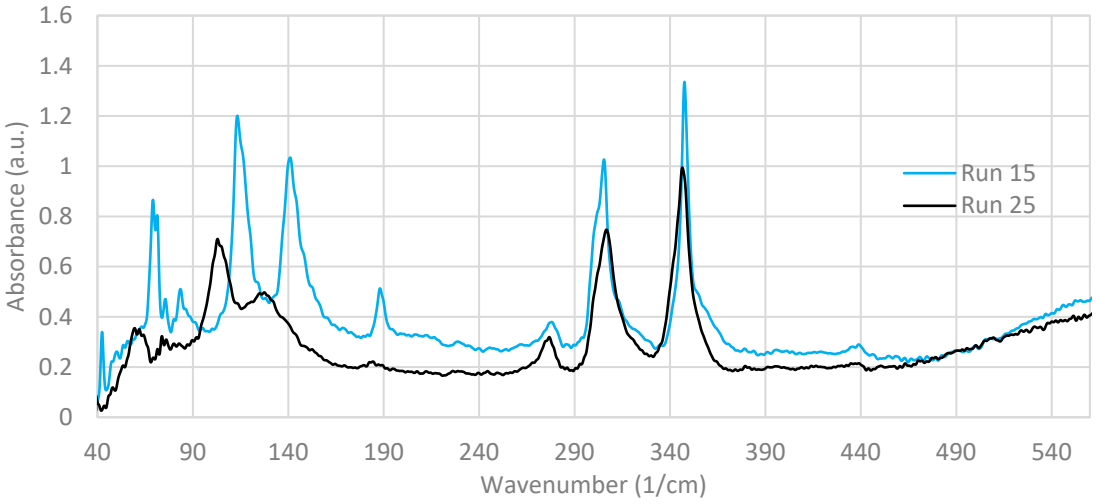

Figure 1-64: Overlayed FIR spectra of triplicate DMSO-d6 in DWLC C with a 20 µm spacer when heated (to 298 K) for the first time, analysed at the Australian Synchrotron (FIR Beamline) with SiBolo detector.

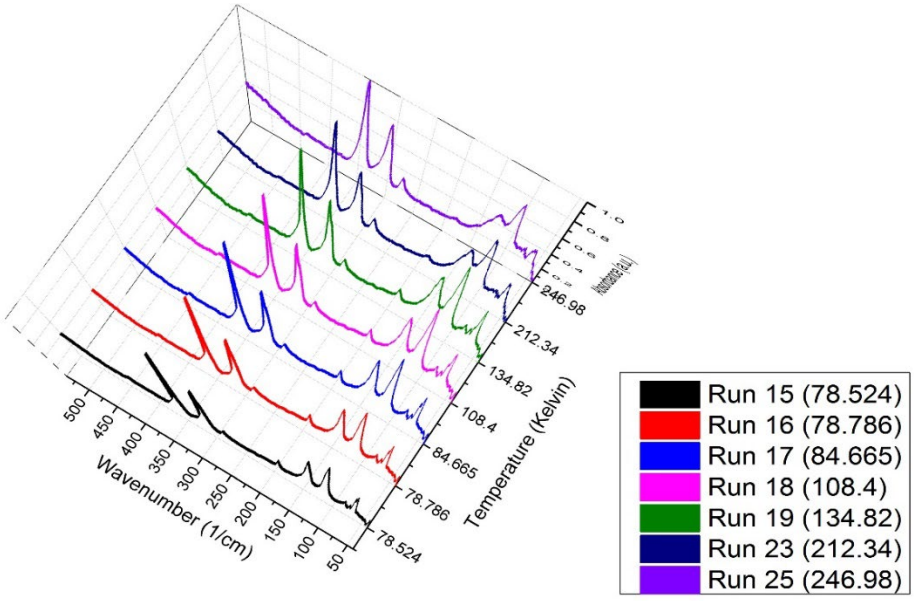

Figure 1-65: 3D Ribbon plot of FIR absorbance spectra for triplicate DMSO-d6 in DWLC C using 20 µm spacer, when heated (to 298 K) for the first time, analysed at the Australian Synchrotron (FIR Beamline) with SiBolo detector.

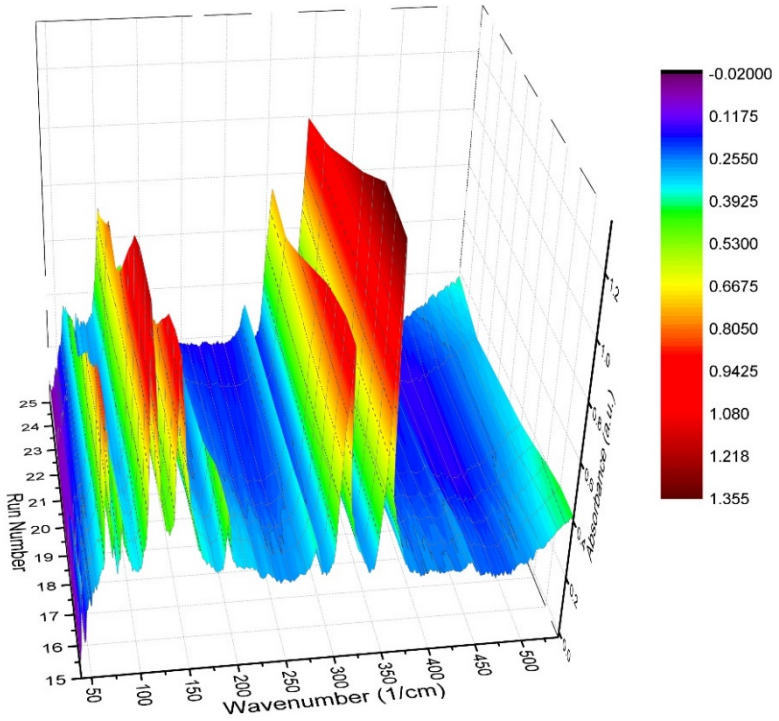

Figure 1-66: 3D Colourmap Surface Contour plot of FIR absorbance spectra for triplicate DMSO-d6 in DWLC C using 20 µm spacer, when heated (to 298 K) for the first time, analysed at the Australian Synchrotron (FIR Beamline) with SiBolo detector.

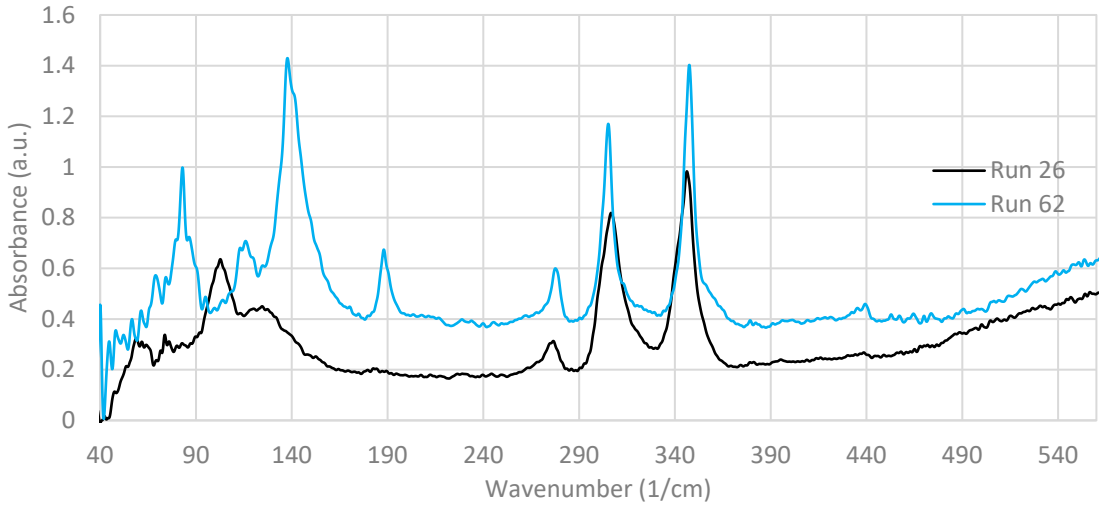

Figure 1-67: Overlayed FIR spectra of triplicate DMSO-d6 in DWLC C with a 20 µm spacer when cooled (to 78 K) for the second time, analysed at the Australian Synchrotron (FIR Beamline) with SiBolo detector.

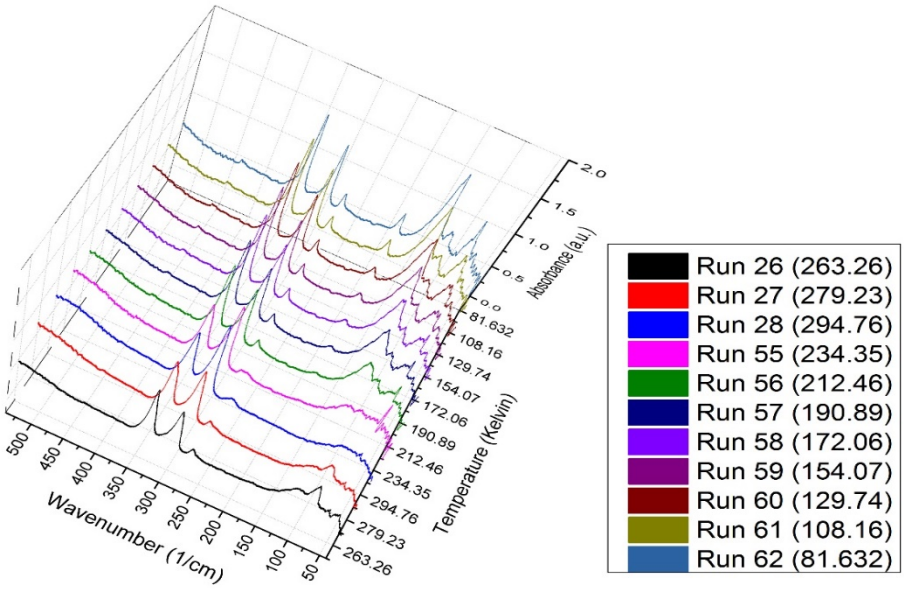

Figure 1-68: 3D Ribbon plot of FIR absorbance spectra for triplicate DMSO-d6 in DWLC C using 20 µm spacer, when cooled (to 78 K) for the second time, analysed at the Australian Synchrotron (FIR Beamline) with SiBolo detector.

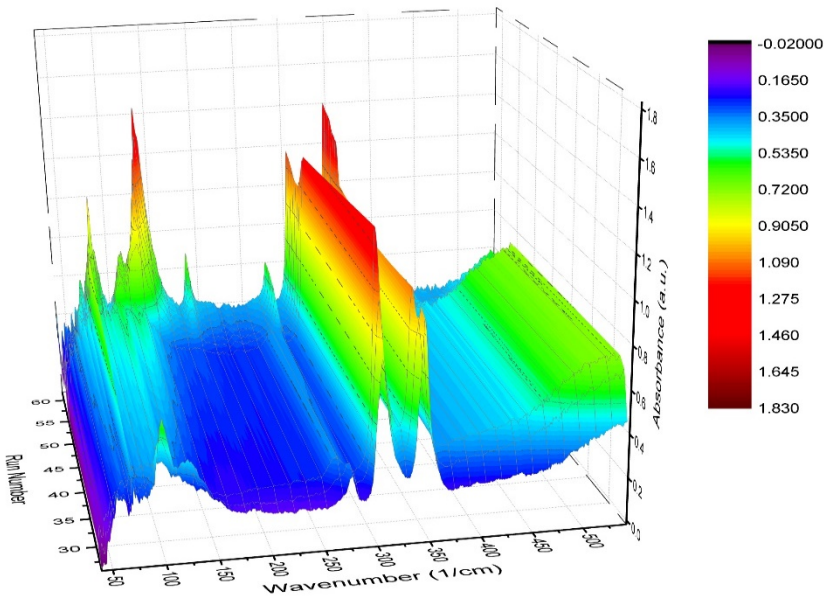

Figure 1-69: 3D Colourmap Surface Contour plot of FIR absorbance spectra for triplicate DMSO-d6 in DWLC C using 20 µm spacer, when cooled (to 78 K) for the second ti me, analysed at the Australian Synchrotron (FIR Beamline) with SiBolo detector.

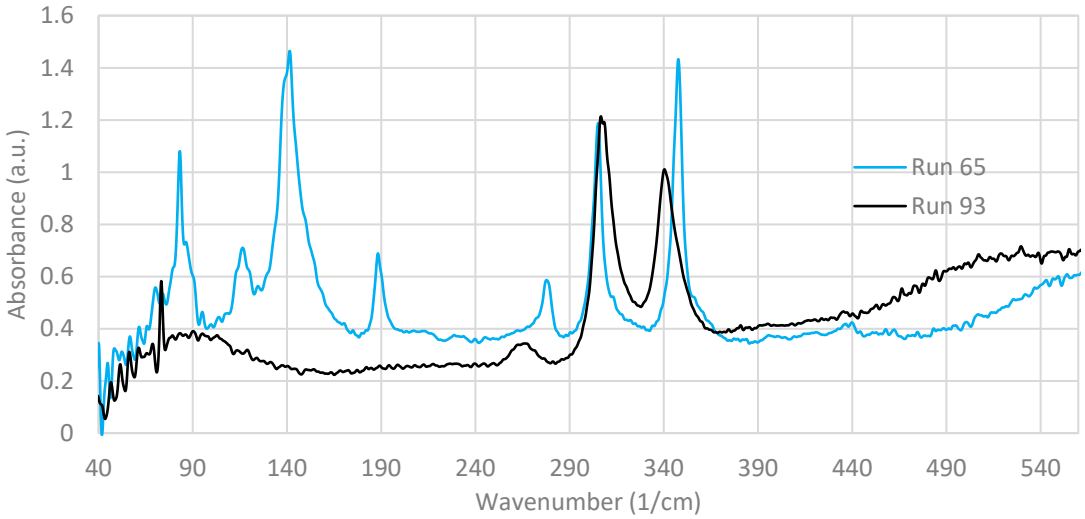

Figure 1-70: Overlayed FIR spectra of triplicate DMSO-d6 in DWLC C with a 20 µm spacer when heated (to 298 K) for the second time, analysed at the Australian Synchrotron (FIR Beamline) with SiBolo detector.

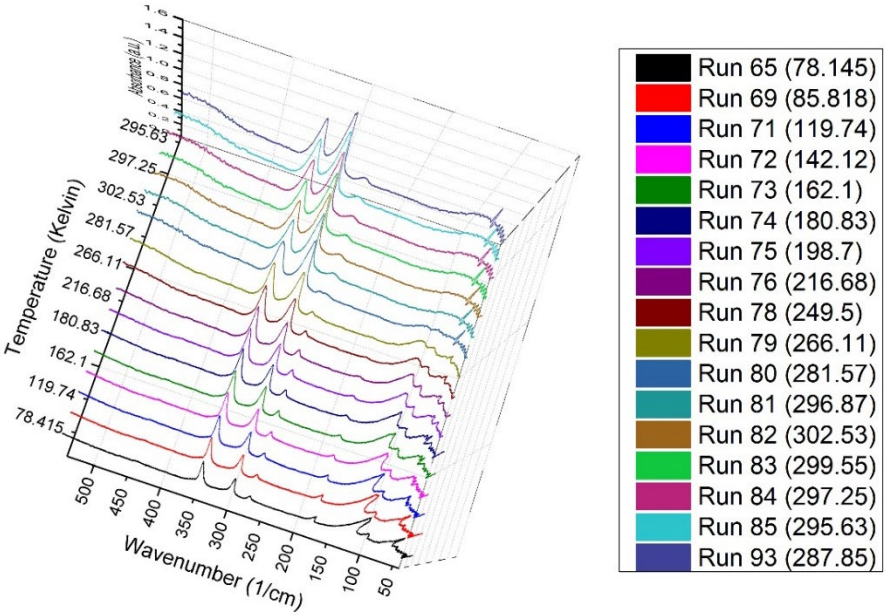

Figure 1-71: 3D Ribbon plot of FIR absorbance spectra for triplicate DMSO-d6 in DWLC C using 20 µm spacer, when heated (to 298 K) for the second time, analysed at the Australian Synchrotron (FIR Beamline) with SiBolo detector.

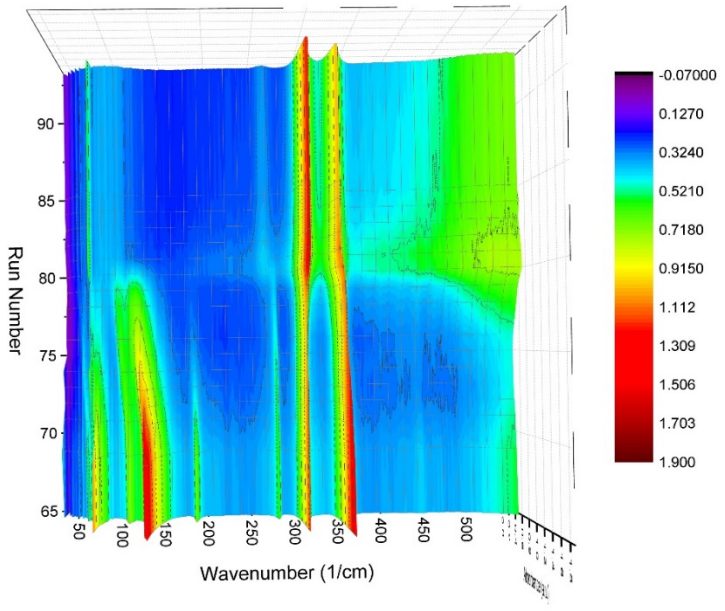

Figure 1-72: 3D Colourmap Surface Contour plot of FIR absorbance spectra for triplicate DMSO-d6 in DWLC C using 20 µm spacer, when heated (to 298 K) for the second time, analysed at the Australian Synchrotron (FIR Beamline) with SiBolo detector.

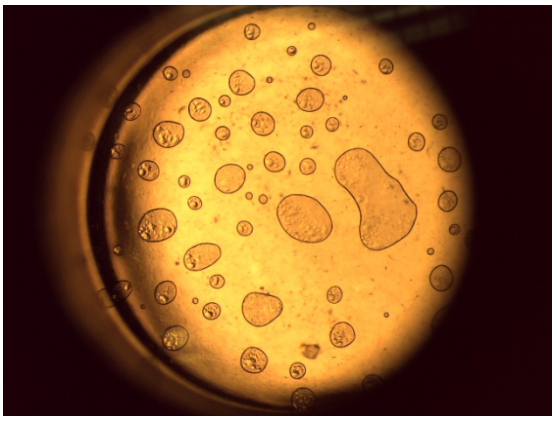

Figure 1-73: Image of triplicate assembled DWLC C using 20 µm spacer containing DMSO-d6, after cryogenic analysis (two cooling cycles).

1.2.3.4 Biliverdin

A pure biliverdin pellet was sandwiched between two sheets of polyethylene bag from the laboratory. This was analysed and provided the spectrum below showing oscillations between 50-650 wavenumbers, which is from bag rather than biliverdin. Similar results were received by the PE bag blank.

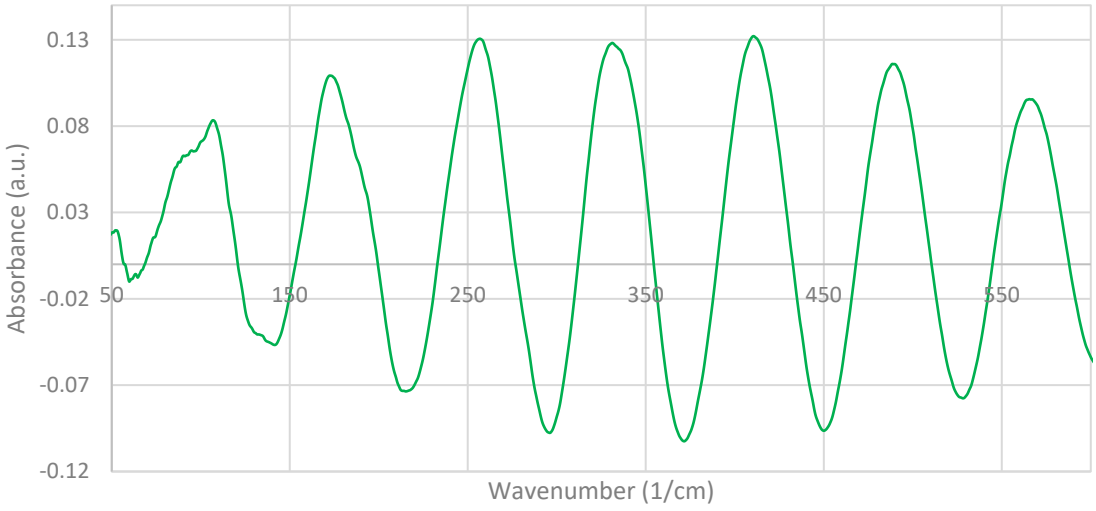

Figure 4-74: FIR spectra of pressed biliverdin pellet (approx. 1 mg) in between two sheets of PE bag, analysed on the THz/FIR beamline at the Australian Synchrotron using a SiBolo detector with amplitude of 18000.

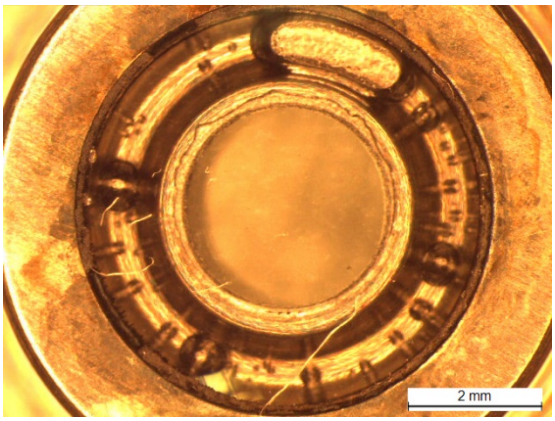

Figure 1-75: Image of dismantled Cell A's diamond window (flange side of cell) with biliverdin contamination in glue used to hold window.

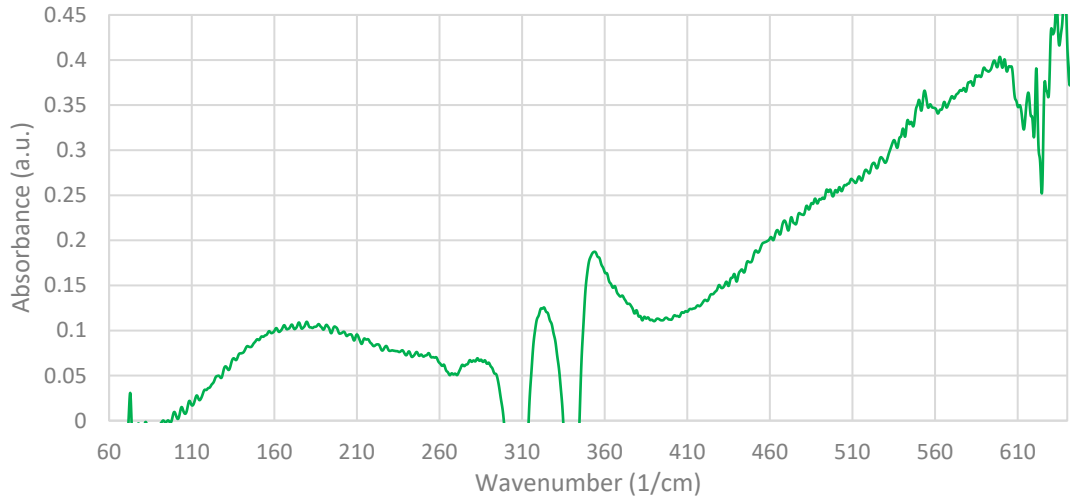

Figure 1-76: FIR absorbance spectra of duplicate biliverdin in DMSO-d_6 (0.25 mg/µL) in DWLC C using 20 µm spacer, analysed at the Australian Synchrotron (FIR Beamline) with SiBolo detector. Amplitude 5140.

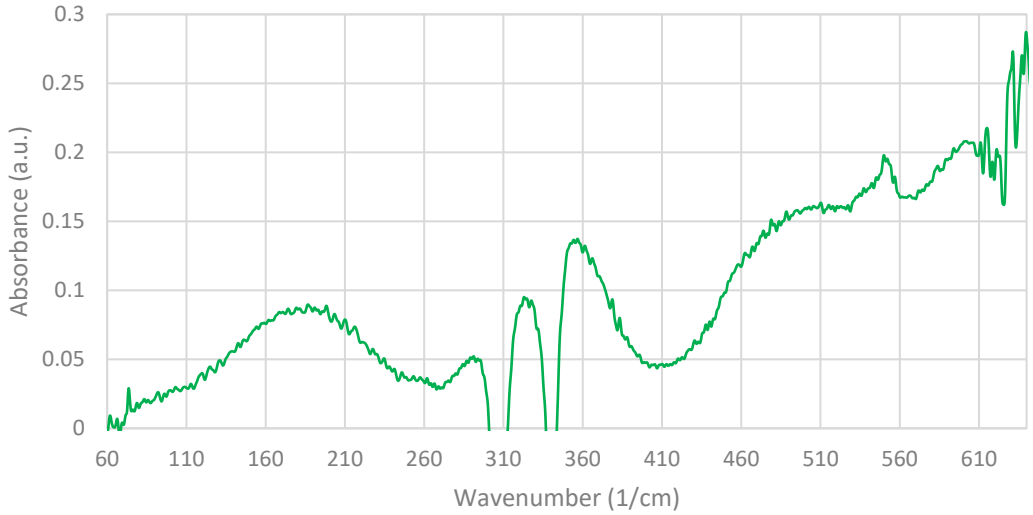

Figure 1-77: FIR absorbance spectra of duplicate biliverdin in DMSO-d_6 (0.4 mg/µL) in DWLC C using 20 µm spacer, analysed at the Australian Synchrotron (FIR Beamline) with SiBolo detector. Amplitude 5360.

1.2.3.5 Bilirubin

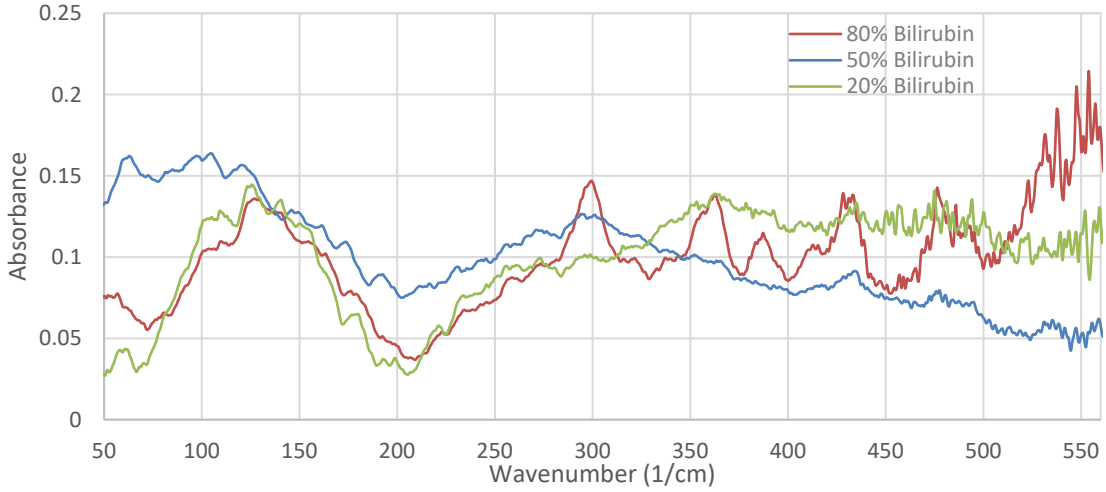

Figure 1-78: FIR overlayed spectra of pressed bilirubin in PE pellets (weights approx. 1 mg) at different concentrations, normalised between 50 and 500 wavenumbers, analysed on the THz/FIR beamline at the Australian Synchrotron using the SiBolo detector with amplitudes of 1210 (80% bilirubin), 4100 (50% bilirubin) & 840 (20% bilirubin).

Above spectra overlay is of very rough dilutions and during analysis signal loss was experienced.

Figure 1-79: Overlayed absorbance spectra of incubated (40 degrees water bath) bilirubin in DMSO-d6 (4 mg in 25 µL DMSO-d6) in DWLC C using 20 µm spacer, analysed overnight at the Australian Synchrotron (FIR Beamline) with SiBolo detector. Amplitude 5380.

Pressure at beginning of analysis in duplicate was 3×10^{-5} and 5.7×10^{-6} just before analysis was completed.

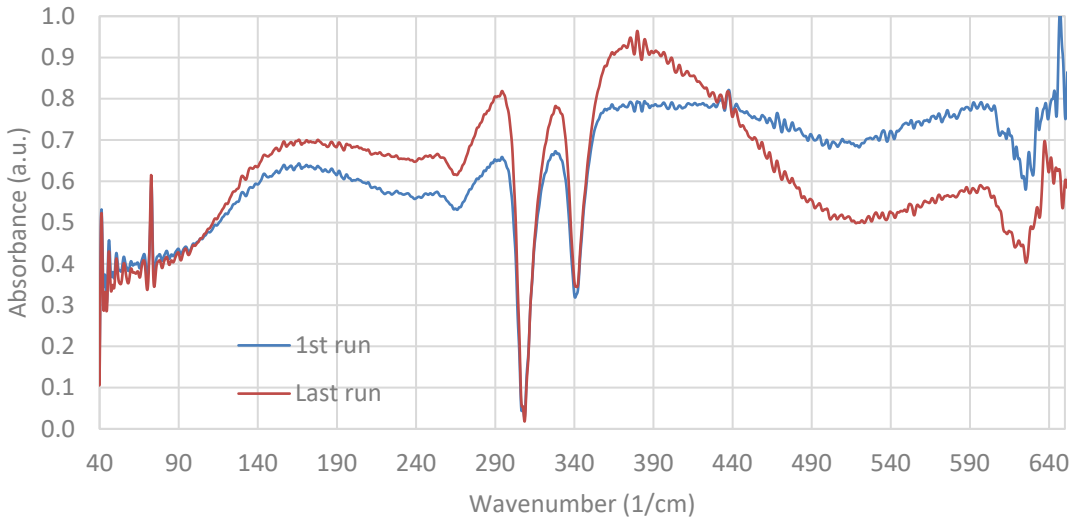

Figure 1-80: Overlayed absorbance spectra of incubated (40 degrees water bath) bilirubin in DMSO-d6 (4 mg in 25 µL DMSO-d6) in DWLC C using 20 µm spacer, analysed overnight at the Australian Synchrotron (FIR Beamline) with SiBolo detector. Amplitude 6300.

Pressure at beginning of analysis in triplicate was 9.7×10^{-5} and 1.8×10^{-5} just before analysis was completed.

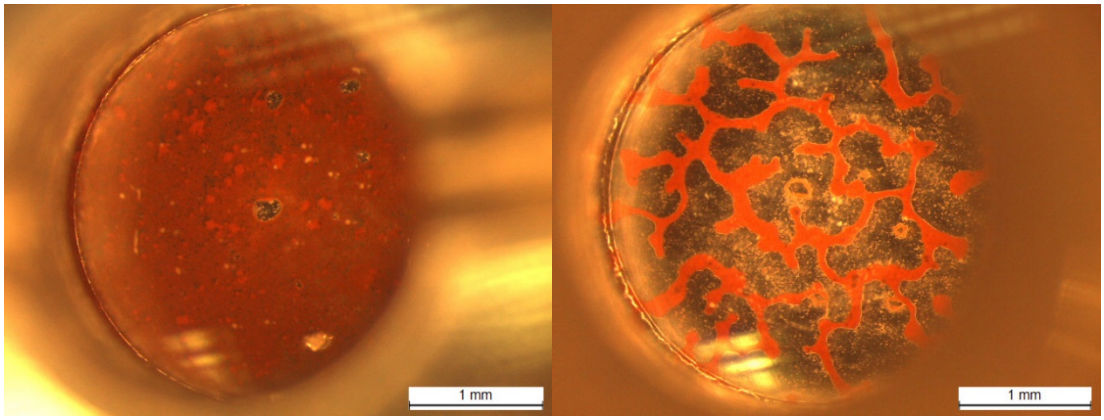

Figure 1-81: Images of duplicate incubated (40 degrees water bath) bilirubin sample in DMSO-d6 (4 mg in 25 µL DMSO-d6) in DWLC C using 20 µm spacer, before analysis (left) and after analysis (right) at the Australian Synchrotron (FIR Beamline) with SiBolo detector.

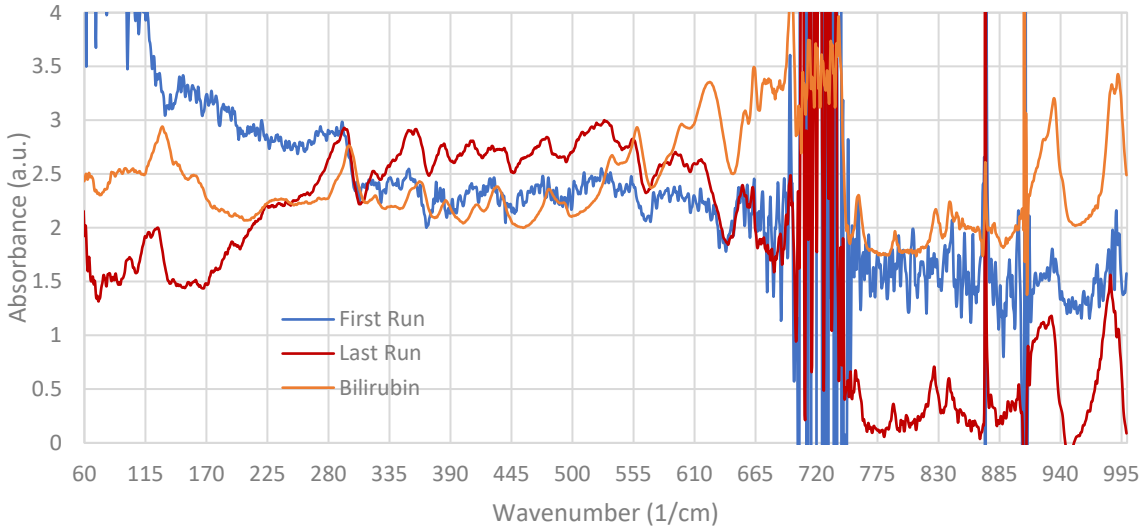

Figure 1-82: FIR-ATR overlayed spectra of bilirubin in defibrinated Sheep's blood (7.1×10^{-2} mg/µL) as it dries overnight, analysed at the Australian Synchrotron with SiBolo detector.

1.2.3.6 Bilirubin Conjugate

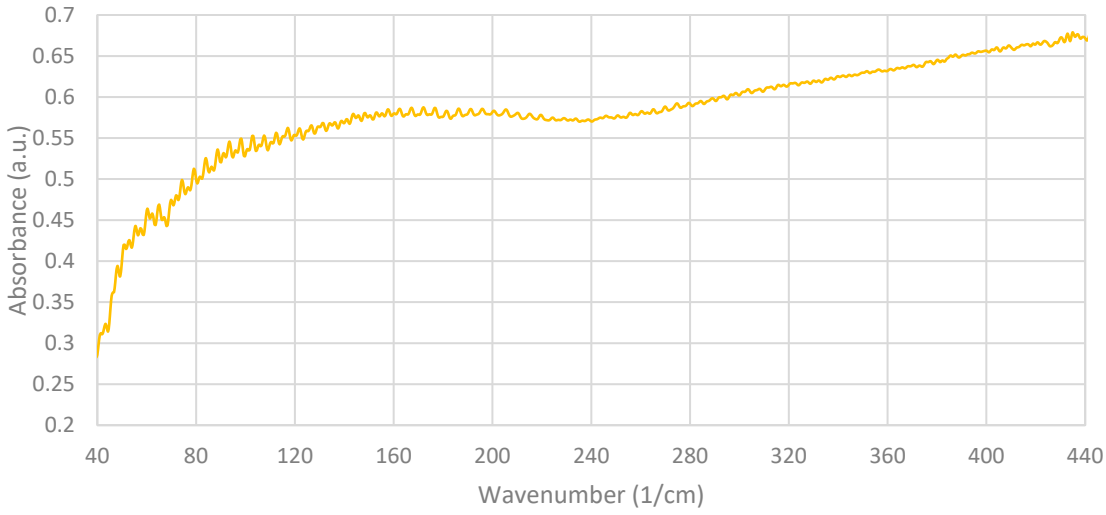

Figure 1-83: FIR spectrum of bilirubin conjugate in water (93 mg/mL) in DWLC C with a 20 µm spacer, analysed at the Australian Synchrotron (THz/FIR Beamline) with SiBolo detector and amplitude of 4300.

1.2.3.7 Biliverdin and Bilirubin Mixtures

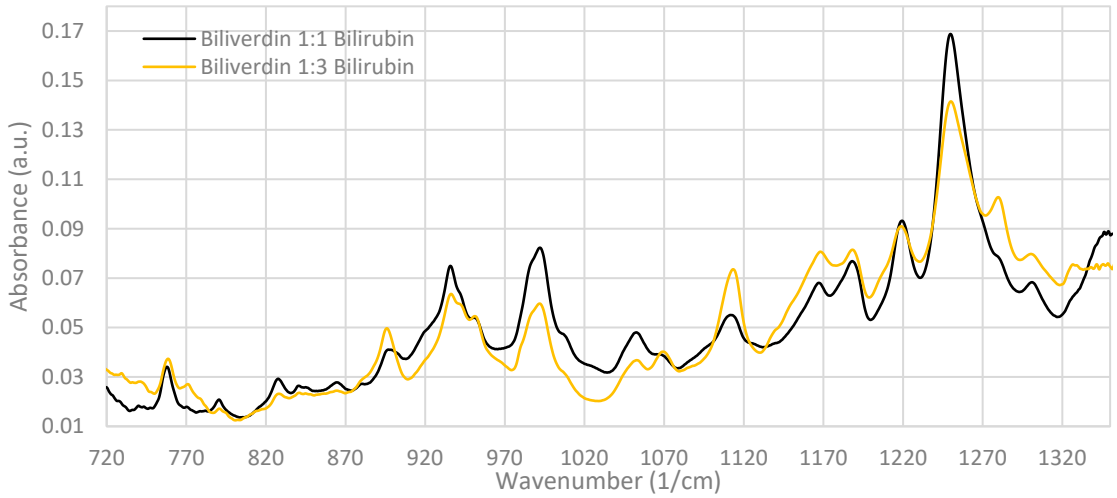

Figure 1-84: Duplicate of overlayed spectra of pressed Biliverdin and Bilirubin mixtures in KBr pellets (each approx. 1 mg) at various concentrations, normalised between 720-1350 wavenumbers analysed at the Australian Synchrotron (FIR Beamline) with MCT_N detector. Amplitude 23700 for 1:1 and 25800 for 1:3 ratio dilutions.

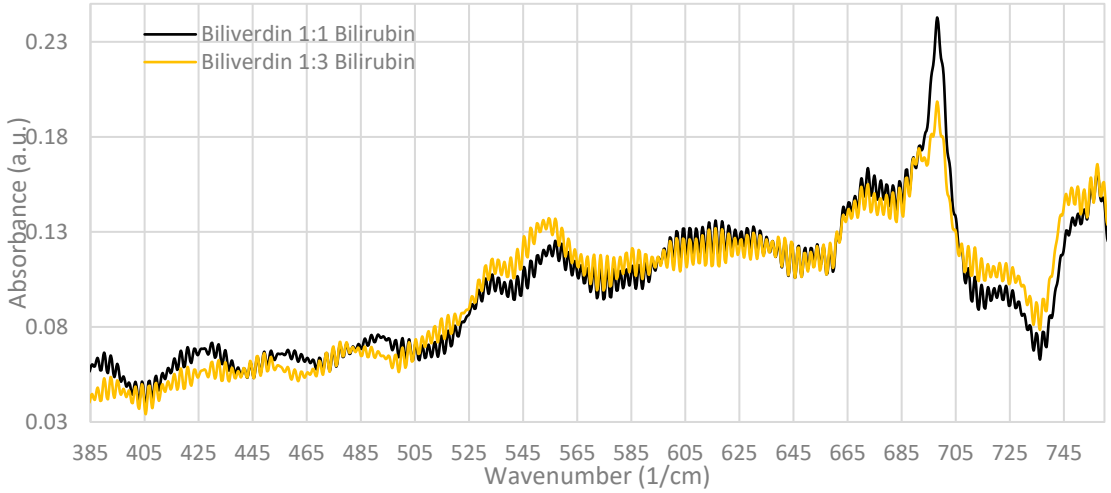

Figure 1-85: Duplicate of overlayed spectra of pressed Biliverdin and Bilirubin mixtures in KBr pellets (each approx. 1 mg) at various concentrations, normalised between 385-760 wavenumbers analysed at the Australian Synchrotron (FIR Beamline) with Si:B detector. Amplitude 23680 for 1:1 and 20800 for 1:3 ratio dilutions.

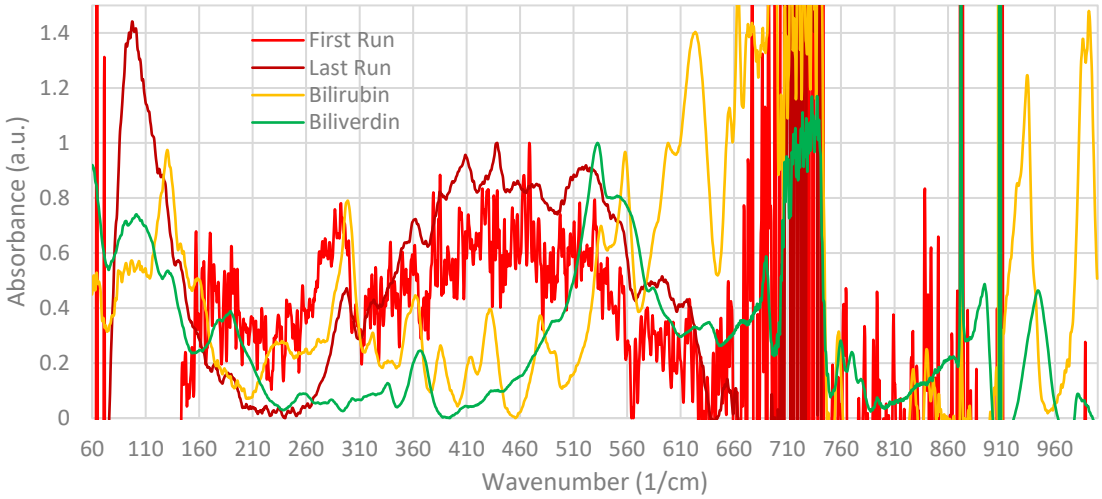

Figure 1-86: FIR-ATR overlayed spectra of biliverdin and bilirubin (1:1 ratio) in defibrinated Sheep's blood (3.3×10^{-2} mg/µL) as it dries including the first run, analysed at the Australian Synchrotron with SiBolo detector.

1.2.3.8 Ferritin

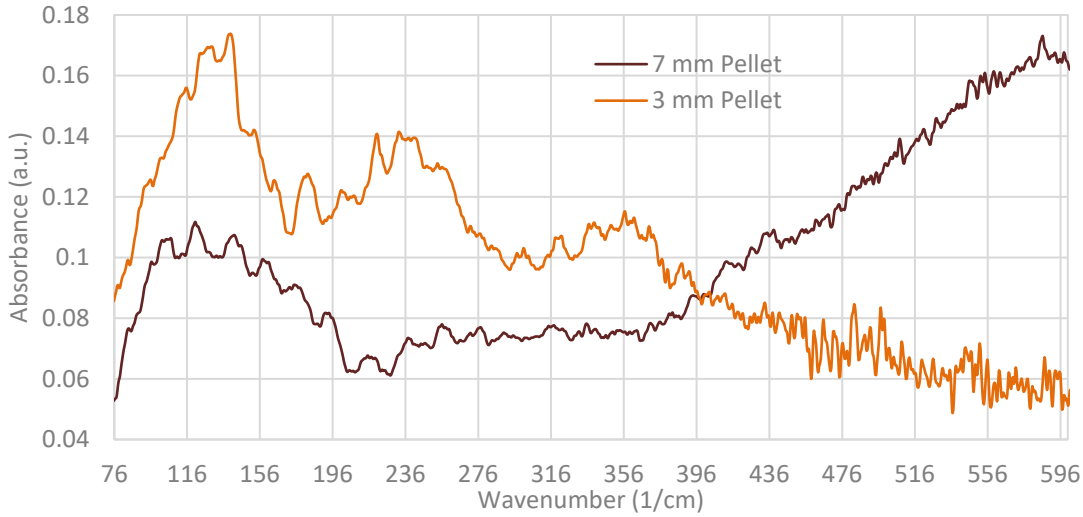

Figure 1-87: FIR overlayed spectra of pressed vacuum-dried ferritins at 5% in PE pellets of various sizes (weight 1 mg for 3 mm & 5 mg for 7 mm), normalised between 50 and 600 wavenumbers, analysed on the THz/FIR beamline at the Australian Synchrotron using a SiBolo detector. 3 mm pellet amplitude was 290.

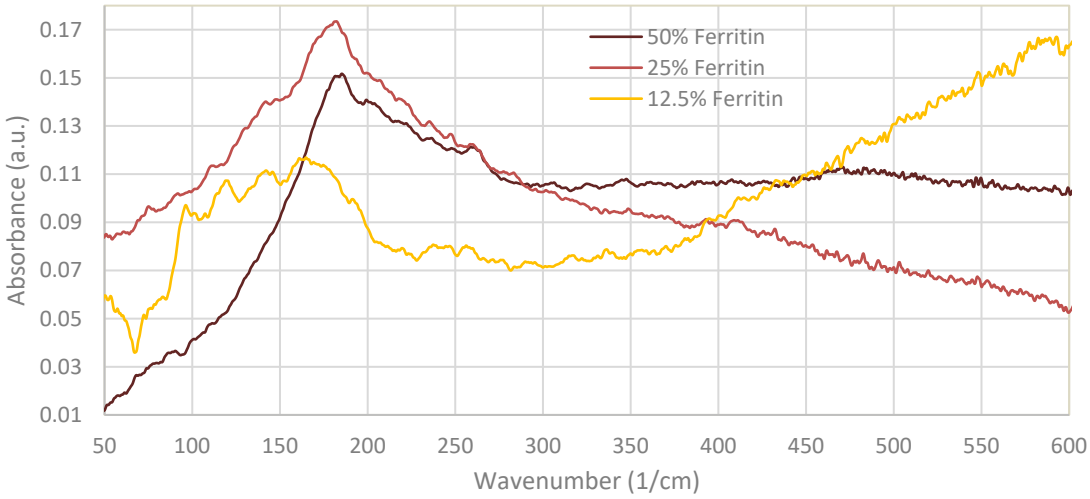

Figure 1-88: FIR overlayed spectra of pressed vacuum-dried ferritins in PE pellets (weights approx. 1 mg) at different concentrations, normalised between 50 and 600 wavenumbers, analysed on the THz/FIR beamline at the Australian Synchrotron using a SiBolo detector with amplitudes of 1258 (50% ferritin), 1081 (25% ferritin duplicate) & 9177 (12.5% ferritin).

In the below overlayed spectra, a broad absorption is observed at 280 wavenumbers with two small and weak peaks at 399 and 445 wavenumbers. The initial replicate leaked under the retainer seal as the ATR anvil refused to tighten. As such, there was less sample, and the water background could not be subtracted.

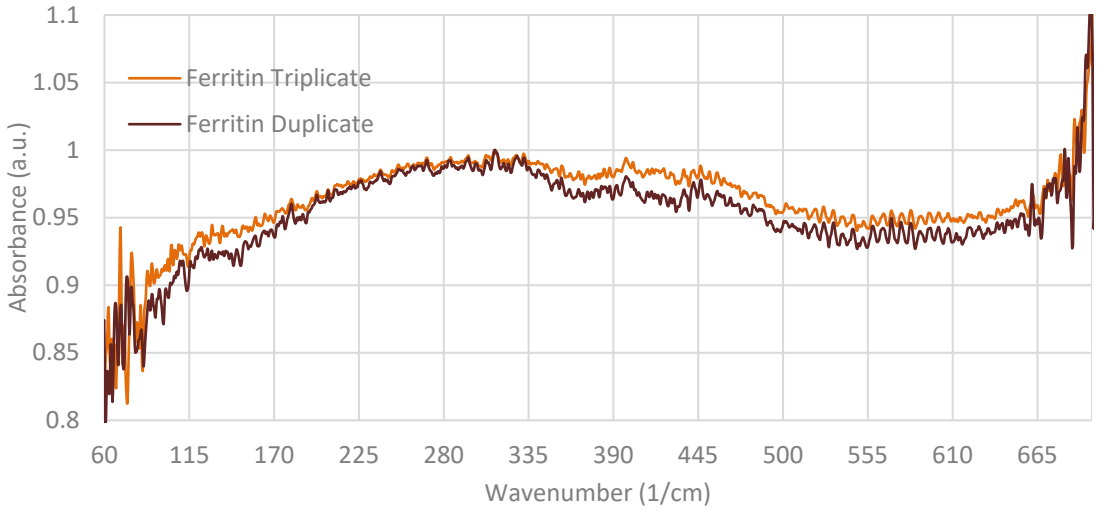

Figure 1-89: FIR-ATR overlayed spectra of ferritin (from stock solution of 44 mg/mL in NaCl) duplicates, analysed at the Australian Synchrotron with SiBolo detector.

The 5% and 50-fold ferritin dilutions in KBr presents a sharp peak at 750 wavenumbers. Two are also observed at 688 and 705 wavenumbers for the 5% sample as well as weak broad peaks at approximately 460 and 585 wavenumbers. The 50-fold dilution exhibits a similar spectrum, although possesses a large amount of oscillation to the second order. It is noted that only 3 runs of this were averaged

when using the MCT_N detector due to this extreme oscillation. Fringing and oscillation corroborate effects due to protein structure as discussed for dried defibrinated blood.

The following functionality may apply; Alkanes, C=C-H Alkenes, neighbouring aromatic C-H, C-Cl, -CH=CH- Trans, N^+-O^-, -C-O, -SO_2, -C=S, -SO, -SO_2N-, -SO_2O, P-O-Aryl, -P=O, -POOH, N-NO_2, O-NO_2, -O-H, P-O-Alkyl and C-NO_2. Extensive fringing is a direct result from beamline issues unable to be troubleshooted by the Beamline Scientist during that beamtime.

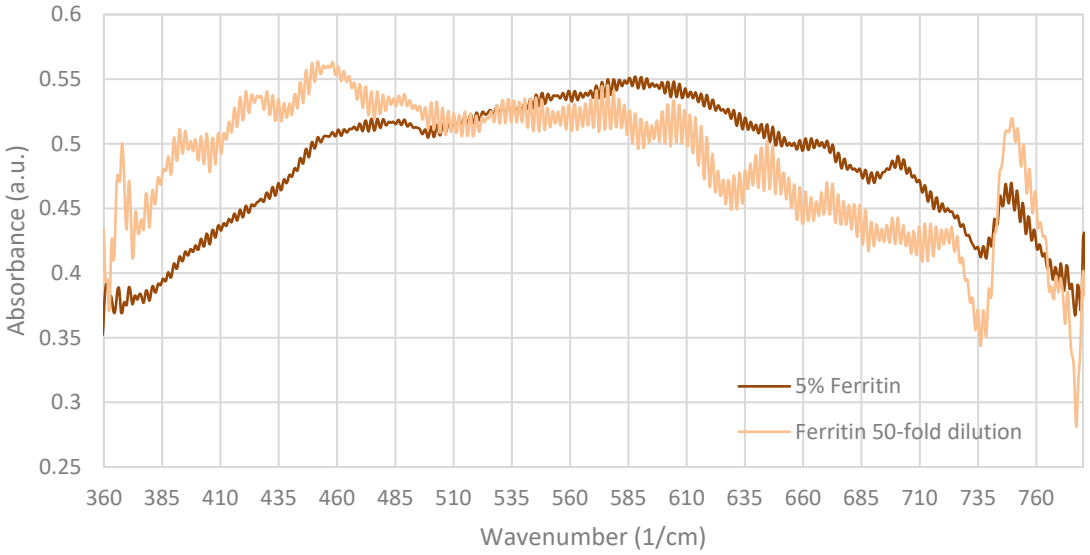

Figure 4-90: FIR overlayed spectra of pressed ferritin in KBr pellets (weights approx. 1 mg) at various concentrations, normalised between 383-720 wavenumbers analysed on the THz/FIR beamline at the Australian Synchrotron using a Si:B detector with amplitudes of 10000 (5% ferritin) & 19460 (50-fold ferritin dilution).

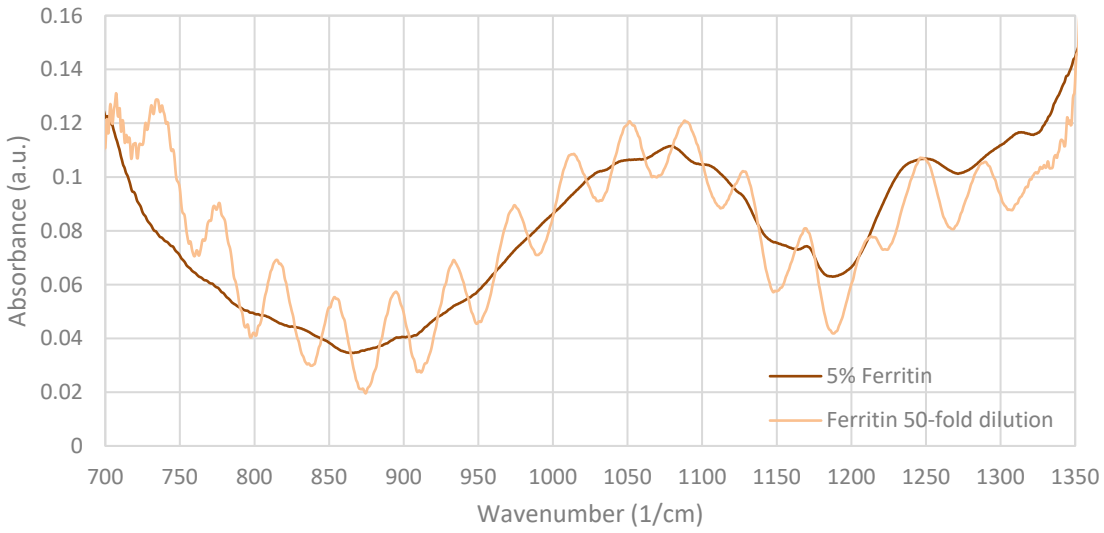

Figure 4-91: FIR overlayed spectra of pressed ferritin in KBr pellets (weights approx. 1 mg) at various concentrations, normalised between 700-1350 wavenumbers analysed on the THz/FIR beamline at the Australian Synchrotron using an MCT_N detector with amplitudes of 18686 (5% ferritin) & 30000 (50-fold ferritin dilution).

1.2.4 Nuclear Magnetic Resonance (NMR) to Investigate Purity of Biliverdin and Bilirubin

Bilirubin has 36 protons which were confirmed present on H^1NMR spectra below, matching spectra from the commercial supplier [2]. It is noted that peaks at approximately 2.5-3 ppm representative of $-CH_2$ proton environments are in addition to supplier data. Water (1.5 ppm), DMSO-d_6 (6.6 ppm) and ether (1.25 and 3.5 ppm) were also found to be present in the bilirubin samples analysed. It is possible that ether results from the manufacture process where it may used to extract organic material.

Baselines for both bilirubin and biliverdin samples are noisy as the molecules may take longer to relax into solution; they are not fully solvated or dissolved. Number of scans could be increased to reduce noise, however for the purposes of qualitative analysis, the below results suffice.

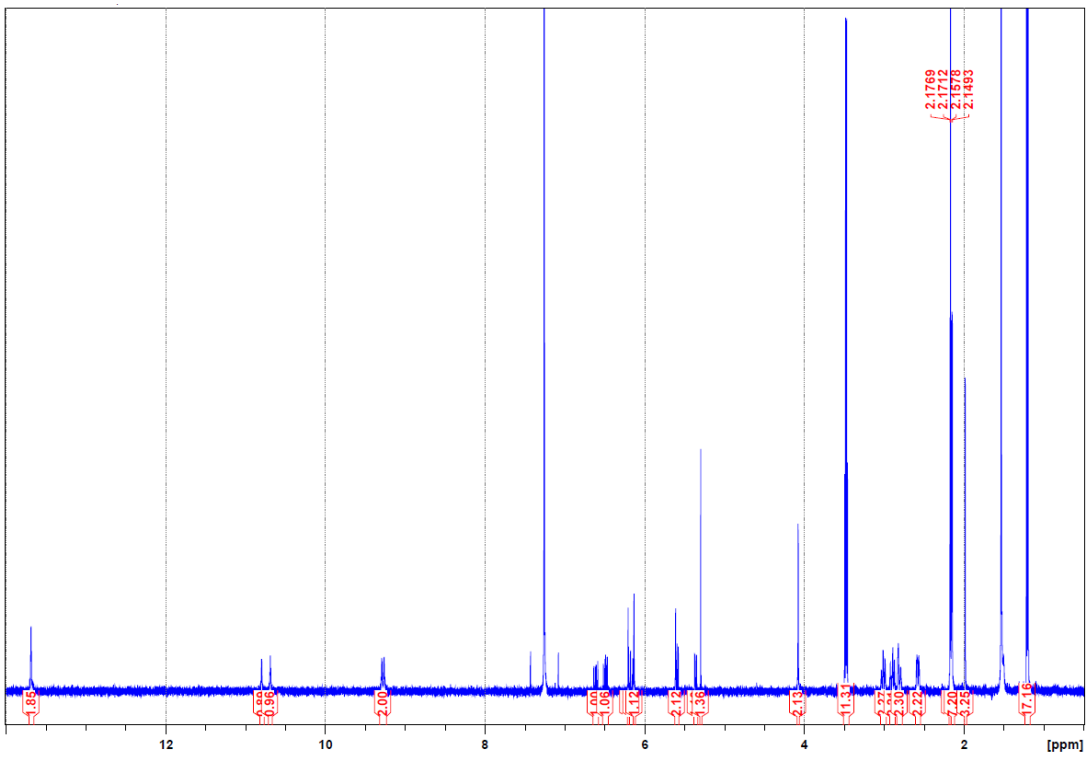

Figure 1-92: H[1]NMR 1-14 ppm spectrum of bilirubin in DMSO-d_6 taken using Bruker TOPSPIN 3 600 MHz NMR. Integration has been applied to peaks using Bruker software.

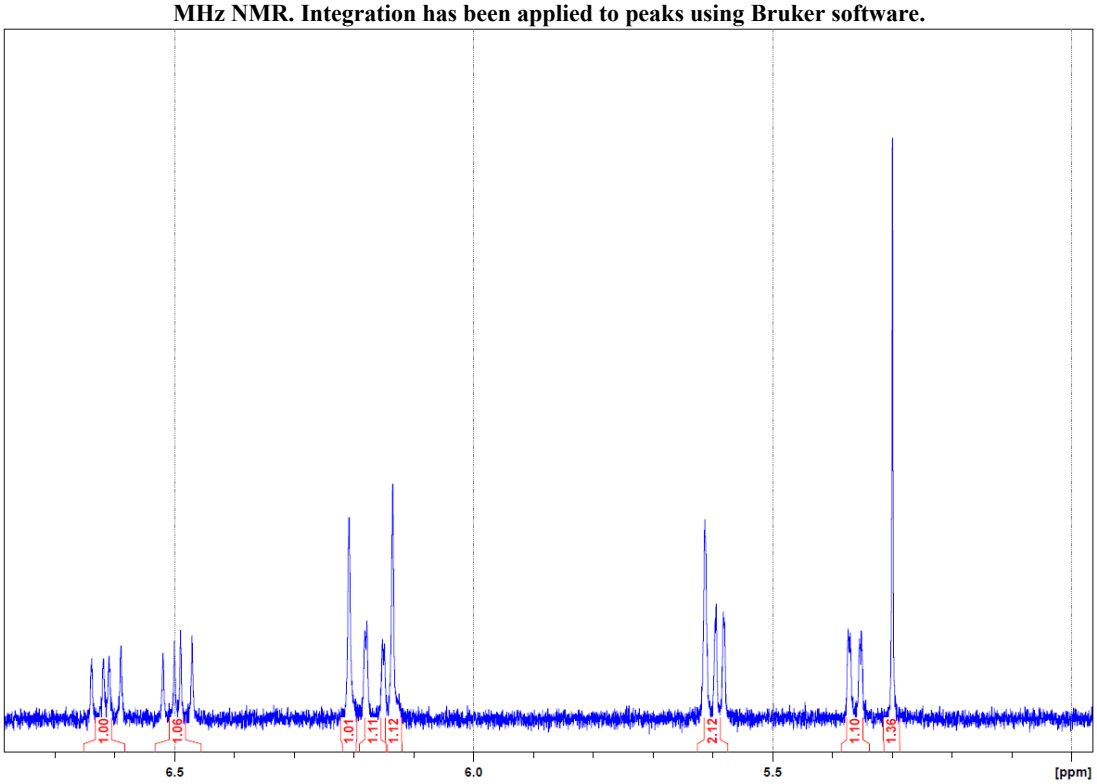

Figure 1-93: H[1]NMR 5-6.9 ppm spectrum of bilirubin in DMSO-d_6 taken using Bruker TOPSPIN 3 600 MHz NMR. Integration has been applied to peaks using Bruker software.

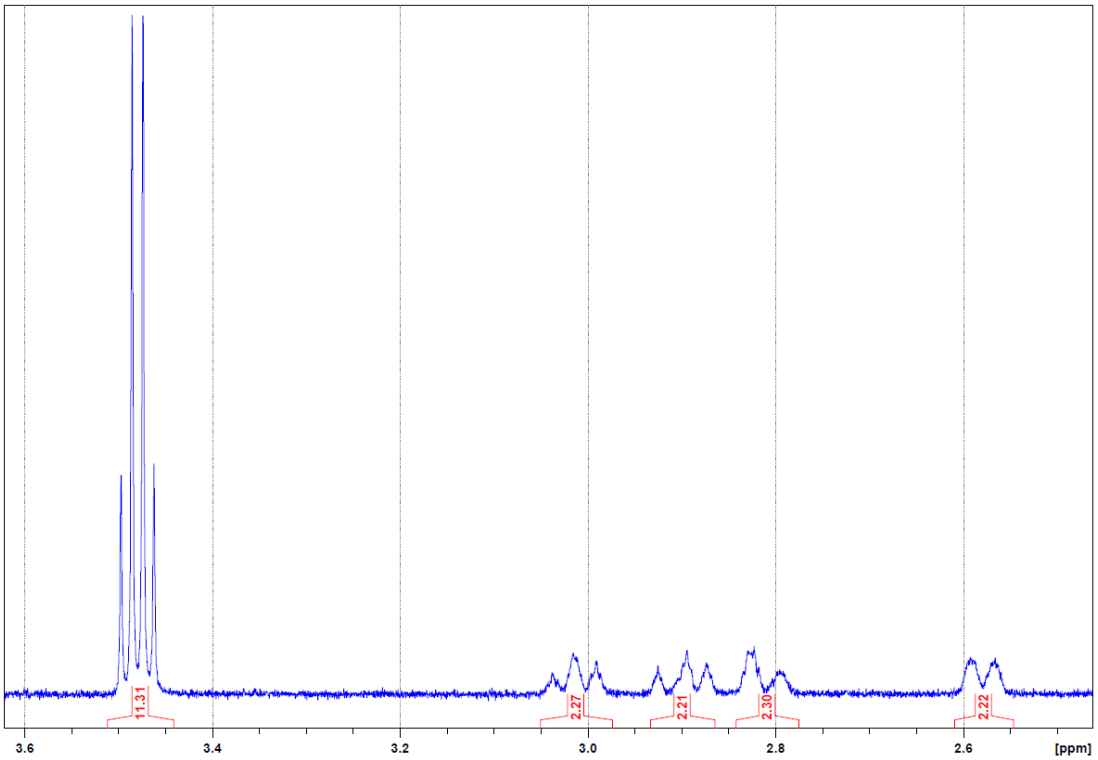

Figure 1-94: H[1]NMR 2.5-3.6 ppm spectrum of bilirubin in DMSO-d$_6$ taken using Bruker TOPSPIN 3 600 MHz NMR. Integration has been applied to peaks using Bruker software.

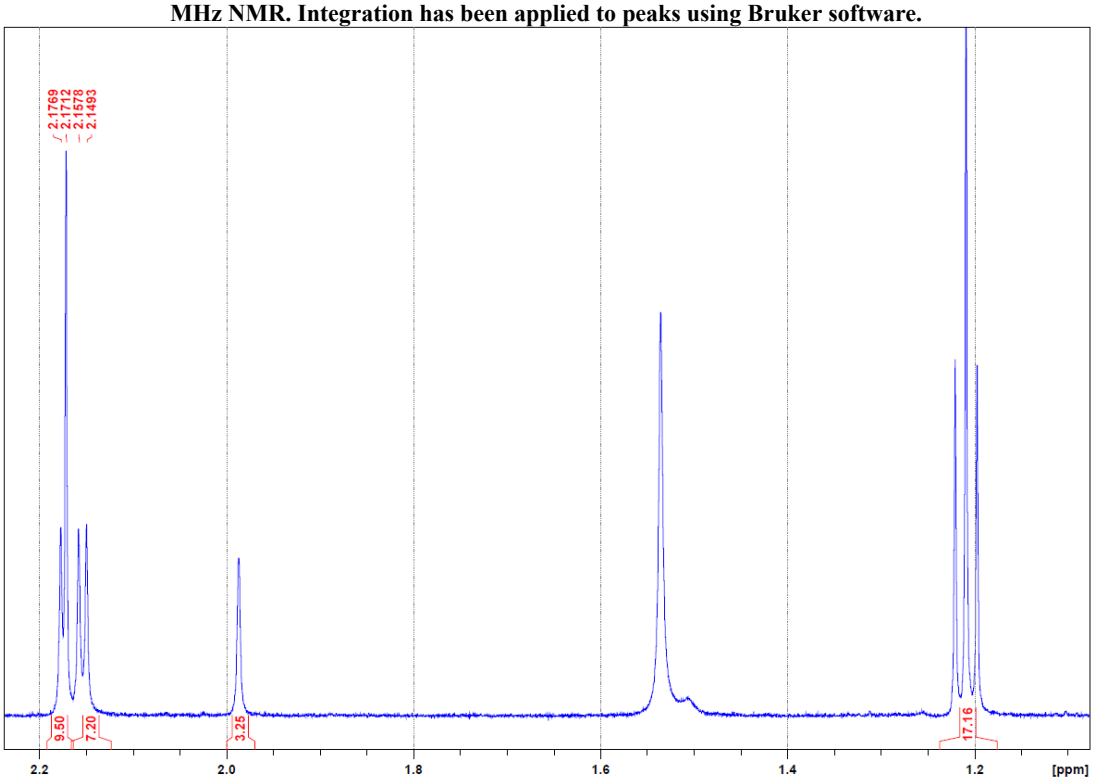

Figure 1-95: H[1]NMR 1.1-2.2 ppm spectrum of bilirubin in DMSO-d$_6$ taken using Bruker TOPSPIN 3 600 MHz NMR. Integration has been applied to peaks using Bruker software.

Biliverdin hydrochloride has 34-35 protons which were confirmed present on H[1]NMR spectra below, matching spectra from literature [3]. In addition are peaks at approximately 2.5 and 2.3 ppm, representative of DMSO-d$_6$ and acetone,

respectively. Acetone may be attributed to cleaning the NMR tubes prior to analysis.

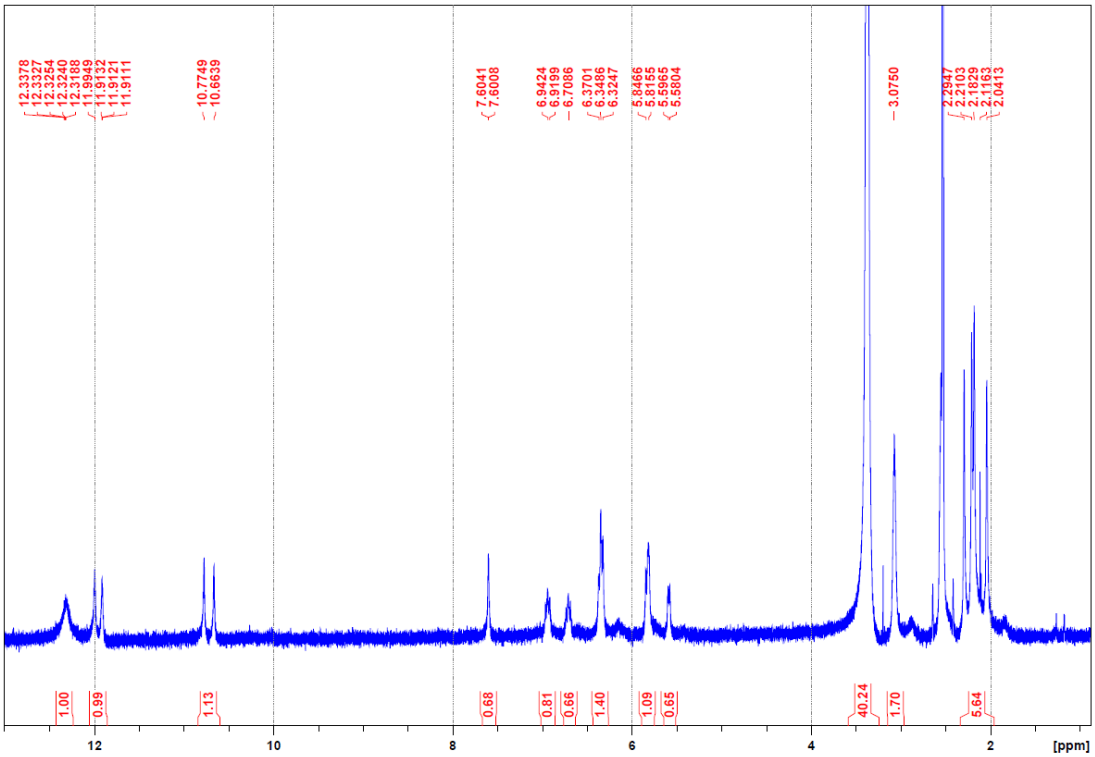

Figure 1-96: H[1]NMR 1-13 ppm spectrum of biliverdin in DMSO-d_6 taken using Bruker TOPSPIN 3 600 MHz NMR. Integration has been applied to peaks using Bruker software.

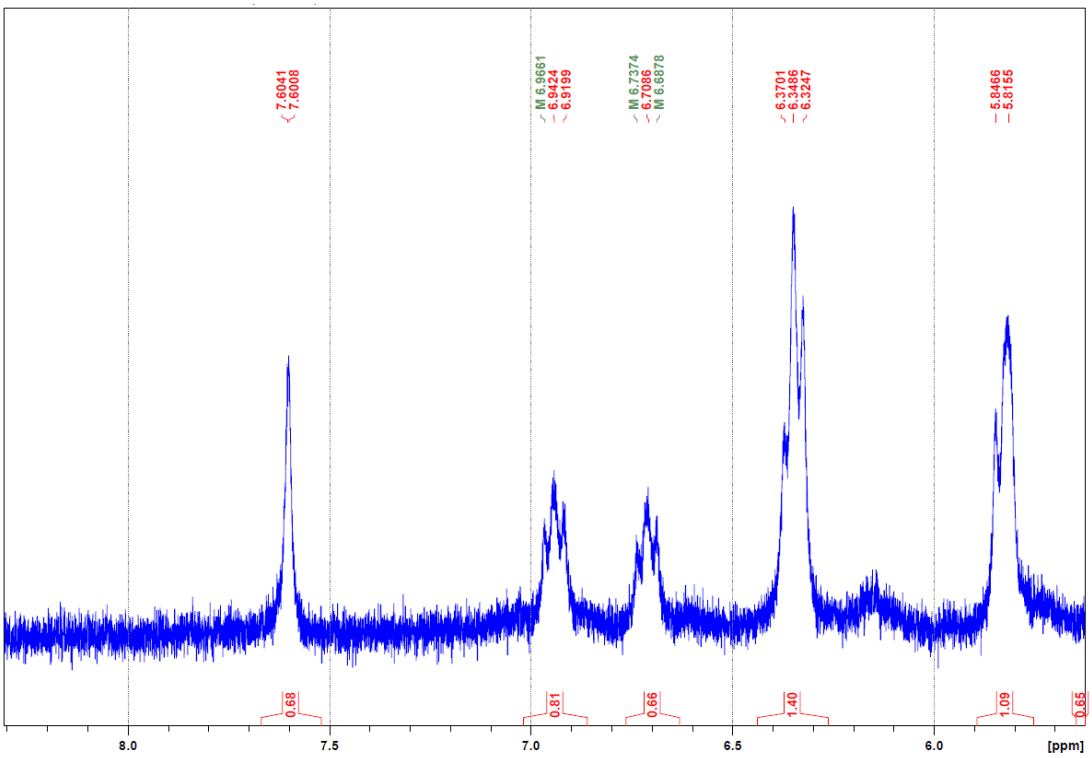

Figure 1-97: H[1]NMR 5.6-8.3 ppm spectrum of biliverdin in DMSO-d_6 taken using Bruker TOPSPIN 3 600 MHz NMR. Integration has been applied to peaks using Bruker software.

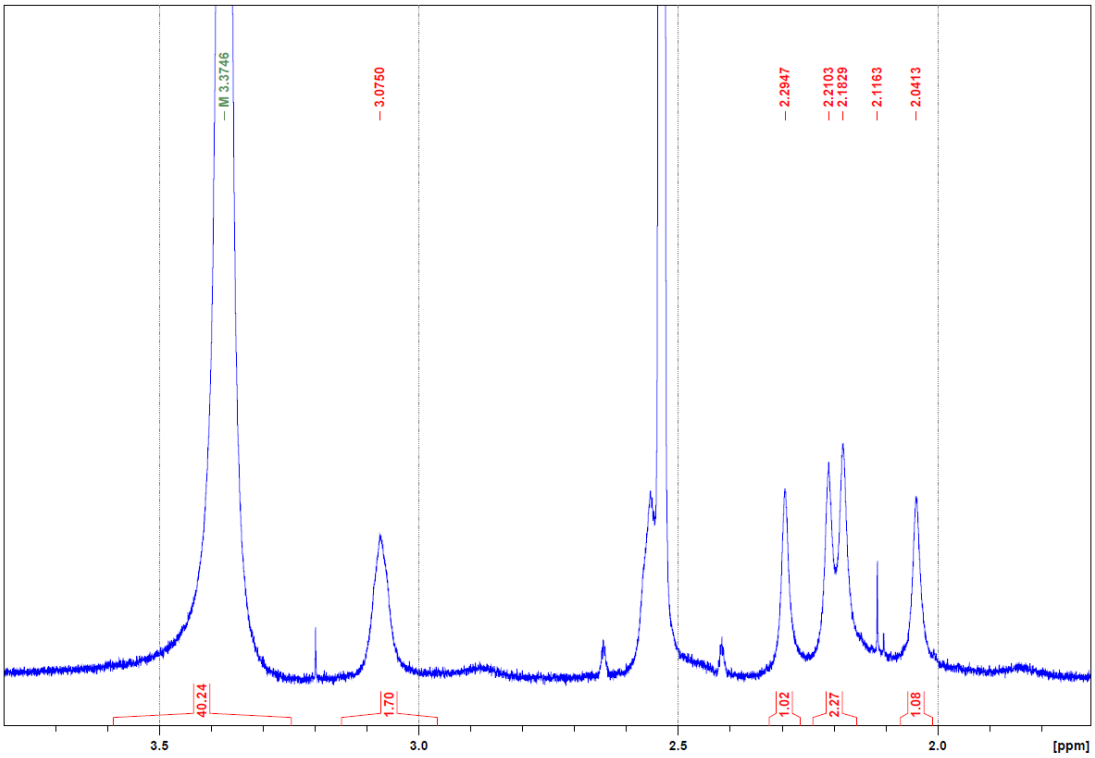

Figure 1-98: H[1]NMR 1.7-3.8 ppm spectrum of bilirubin in DMSO-d_6 taken using Bruker TOPSPIN 3 600 MHz NMR. Integration has been applied to peaks using Bruker software.

1. Yano, T., Aimi, T., Nakano, Y. & Tamai, M., *Prediction of the concentrations of ethanol and acetic acid in the culture broth of a rice vinegar fermentation using near-infrared spectroscopy.* Journal of Fermentation and Bioengineering, 1997. **84**(5).
2. KGaA, M. *Bilirubin ≥98% (EmM/453 = 60), powder*. 2018 27 October 2018]; Available from: https://www.sigmaaldrich.com/catalog/product/sigma/b4126?lang=en&region=AU&gclid=EAIaIQobChMIiJ6a4Lml3gIVhDUrCh3KjwIfEAAYASAAEgJi0fD_BwE.
3. Chen, D., Brown, J., Kawasaki, Y., Bommer, J. & Takemoto, J., *Scalable production of biliverdin IXα by Escherichia coli.* BMC Biotechnology, 2012. **12**(89).